https://doi.org/10.15388/vu.thesis.87
https://orcid.org/0000-0003-2325-2457

VILNIAUS UNIVERSITETAS
CENTER FOR PHYSICAL SCIENCES AND TECHNOLOGY

Tomas
SABIROVAS

Formation and investigation of phospholipid bilayers on metal/metal oxide surfaces

DOCTORAL DISSERTATION

Natural sciences,
Chemistry (N 003)

VILNIUS 2020

This dissertation was prepared between 2016 and 2020 at Vilnius University, Faculty of Chemistry and Geosciences. The part of this research was partially supported by Research Council of Lithuania.

Academic supervisor:
Assoc. Prof. Dr. Aušra Valiūnienė (Vilnius University, Natural Sciences, chemistry – N 003).

This doctoral dissertation will be defended in a public meeting of the Dissertation Defense Panel:
Chairman – **Prof. Habil. Dr. Aivaras Kareiva** (Vilnius University, Natural Sciences, chemistry – N 003).
Members:
Prof. Dr. Henrikas Cesiulis (Vilnius University, Natural Sciences, chemistry – N 003),
Dr. Arūnas Jagminas (Center for Physical Sciences and Technology, Natural Sciences, chemistry – N 003),
Dr. Urtė Samukaitė – Bubnienė (Vilnius University, Natural Sciences, chemistry – N 003),
Prof. Dr. Vida Vičkačkaitė (Vilnius University, Natural Sciences, chemistry – N 003).

The dissertation shall be defended at a public meeting of the Dissertation Defense Panel at 14 p.m. on 2 October 2020 at the Inorganic Chemistry Auditorium (141) of the Faculty of Chemistry and Geosciences of Vilnius University. Address: Naugarduko str. 24, LT-03225, Vilnius, Lithuania, tel. (8 5) 219 3108; e-mail: info@chgf.vu.lt

The text of this dissertation can be accessed at the Library of Vilnius University and at the Library of FTMC, as well as on the website of Vilnius University: www.vu.lt/lt/naujienos/ivykiu-kalendorius

https://doi.org/10.15388/vu.thesis.87
https://orcid.org/0000-0003-2325-2457

VILNIAUS UNIVERSITETAS
FIZINIŲ IR TECHNOLOGIJOS MOKSLŲ CENTRAS

Tomas
SABIROVAS

Fosfolipidinių membranų formavimas ir tyrimas ant metalo/metalo oksido paviršių

DAKTARO DISERTACIJA

Gamtos mokslai,
Chemija (N 003)

VILNIUS 2020

Disertacija rengta 2016 – 2020 metais Vilniaus universiteto Chemijos ir Geomokslų fakultete.
Dalį mokslinių tyrimų rėmė Lietuvos mokslo taryba,

Mokslinė vadovė:
doc. dr. Aušra Valiūnienė (Vilniaus universitetas, gamtos mokslai, chemija – N 003).

Gynimo taryba:
Pirmininkas – **prof. habil. dr. Aivaras Kareiva** (Vilniaus universitetas, gamtos mokslai, chemija – N 003).
Nariai:
prof. dr. Henrikas Cesiulis (Vilniaus universitetas, gamtos mokslai, chemija – N 003),
dr. Arūnas Jagminas (Fizinių ir technologijos mokslų centras, gamtos mokslai, chemija – N 003),
dr. Urtė Samukaitė – Bubnienė (Vilniaus universitetas, gamtos mokslai, chemija – N 003),
prof. dr. Vida Vičkačkaitė (Vilniaus universitetas, gamtos mokslai, chemija – N 003).

Disertacija ginama viešame Gynimo tarybos posėdyje 2020 m. spalio mėn. 2 d. 14 val. Chemijos ir Geomokslų fakulteto Neorganinės chemijos auditorijoje (141). Adresas: Naugarduko g. 24, LT03225, Vilnius, Lietuva, tel. (8 5) 219 3108; el. paštas: info@chgf.vu.lt

Disertaciją galima peržiūrėti Vilniaus universiteto, FTMC Chemijos instituto bibliotekose ir VU interneto svetainėje adresu: https://www.vu.lt/naujienos/ivykiu-kalendorius

TABLE OF CONTENTS

LIST OF ABBREVIATIONS

ATR-FTIR – Attenuated total reflectance Fourier-transform infrared spectroscopy

BLM – bilayer lipid membrane

CA – contact angle

Chol – cholesterol

CV – cyclic voltammetry

DOPC - 1,2-dioleoyl-sn-glycero-3-phosphocholine

DPhyPC - 1,2-diphytanoyl-sn-glycero-3-phosphocholine

EIS – electrochemical impedance spectroscopy

FFT EIS – fast Fourier-transform electrochemical impedance spectroscopy

hBLM – hybrid bilayer lipid membrane

mhBLM – mixed hybrid bilayer lipid membrane

GPL - glycerophospholipid

MTS – methyltrichlorosilane

OTS – octadecyltrichlorosilane

PLA2 – phospholipase A_2

PLY – pneumolysin

SAM – self-assembled monolayer

sBLM – solid-supported bilayer lipid membrane

tBLM – tethered bilayer lipid membrane

αHL – α-hemolysin

INTRODUCTION

Plasma membrane is one of the most essential structures in the cell which separates cell interior from the environment and/or extracellular matrix. Wide range of proteins are incorporated in the cell membrane. These proteins are responsible for a number of functions: compartmentalization of life components, cell-to-cell electric and/or chemical communications, recognition, biosignaling, and others. To simplify this complex system, various lipid bilayer models were developed and used for biochemical and biophysical studies involving protein-lipid interaction [1], ion transportation [2-3]. Medical diagnostics [4-5], drug screening [6-7], and environmental control [8-9] are often based on artificial lipid membranes by the combination of biological recognition with a physicochemical transducer. The obvious advantages of membrane-based biosensors are nature-like environment and relatively simple preparation through a self-assembly process.

By the pioneering work of Mueller on bilayer lipid membranes ("black lipid membranes") [10-11], various approaches were developed for the formation of artificial lipid membranes. Among those, solid supported lipid bilayers received considerable recognition. Several different strategies can be adopted for the formation of the lipid membrane on a solid support. One of them is supported lipid bilayers, where lipid bilayer is formed directly on the substrate such as oxidized silicon [12], silica [13], mica [14], aluminum [15], titanium [16], etc. The advantage of using solid supports is an increase in the robustness and stability of artificial membranes. Ability to probe the surface with powerful analytical techniques (e.g. quartz crystal microbalance [17], atomic force microscopy [18], surface plasmon resonance [19], electrochemical impedance spectroscopy [20]) is another equally important advantage of using solid supports. Nevertheless, the major drawback of supported lipid bilayers is the thin water layer between the bilayer and solid support, so the incorporation of transmembrane proteins often presents unfavorable interactions with the substrate and leads to loss of their lateral mobility [21].

Another widely used strategy is to form artificial bilayers on modified surfaces with a polymer layer [22-24] or self-assembled monolayers [25-28]. Such functionalization of the surface decouples the artificial membrane from the substrate and, in principle, allows for transmembrane proteins to preserve their function. The modification of the surface by molecular anchors is often achieved either by thiol-metal or silane-oxide surface chemistry. Mostly gold [26, 28-29] as a substrate has been extensively studied for the formation of

bilayer lipid membranes but other surfaces are viable choice as well e.g. indium tin oxide (ITO) [30], fluorine doped tin oxide (FTO) [31], cadmium tin oxide (CTO) [32], Ti/TiO_2 [33], aluminum [34-37], etc. However, most of the substrates requires special preparation techniques e.g. magnetron sputtering, consequently increasing the total expense towards the investigation of membrane related processes or for application of the electrochemical/electroanalytical devices. Furthermore, mostly used gold surfaces have propensity to denature proteins which leads to biofouling of the surface [38-39]. In contrast, widely used titanium and its alloys exhibit excellent biocompatibility [40], therefore, tailoring titanium surfaces by the phospholipid membranes may expand their utility in implant/replacement medicine. However, preparation of metallurgical titanium surfaces e.g. surface polishing, is challenging due to the hardness of material. Also, application towards phospholipid membrane-based devices might be limited due to the expensive titanium surface. Therefore, other cost-efficient and soft metal surfaces should be explored as well for phospholipid bilayer formation. One of them is aluminum. A major advantages of aluminum compared to titanium surface are effortless preparation of the surface due to the softness of the material and higher affinity towards silane based compounds [41]. For these reasons, artificial bilayers on metallurgical aluminum surface could decrease the total expenditure towards investigation of the membrane related process or as an application towards bioanalytic devices.

The aim of this study was to design biomimetic phospholipid bilayers on metallurgical surfaces of titanium and aluminum.

The objectives of the study:

1. To establish a preparation procedure of metallurgical titanium and aluminum surfaces for formation of silane based self-assembled monolayers.
2. To investigate the formation of the hybrid bilayer lipid membrane on the metallurgical titanium surface and test it`s functionality with membrane damaging toxin phospholipase A_2.
3. To investigate formation of the mixed hybrid bilayer lipid membrane on metallurgical titanium functionalized with the mixed self-assembled monolayer and test it`s functionality with membrane damaging toxins: pneumolysin and α-hemolysin.
4. To investigate the formation of the hybrid bilayer lipid membrane on the metallurgical aluminum and test it`s functionality with membrane damaging toxin – melittin.
5. To investigate reusability of the self-assembled monolayers for the artificial membrane.

SCIENTIFIC NOVELTY

The artificial membranes on solid surfaces have been extensively studied over the past few decades. Mostly, gold surfaces have been employed for application of artificial membranes towards membrane-based biosensor devices. However, preparation of such surfaces is still rather expensive since it requires special preparation techniques e.g. magnetron sputtering. Moreover, formation of the molecular anchors is still time-consuming process. Self-assembled monolayers on gold surfaces, in general, are prone to structural rearrangements, hence, they are mostly disposed after single use. Therefore, in this research metallurgical surfaces of aluminum and titanium were investigated for the first time for the artificial membrane formation on silane–based monolayers. Notably, silane-based monolayers on Ti and Al surfaces were found to be reusable for multiple times of the artificial membrane formation. Also, biological relevance of artificial membranes formed on titanium and aluminum surfaces was shown by using membrane damaging proteins/peptides. All in all, the results presented in this research enable to conclude that surfaces of metallurgical Al and Ti can be successfully employed for artificial membrane formation, significantly reducing total cost of membrane-based biosensor devices.

STATEMENTS FOR DEFENSE:

1. Metallurgical surfaces of titanium and aluminum can be used for hybrid bilayer lipid membrane formation.
2. Mixed hybrid bilayer lipid membrane can be formed on the metallurgical titanium surface by dilution of OTS molecular anchor by short-chain MTS molecule.
3. Artificial bilayers formed on the metallurgical titanium and aluminum surfaces can be used for the detection of the membrane damaging proteins/peptides.
4. Silane-based self-assembled monolayer formed on metallurgical titanium and aluminum surfaces can be reused multiple times for the artificial membrane formation.

1. LITERATURE REVIEW

1.1 Biological membranes

Cell is one of the most essential unit in living organisms. One of the most important structure elements in the cell is plasma membrane, separating cell interior from the environment and/or extracellular matrix. The membrane is responsible for several functions such as compartmentalization of life components, cell-to-cell electric and/or chemical communications, permeabilization of various materials. The membranes are composed of the two-dimensional lipid bilayers, where peripheral and integral proteins are located. In 1972, the fluid mosaic model of the cell membrane was presented by Singer and Nicholson [42] describing the membrane as a fluid in which integral proteins that are either embedded inside the bilayer and peripheral proteins that are arranged on the surface of the membrane are able to move freely. The biological membrane can be considered as a liquid, where the lipids and proteins can diffuse laterally in the bilayer, creating random distribution.

The fluid mosaic model is still relevant nowadays, however, the real situation is far more complicated. In 1997 Simons and Ikonen [43] introduced the lipid rafts, which improved the fluid mosaic model. It was shown that lipids are not equally located across the membrane. The inner and outer leaflet may have different composition. The lipid rafts, consisting of clusters of the more ordered lipids, moves freely in the bilayer. The lipid rafts are functional, for example they are responsible for transmembrane signal transduction at the cell surface, cell adhesion, molecular recognition, etc. [44].

One of the major components of the plasma membranes is lipids. Lipids are amphipathic, consisting of the polar head group and a hydrophobic hydrocarbon part. The major membrane lipids are glycerophospholipids (GPL), sphingolipids, and sterols (mainly cholesterol). Lipids, especially glycerophospholipids and sphingolipids have high chemical diversity. Fatty acids in GPL or sphingolipids vary in chain length, double bond number, double bond position and hydroxylation [45]. Another chemical diversity arrives from the head group substituent of the lipids such as phosphatidylcholine (PC), phosphatidylethanolamine (PE), phosphatidylserine (PS), phosphatidylinositol (PI). The head group and acyl chain composition influence the physical properties of the membrane [46]. The variation in headgroups and aliphatic chains allows the existence of >1,000 different lipid species in any eukaryotic cell [47]. Such high diversity

of lipids is essential for membranes, since, e.g., lipids can function as signaling molecules, chemical identifiers of specific membranes or as energy storage molecules [48].

1.2 Membrane model systems

Plasma membrane is a complex system, consisting of various lipids and proteins, responsible for cell protection, cell-to-cell electric and/or chemical communications, metabolism, etc. To study biological membranes artificial bilayer lipid membranes were required for simplification reasons. Artificial membranes allows to study biochemical and biophysical properties of bilayer lipid membranes such as protein-membrane interactions [49], redox reactions [50], ion permeability [51-52], etc.

Liposomes

Liposomes or vesicles have spherical structure, where the aqueous reservoir is enclosed by the phospholipids (Fig. 1). Usually, such system forms by self-assembly process due to hydrophobic and hydrophilic interaction since phospholipid molecules are amphipathic (having both hydrophobic and hydrophilic part) by their nature [53]. In principle, liposomes can be classified depending on the size and the number of bilayers (lamellarity). Main classification consists of: multilamellar large vesicles (MLV, >500 μm, approx. 5-25 lipid bilayers), large unilamellar vesicles (LUV, >100 nm, 1 lipid bilayer), small unilamellar vesicles (SUV, 20-100 nm, 1 lipid bilayer), giant unilamellar vesicle (GUV, >100 μm, 1 lipid bilayer) [54]. Due to their unique structural properties liposomes, excellent biocompatibility and ability to interact with cells by releasing liposomal components, they are often used as a drug delivery system [54-55]. Various therapeutic agents, both hydrophobic and hydrophilic in their nature can be incorporated into liposomes. The aqueous reservoir inside the liposomes can be exploited for water soluble drugs [56], while the bilayer lipid membrane – for hydrophobic drugs [57].

While liposomes are excellent in the field of the drug delivery, they can also be used for artificial bilayer membrane formation. In this work, liposomes were used as a tool to form bilayer lipid membrane on the functionalized surface. The formation of the bilayer lipid membrane by vesicle fusion method follows these steps: approaching the surface, adsorption, and attachment to the surface, flattening from the edges. The flattened areas expand and spread until liposome collapse by forming the bilayer membrane on solid surfaces [58-59].

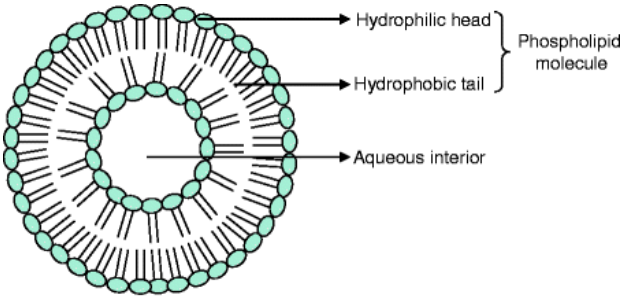

Figure 1. Structure of liposome [60].

Black lipid membranes

The history of artificial bilayer lipid membranes started in 1961 by the pioneering work of Müller et al., who developed black lipid membranes (BLM) [10-11]. BLMs are usually formed by spreading a lipid solution in a small hole inside the wall, separating two aqueous compartments. Such model has advantage comparing to liposomes, since it is suitable for electrical conductivity measurements. The major advantage of the black lipid membranes is their semblance to the biological membrane. Moreover, black lipid membranes are suspended across the mechanical frame, where transmembrane proteins can be incorporated and studied in most natural environment. Nevertheless, the major drawback is the physical stability due to insufficient surface tension required to form BLM over long period of time (only last few hours) [61].

Solid supported lipid membranes

Another method for formation of artificial lipid membranes is to employ a solid supported, which allows to form lipid membranes on various surfaces, i.e., (oxidized silicon [12], silica [13], mica [14], aluminum [15], titanium [16], etc). The major advantage of introducing a solid support for artificial membrane formation is a long-term and high mechanical stability. Moreover, such artificial membranes can be investigated by various surface sensitive techniques such as (quartz crystal microbalance [17], atomic force microscopy [18], surface plasmon resonance [19], electrochemical impedance spectroscopy [20]). Such solid supported bilayer lipid membranes (sBLM) consist of lipid bilayer deposited onto the solid surface, separated by ultrathin water layer [62]. However, the distance between the bilayer lipid membrane and the substrate limits the usage of such model. The incorporation of transmembrane proteins often presents unfavorable interactions with the

substrate and leads to loss of their lateral mobility which change the physiological response of the protein [21].

Hybrid bilayer lipid membrane

Hybrid bilayer lipid membranes is another class of solid supported lipid bilayer. Typically, hybrid bilayer lipid membrane consists of phospholipid layer physisorbed to an immobile self-assembled monolayer (Fig. 2). The polar headgroups of the phospholipids are facing away from the solid substrate to the aqueous solution, and the hydrophobic tails of phospholipids are oriented towards the hydrophobic SAM [63-65]. Such SAM/lipid bilayer lipid membrane exhibit long-term stability. Nevertheless, the main drawback of such model is the rigidity of the membrane [66]. The incorporation of the large integral proteins is hardly achievable, because of the lack of the ionic reservoir between the solid supported and lipid membrane [67].

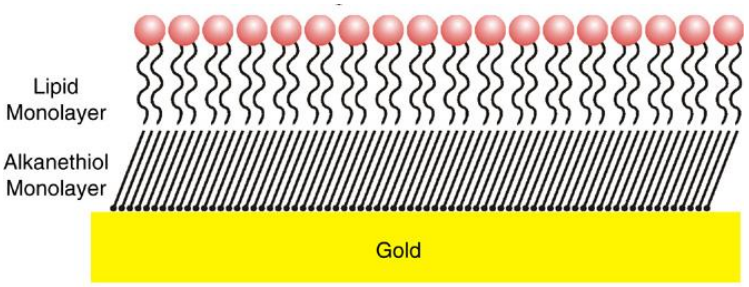

Figure 2. Schematic representation of hybrid bilayer formed on gold surface [62].

Tethered bilayer lipid membrane

In attempt to overcome the absence of ionic reservoir of hybrid bilayers, tethered bilayer lipid membrane (tBLM) model was developed. Main difference between hybrid bilayers and tethered bilayer lipid membranes are introduction of thiolipids, which is a molecular anchor containing a lipid or cholesterol derivative. Thiolipids usually have a hydrophobic headgroup (lipid/cholesterol derivative), a spacer consisting of hydrophilic molecule, and terminal group usually consisting of a thiol or disulfide, which covalently binds to the substrate [26-28, 68]. Such structural configuration of a spacer group, which provides a physical separation of the bilayer from the solid support, allows to form an ionic (aqueous) reservoir between the bilayer lipid membranes (submembrane space). The submembrane space is designed in a way that allows accommodate hydrophilic part of the transmembrane proteins,

similar to that of the cell. Such aqueous reservoir is the major advantage of the tBLM over other artificial membrane models, together with high electrical insulation.

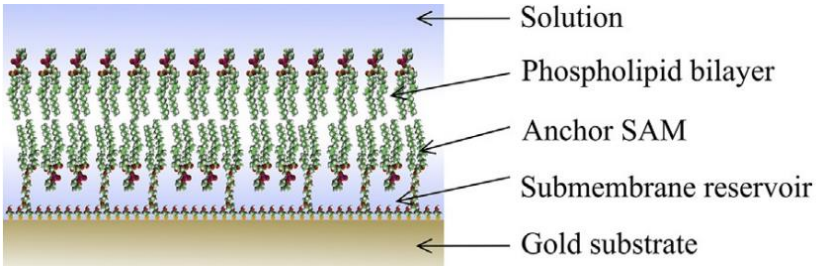

Figure 3. Schematic representation of tethered bilayer lipid membrane on gold substrate [69].

1.3 Silane based self-assembled monolayers

Large variety of the self-assembled assembled monolayers have been studied since their introduction in 1980 by Sagiv [70]. Typically, SAMs are composed of the three parts: i) the head group, which binds to the surface, ii) alkylchain, which provides stability and ordering of the SAM mostly due to the van der Waals interaction [71] and iii) terminal group, which determines the chemical functionality [72] and surface energy [73]. The most studied self-assembled monolayers are either based on thiols [74] or silanes [75].

Typically, for the silane based self-assembled monolayer formation, hydroxilated surfaces are dipped into the reaction bath containing the solution of the desired silane molecule. As a reference, the mechanism of the SAM formation on silicon substrate is displayed in Fig. 4, consisting of the four steps [76-78]. The first step, physisorption process takes place at hydrated surface. In the second step, in the presence of the adsorbed water layer on the surface, the silane molecules in close proximity to the substrate hydrolyze into polar trihydroxysilane $Si(OH)_3$. The third step occurs when the polar $Si(OH)_3$ groups form covalent bonds with the surface hydroxyl groups. Afterwards, condensation reactions between neighbor silane molecules occurs by forming silanol groups. During the first three stages, only few molecules will be absorbed on the surface and monolayer is in a disorder state. Nevertheless, well-ordered, or compact monolayer will be obtained (step 4) by increasing the time of the silanization. The process can be facilitated by curing the substrate in an oven at 100-200 °C [79].

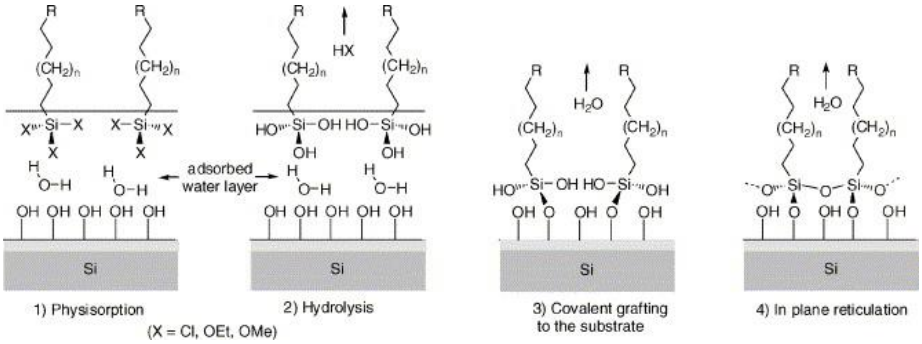

Figure 4. Schematic showing different steps involved in the mechanism of SAM formation on a hydrated silicon surface [78].

Main advantage of silane based SAMs in contrast with thiol based SAMs is a higher physical and chemical stability. However, silane based SAMs are much more complicated in preparation. In particular, the reactivity of alkyltrichlorosilane based SAMs are much higher in a presence of water. Precise control of water is very important for the formation of the closely packed SAMs [80]. In an absence of water, incomplete monolayers can be formed [76], while the excess of water results in the polymerization of silane molecules in the solution [81]. Another important advantage of silane based SAM over the thiol based SAMs is thermal stability up to 250 degrees [82-83].

Chemical and thermal stability, mechanical robustness presents silane based SAMs as an ideal platform to study wide range of physical and chemical properties such as adhesion [84], adsorption [85], friction [86]. Ability to functionalize various surfaces with silane based SAMs such as silicon [78, 82], glass [81], mica [87], Al [34, 88], Ti [89-90], and other relevant surfaces provides the possibility to apply such surface for wide range of the research areas such as electronics [78, 91], protective coatings [92], biosensors [71], etc. Especially SAMs as a biosensor platform are exceptional due to i) relatively easy formation of defect free, ordered and stable monolayers, ii) membrane like microenvironment, provided by the SAM surface, which is suitable for biomolecules immobilization, iii) the flexibility to design the SAM head group with different functional groups, iv) stability for extended periods, v) ability to use surface sensitive techniques to study processes such as protein adsorption, bilayer lipid membrane formation, antibody-antigen interactions, etc. [71]. In particular, silane based SAMs provides a possibility to tailor various metal/metal oxide surfaces for bilayer membrane formation applications. As mentioned earlier, a covalently attached linker of SAM to the

surface endows the lipid film much greater robustness compared to black lipid membranes or supported lipid membranes. However, mostly gold substrates have been employed for bilayer lipid membrane formation based on thiol SAMs [26, 28, 66]. However, gold surfaces are quite expensive in the context of the disposable/reusable biosensors. Therefore, the ability to form bilayer lipid membranes on other substrates for cheap and disposable/reusable biosensors could be considered. Especially, metallurgical substrates, having straightforward surface preparation by a simple mechanical polishing could provide a convenient platform for bilayer lipid membrane formation on silane based SAMs. Hence, in this study for the first-time silane based self-assembled monolayers were formed on metallurgical Al and Ti surface for immobilization of the bilayer lipid membrane.

1.4 Electrochemical impedance spectroscopy

Electrochemical impedance spectroscopy (EIS) is an analytical tool for investigating electrical properties of the material such as resistivity, dielectric constant, and capacitance. In principle, impedance, Z, is defined in terms of current, I, and potential, E [93]:

$$Z = \frac{E}{I} \tag{1}$$

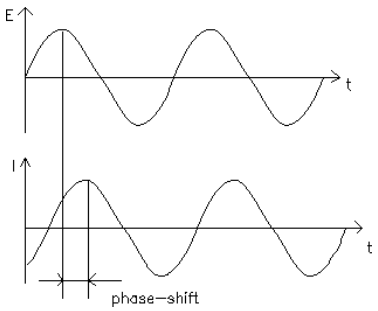

Figure 5. Sinusoidal alternating current response.

The applied voltage can be expressed as a function of time:

$$E(t) = E_0 \cos(\omega t) \tag{2}$$

then, the response signal of the current is shifted by the phase (ϕ)

$$I(t) = I_0 cos(\omega t - \phi) \quad (3)$$

where I_t – is the current at specific time, I_0 – amplitude of the signal, ϕ – phase shift and ω – radial frequency (rad/s) which can be expressed as $\omega = 2\pi f$, where f – frequency (Hz).

Therefore, by applying Ohm`s law and Euler`s relationship, impedance, Z, can be expressed as a complex number:

$$Z = \frac{E_t}{I_t} = \frac{E_0 \cos(\omega t)}{I_0 cos(\omega t - \phi)} = \frac{E_0 e^{j\omega t}}{I_0 e^{j\omega t - \phi}} = Z_0(cos\phi + jsin\phi) \quad (4)$$

where Z_o is the magnitude.

Impedance can be described as a vector since it has a magnitude Z_0 and a direction (phase shift ϕ). Thus, in a complex plane (Nyquist plot, Fig. 5), the impedance vector, |Z|, is composed by two components: the real part, Z_{Re}, and imaginary part, Z_{Im}. Accordingly, the value of impedance and phase angle can be calculated:

$$|Z| = \sqrt{Z_{Re}^2 + Z_{Im}^2} \quad (5)$$

$$tg(\phi) = \frac{Z_{Im}}{Z_{Re}} \quad (6)$$

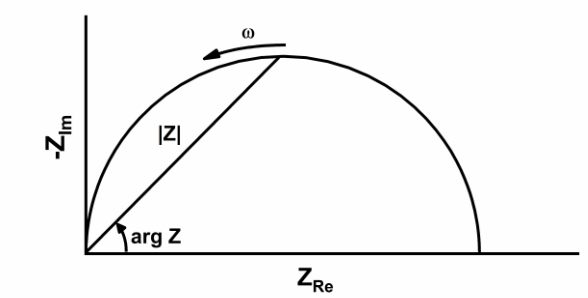

Figure 6. Nyquist plot representation of the impedance spectroscopy data.

The data of EIS can be displayed differently, but usually, both the Bode and Nyquist representation is used. The Bode impedance representation consists of two plots (Fig. 7). In one plot, the absolute magnitude of the impedance is plotted against the frequency, f. In another one the phase angle is plotted vs the frequency. The Bode plot gives information on the impedance and phase shift as a function of frequency.

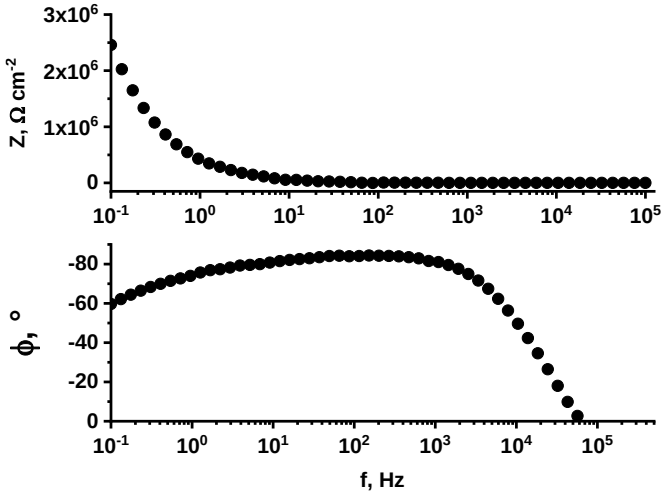

Figure 7. Bode plot representation of the impedance spectroscopy data.

Another important expression is also used to study the system with the EIS – admittance. Relation between impedance, Z, and admittance, Y, can be described:

$$Y = \frac{1}{Z} = Y_{Re} + jY_{Im} \quad (7)$$

where Y – admittance (S), Y_{Re} and Y_{Im} are real and imaginary parts of the admittance. Dividing eq. (7) by $j\omega$, complex capacitance can be obtained:

$$C = \frac{Y}{j\omega} = \frac{Y_{Re}}{j\omega} + \frac{jY_{Im}}{j\omega} = C_{Re} + jC_{Im} \quad (8)$$

Eq. (8) representation is called Cole-Cole plots or complex capacitance plots (Fig. 8).

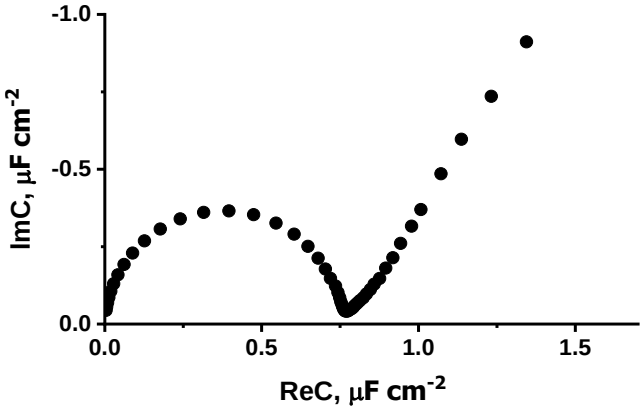

Figure 8. Cole-Cole plot representation of the impedance spectroscopy data

Cole-Cole plots are useful to study the dielectric properties of the surface [20, 28]. The insulating layer showing near or ideal capacitive behavior exhibits semi-circular shape, which is typical for ideally polarizable interfaces. An example of such cases is self-assembled monolayer and bilayer lipid membranes [27, 69]. Furthermore, phospholipid bilayer capacitance is one of the main parameters, which may vary upon interaction with proteins/peptides.

Therefore, in this work mainly complex capacitance plots were used to study self-assembled monolayer and artificial bilayer formation. For dielectric surfaces exhibiting ideally polarizable interfaces, the capacitance value can be estimated from the frequency at maximum peak of ImC [69, 94]. Ideally, the diameter of the semicircle is equal to the capacitance of the electrical double layer at the interface. Thus, in this study the values of complex capacitances were obtained by taking the radius of the semicircle in Cole-Cole plot and multiplying it by two.

2. MATERIALS AND METHODS

2.1 Preparation of the titanium and aluminum surfaces

Metallurgical titanium (25 × 55 mm, thickness 0.125 mm) (>99.0 %, Goodfellow GmbH) and metallurgical aluminum (25 × 55 mm, thickness 0.125 mm) (>99.0 %, Goodfellow GmbH) plates were polished with 200,000 grit diamond lapidary paste with 50 % the concentration of the diamond powder (size ≤ 0.1 μm) at the speed of 1000 rpm until a mirror-like surface finish was observed. Polished titanium and aluminum surfaces were cleaned using two different protocols. Polished titanium plate was cleaned by ultrasound in hexane (≥99 %, Reachem, Slovakia) or acetone (≥99,5 %, Sigma-Aldrich), (ii) in 2 % cleaning solution of MICRO®-90 (Sigma-Aldrich), (iii) in 2-propanol (≥99.5 %, Sigma-Aldrich) and (iv) in Milli-Q water (Milli Q-plus-Millipore system (USA)) for 10 min. Polished aluminum plate was cleaned by ultrasound for 10 minutes (i) in hexane (ii) in 2-propanol and 2 minutes in Milli-Q water. After cleaning, titanium and aluminum plates were dried under nitrogen stream.

2.2 Self-assembled monolayer formation

Freshly polished and cleaned aluminum and titanium surfaces were used for the formation of octadecyltrichlorosilane (OTS) (>90%, Sigma-Aldrich) self-assembled monolayer. Methyltrichlorosilane (MTS) (97%, Alfa-Aesar) was used for the formation of the mixed self-assembled monolayer on titanium surface. The silanization solution was prepared by heating 45 mL heptane to 60-65 °C and adding 0.1 % (v/v, 2.5 mM), 1 % (v/v, 25 mM) or 5 % (v/v, 125 mM) of OTS. The total concentration of OTS and MTS for mixed self-assembled monolayer formation on titanium plate was 0.1 % (v/v, 2.5 mM). Then, the titanium or aluminum plates were immersed into a silanization solution for 45 min. After that, the functionalized plates were rinsed in heptane and dried under nitrogen stream. Finally, silanized plates were heated at 100 °C for 1h in air environment to remove adsorbed water and solvent residues, unless indicated otherwise.

2.3 Phospholipid bilayer lipid membrane formation

Bilayer lipid membranes were formed by vesicle fusion method [95]. Vesicle solution was prepared from 1,2-diphytanoyl-sn-glycero-3-phosphocholine (DPhyPC), 1,2-dioleoyl-sn-glycero-3-phosphocholine (DOPC) (Avanti Polar Lipids, Inc., USA) or a mixture of (DOPC) and cholesterol (Chol) (Avanti Polar Lipids, Inc., USA). Vesicle solution of 1.5 mM was used in all experiments. The lipids were dissolved in chloroform (99 %, Sigma-Aldrich) to a concentration of 10 mM. In order to prepare 1.5 mM vesicle solution, a desired amount of lipid-chloroform solution was transferred to a separate vial and evaporated under a nitrogen stream until formation of a lipid film on the bottom of the vial. The lipid film was re-suspended in a phosphate buffer solution (PBS, 0.1 M NaCl (Reachem Slovakia p. a.), 0.01 M NaH_2PO_4 (Reachem Slovakia, p. a.)), which pH was adjusted to 4.5 with NaOH (Reachem Slovakia p. a.). For phospholipid bilayer lipid formation on aluminum surface pH of PBS was adjusted to 7.1.

2.4 Regeneration of self-assembled monolayer

Regeneration of the self-assembled monolayer was carried as follows: (i) hybrid bilayer lipid membrane was formed on the functionalized metallurgical surfaces via vesicle fusion method, (ii) the electrochemical cell was washed with a copious amount of phosphate buffer (pH 7.1), (iii) the phosphate buffer solution was drained out of the cell, (iv) a solution consisting of 2-propanol and Milli-Q water (volume % ratio 50/50) was added into the cell with a pipette and re-suspended a few times to disintegrate the hybrid bilayer (the action was repeated for minimum of 3 times), (v) the cell was washed with a copious amount of phosphate buffer (pH 7.1) and thus completing the first regeneration of the self-assembled monolayer.

2.5 Electrochemical measurements

Measurements of electrochemical impedance spectroscopy (EIS) and cyclic voltammetry (CV) were carried out in phosphate buffer (pH adjusted to 7.1). A three-electrode conventional system configuration was used for measurements, where aluminum or titanium plate served as a working electrode, saturated silver-silver chloride ($Ag/AgCl/NaCl_{(sat.)}$) microelectrode

(M-401F, Bedford, USA) as a reference electrode and platinum (99.99 % purity, Aldrich) wire as an auxiliary electrode, which was coiled around the barrel of the reference electrode. CV measurements were carried out at a scan rate of 10 mVs^{-1} and a scan step at 1 mV using the μAutolab (Utrecht, the Netherlands). EIS was measured using μAutolab (unless indicated otherwise) (Utrecht, the Netherlands) in a frequency range from 0.1 Hz to 50 kHz or using fast Fourier transform (FFT) electrochemical impedance spectrometer EIS-128/16 (University of Kiel, Germany)[96], in a frequency range between 0.7 Hz and 50 kHz (unless indicated otherwise). Additional platinum wire electrode (connected to the 1 μF capacitor) was used as a quasi-reference electrode to reduce the impedance of the reference electrode at the higher frequencies for FFT-EIS measurements. The obtained data was normalized to the geometric surface area of 0.32 cm^2 of the working electrode. At least 2 and up to 20 experiments were carried out for determining standard deviations.

2.6 Attenuated total reflection Fourier transform infrared spectroscopy

Fourier-transform infrared (FTIR) spectra of aluminum functionalized with OTS self-assembled monolayer were registered using the spectrometer Bruker Alpha (Germany) equipped with a diamond attenuated total reflection (ATR) detector. The spectra were acquired in the wavenumbers range from 4000 cm^{-1} to 400 cm^{-1} at 4 cm^{-1} resolution from 100 scans. The spectrum of the aluminum was used as a reference and all experiments were carried out at ambient conditions.

2.7 Contact angle measurements

The contact angle was measured with Theta Lite Optical Tensiometer from Biolin Scientific (Finland) company by placing 6-8 droplets of 10 μL Milli-Q water. The contact angle measurements were performed immediately after the aluminum or titanium plates were cleaned or silanized. Standard deviations were obtained from minimum of 5 different samples.

3. RESULTS AND DISCUSSION

3.1 Hybrid bilayer membrane formation on metallurgical titanium surface

3.1.1 Properties of titanium plate electrode cleaned by different solvents

The first step for assembling hybrid bilayers is preparation of a substrate. The substrate preparation is an essential step for formation of the artificial membranes. In this section commercially produced metallurgical titanium plate surface was used. Firstly, titanium surface was cleaned and polished to mirror-like appearance. The polished surface exhibited hydrophilicity, which is needed for functionalization of octadecyltrichlorosilane. After the silanization, the surface became hydrophobic as determined by the contact angle measurements. Polished Ti surface was rather hydrophilic exhibiting contact angles of approx. 50° ± 5° (Fig. 9, A). The value is comparable to a value reported earlier for a magnetron sputtered thin-film Ti electrode [33]. However, these contact angles are higher than those obtained for gold [28] or cadmium stannate [32] substrates. To obtain more hydrophilic Ti surfaces the effect of the cleaning solvent was investigated. Figure 9, A shows that replacing hexane with acetone consistently causes lower contact angle values. Different contact angles may reflect different chemical compositions of the oxide covered surfaces. For example, according to Eslamibidgoli et al. [97] the surfaces of NiOOH and $Ni(OH)_2$ have different wettability parameters. Water interacts weakly with $Ni(OH)_2$ due to weak dipole moment of the surface. The surface of NiOOH has strong interaction with water because of its high dipole moment, moreover, unsaturated O atoms forms hydrogen bonds with water which leads to a stronger interaction with water molecules. The origin of this effect remains elusive, though surface density of the hydroxyl groups can be a primary reason for this effect based on consistently higher contact angle values on hexane cleaned titanium surface.

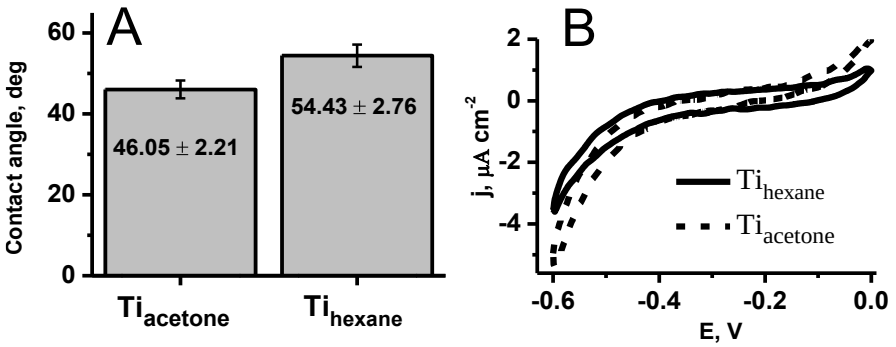

Figure 9. Properties of Ti surface cleaned by using different solvents detected A – by measuring contact angles; B – by recording cyclic voltammograms in phosphate buffer solution pH 7.1.

Ti electrodes treated using different cleaning solutions were analyzed by the cyclic voltammetry. Fig. 9, B compares cyclic voltammetry traces from Ti electrodes cleaned with acetone ($Ti_{acetone}$) and Ti electrodes cleaned with hexane (Ti_{hexane}). $Ti_{acetone}$ electrode showed ideally polarizable interval (Fig. 9, B, dashed line) of potentials from -0.4 V to -0.2 V displayed in the cathodic range of CV (vs $Ag/AgCl/NaCl_{(sat.)}$). For Ti_{hexane} surface the ideally polarizable interval of potentials slightly extended to the anodic direction up to -0.05 V (Fig. 9, B, solid line) indicating wider potential range relevant for further experiments of EIS.

Fig. 10 displays electrochemical impedance spectra obtained on Ti_{hexane} and $Ti_{acetone}$ electrodes plotted in the complex capacitance format [94]. Independently on the used electrode, the obtained complex capacitance plots exhibited semi-circular shape similar to ones observed earlier for sputtered Ti thin-film electrodes [33]. Such a shape is typical for ideally polarizable interfaces exhibiting near ideal capacitive behavior [98]. The complex capacitances values of the $Ti_{acetone}$ and Ti_{hexane} electrodes were found to be 23.78 ± 4.50 μF cm^{-2} and 29.18 ± 4.24 μF cm^{-2}, respectively. Slightly higher complex capacitances values were observed for Ti_{hexane}. This may attest for the thinner dielectric oxide layer on Ti_{hexane} interface, which though exhibits slightly less polar environment as deduced from the contact angle data in Fig. 9, A.

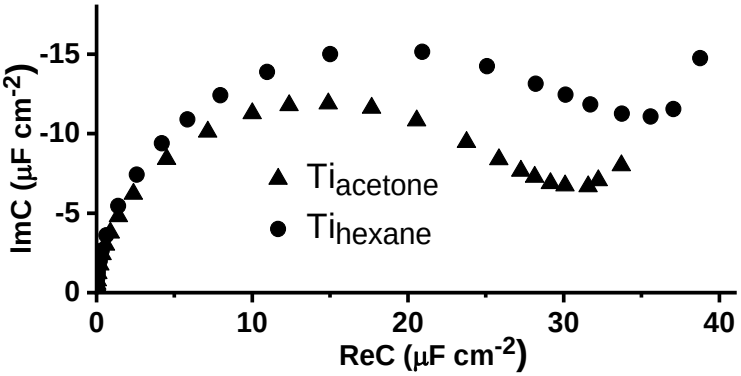

Figure 10. FFT electrochemical impedance spectra (Cole-Cole plots) of titanium electrode cleaned with different solvents obtained at potential of -0.3 V vs Ag/AgCl/$NaCl_{(sat.)}$ in phosphate buffer solution pH 7.1.

3.1.2 Influence of cleaning solvent of Ti substrate and effect of heating on the properties of SAM

Preparation of Ti plate electrodes by using different cleaning solutions allowed obtaining slight differences in their surface properties. Firstly, higher hydrophilicity was obtained for $Ti_{acetone}$ electrode (Fig. 9, A). This feature is an important reason for choosing this type of the electrode for further modification with OTS SAM. Secondly, by testing the electrodes with EIS (Fig. 10) it was found that surface of $Ti_{acetone}$ electrode exhibits higher homogeneity properties comparing to Ti_{hexane} electrode, i) because of its smaller value of complex capacitance and ii) because of its more completed semicircle obtained in Cole-Cole plot (Fig. 10). However, cyclic voltammogram of $Ti_{acetone}$ electrode (Fig. 9, B) showed narrower ideally polarizable interval of potentials than Ti_{hexane} electrode. These were the reasons to continue experiments by using both types of Ti electrodes.

Table 1 summarizes CA data obtained in the course of silanization of $Ti_{acetone}$ and Ti_{hexane} electrodes by using different concentrations of OTS. As expected, a clear increase of CA's was observed for the both types of electrodes after the silanization. An increase of CA's was dependent on OTS concentration reaching maximal contact angle values of 98.82° ± 1.86° upon silanization in 5% OTS solution for $Ti_{acetone}$ electrode, and value of 101.84° ± 1.53° for Ti_{hexane} electrode in 1% OTS solution. In all the cases the values of the CA exceeded threshold of 90°, indicated earlier as a threshold at which compact lipid overlayers can be formed [7].

Table 1. Comparison of contact angles of the $Ti_{acetone}$ and Ti_{hexane} electrodes, unheated and heated after the silanization in OTS solution of different concentrations.

Cleaning solvent of Ti surface	Concentration of OTS, %	Contact angles, degrees (without heating)	Contact angles, degrees (after heating at 100 °C for 1 hour)
Acetone	0.1	95.31 ± 1.81	95.84 ± 1.86
	1	98.01 ± 1.86	101.90 ± 1.94
	5	98.82 ± 1.86	101.45 ± 2.27
Hexane	0.1	99.87 ± 0.98	102.27 ± 1.76
	1	101.84 ± 1.53	100.24 ± 1.92
	5	96.27 ± 1.47	103.81 ± 5.60

The next series of experiments were carried out by applying heating of silanized Ti surfaces at 100 °C for 1 hour in order to remove impurities of water molecules expecting to obtain more uniform and stable monolayer [99]. CA values increased slightly (Table 1) in all the cases exceeding 100° except for $Ti_{acetone}$ electrode silanized in 0.1 % OTS solution (95.84° ± 1.86°). Also, the positive effect of the heating was observed analyzing cyclic voltammetry curves (Fig. 11). The wider ideally polarizable interval of potentials was obtained in the anodic range of CV (vs Ag/AgCl, $NaCl_{(sat.)}$ electrode) for the silanized and heated Ti_{hexane} electrode comparing to that obtained for the silanized and unheated Ti_{hexane} electrode.

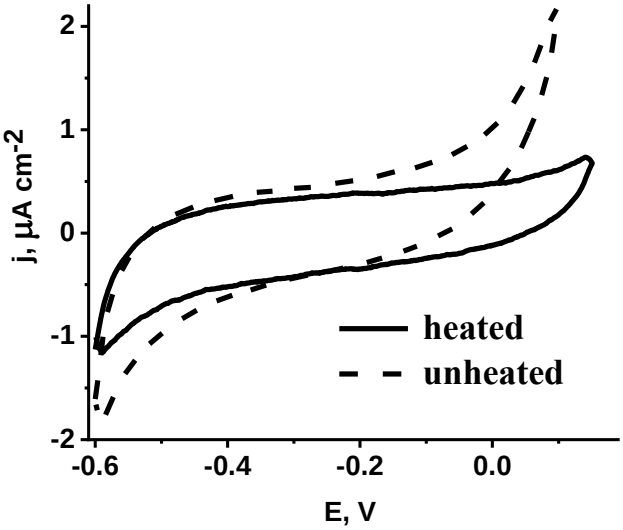

Figure 11. Cyclic voltammograms of unheated (dashed line) and heated at 100 °C for 1 hour (solid line) Ti_{hexane} electrode after the silanization in 0.1% OTS solution.

3.1.3 Electrochemical impedance spectroscopy and evaluation of complex capacitances

Formation of OTS monolayer was monitored by the EIS. For both acetone and hexane incubated electrodes the decrease of the electrode capacitance was observed. Comparison of the complex capacitances of $Ti_{acetone}$ and Ti_{hexane} electrodes before and after silanization with following heating at 100 °C for 1 hour is presented in Figure 12. The lowest values of capacitance with the smallest parameter scatter (Fig. 12, grey columns) were observed when 0.1 % OTS concentration solution was used during silanization procedure. Increase in OTS concentration to 5 % results in much higher value of complex capacitances. These features attest for the formation of a more defective and possibly inhomogeneous OTS monolayer. It is interesting to note that the differential capacitances of both $Ti_{acetone}$ and Ti_{hexane} electrodes always decrease upon silanization, however, lower values were consistently observed for Ti_{hexane} electrodes silanized in 0.1 % OTS solution (1.02 ± 0.17 μF cm^{-2}) and in 1 % OTS solution (1.08 ± 0.22 μF cm^{-2}). Higher values of complex capacitances were obtained for the $Ti_{acetone}$ electrode (from 1.26 ± 0.16 μF cm^{-2} to 1.96 ± 0.38 μF cm^{-2}), indicating hexane to be a more efficient as a cleaning solvent for Ti surface than acetone. This finding is consistent with contact

angle measurements showing lower CA values in case of $Ti_{acetone}$ electrodes (Fig. 9, A) suggesting higher hydrophilicity of $Ti_{acetone}$ surfaces, and relatively higher hydrophobicity of Ti_{hexane}. These observations possibly confirm the assumption that Ti_{hexane} may have higher density of the surface hydroxyl groups than $Ti_{acetone}$. Since hydroxyl groups are essential for forming silane bonds, Ti_{hexane} exhibited consistently denser OTS monolayers as deducted from the capacitance of OTS modified Ti_{hexane} electrode. The obtained values of complex capacitance are very comparable to the thiolate self-assembled monolayers on gold [28, 100], and indicates the formation of a relatively compact and reproducible anchor monolayer of OTS on Ti_{hexane} surface.

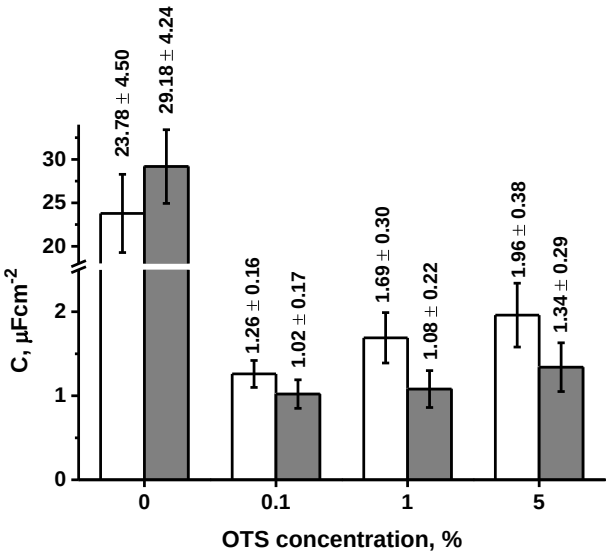

Figure 12. Differential capacitances of Ti_{hexane} (grey columns) and $Ti_{acetone}$ (white columns) electrodes, silanized using various OTS concentrations.

3.1.4 Calculation of the OTS monolayer thickness

EIS data obtained for silanized Ti electrode (Fig. 12) gave possibility to estimate the thickness value of the OTS layer, taking into account that capacitance of the SAM modeled as a parallel plate capacitor can be easily calculated using the following equation:

$$C = (\varepsilon\varepsilon_0)/d \qquad (9)$$

In this case the thickness of OTS SAM, d (cm), can be calculated by using ε – dielectric permittivity of OTS monolayer (2.3), ε_0 – vacuum permittivity (8.85×10^{-14} F cm^{-1}) and C – complex capacitance of silanized Ti electrode, $C_{Ti/OTS}$ (F cm^{-2}), which can be expressed as a sum of two terms:

$$C_{Ti/OTS}^{-1} = C_{Ti}^{-1} + C_{OTS}^{-1} \quad (10)$$

where C_{Ti} – complex capacitance of Ti plate electrode before silanization, C_{OTS} – complex capacitance of OTS monolayer.

The capacitance of OTS film (C_{OTS}) for the Ti_{hexane} electrode silanized in 0.1 % OTS solution was calculated to be equal to 1.05 μF cm^{-2} according to equation (10) by using the experimental data in Fig. 10 (C_{Ti} = 29.18 μF cm^{-2}) and Fig. 12 ($C_{Ti/OTS}$ = 1.02 μF cm^{-2}). By inserting the obtained C_{OTS} value into eq. (9), the thickness of OTS film was estimated to be 1.94 nm. For Ti_{hexane} electrode silanized in 1 % OTS solution, the thickness does not change significantly and was calculated to be equal to 1.69 nm. These values of thickness are comparable to those obtained for OTS monolayer on thin-film Ti electrode when measured with spectroscopic ellipsometry and calculated theoretically, which were found to be approximately 2.0 – 2.3 nm [33]. In this case, it conclude that nearly 90 % of the surface of Ti_{hexane} electrode silanized in 0.1 % or in 1 % OTS solution is covered by compact OTS monolayer.

Summarizing, CA data (Fig. 9, A) together with the electrochemical experiments using CV and EIS methods (Fig. 11, 12) indicate that formation of a compact hydrophobic OTS monolayer occurs on Ti_{hexane} surface which can be further used for phospholipid hybrid bilayer formation.

3.1.5 Formation of hybrid bilayer

The formation of the hybrid bilayer was tested with EIS. The effect on capacitance decrease of OTS functionalized Ti_{hexane} electrode triggered by the interaction with DOPC:Chol (molar % ratio 6:4) vesicles are shown in Cole-Cole plot (Fig. 13). It was found out that 20 minutes of incubation time was needed for approaching the lowest value of capacitance (0.61 ± 0.06 μFcm^{-2}). This value of a capacitance is very close to those observed for hybrid bilayer on silanized thin-film Ti electrode [33] and on thiolipid molecular anchors [101]. Consequently, these results show that silanized Ti surface is completely covered by phospholipid film.

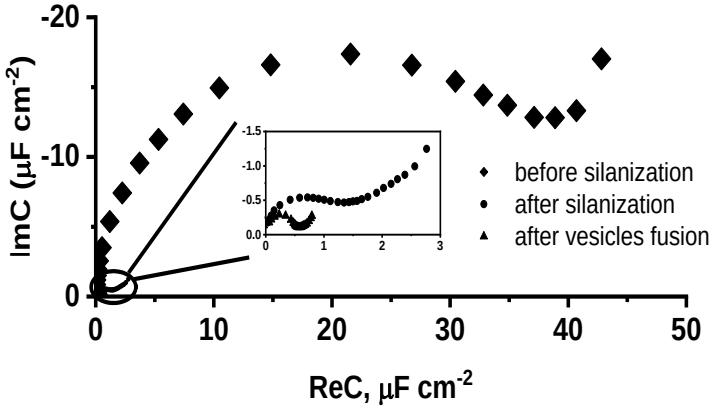

Figure 13. FFT electrochemical impedance spectra of Ti_{hexane} electrode: diamonds – neat Ti_{hexane} electrode; circles – after silanization in 0.1 % OTS solution with following heating; triangles – after 20 min of DOPC (60 %)/Cholesterol (40 %) vesicles fusion. Electrode potential: 0 V vs Ag/AgCl/ $NaCl_{(sat.)}$.

Capacitance of the hybrid bilayer, C_{HB}, which can be considered as a composite of OTS and DOPC-Chol layer, can be evaluated using the following equation:

$$C_{hBLM}^{-1} = C_{Ti}^{-1} + C_{HB}^{-1} \quad (11)$$

in which C_{hBLM} = 0.61 μF cm^{-2} (from EIS data in Fig. 13). By using the calculated value of C_{HB} = 0.62 μF cm^{-2} and assuming that the average relative dielectric constant as 2.5, the thickness of a composite of OTS and DOPC-Chol layer was calculated to be equal to 3.57 nm. This value is similar for covered by DOPC-Chol bilayer tethered on gold surface [102]. The obtained quantitative data of DOPC-Chol layer similar with those proposed previously by other author [103-104], enable us to conclude that hybrid bilayer on OTS anchors can be formed on metallurgical Ti substrate.

3.1.6 Hybrid bilayer regeneration

In order to determine the reusability of the OTS SAM for hybrid bilayer formation, the EIS data were collected by repeating the processes of vesicle fusion and monitoring changes of electrochemical impedance spectra. In the first cycle of measurements, OTS monolayer was formed and EIS was

measured (Fig. 14, filled circles), then DOPC:Chol (molar % ratio 6:4) membrane was formed and EIS was measured again (Fig. 14, open circles). Afterward, the membrane was flushed with isopropanol/water mixture (50:50 %) and the second cycle of measurements was carried out by measuring EIS of residual OTS monolayer (Fig. 14, filled circles) and of bilayer (Fig. 14, filled triangles) formed on it. It is seen from EIS data in Fig. 14 that despite some loss of OTS monolayer after every cycle, as many as 3 cycles were achieved with almost identical capacitance value of silanized Ti_{hexane} electrode. Only on the 4th cycle a slight increase in capacitance was observed. Schematic representation of the designed system is represented in Fig. 15.

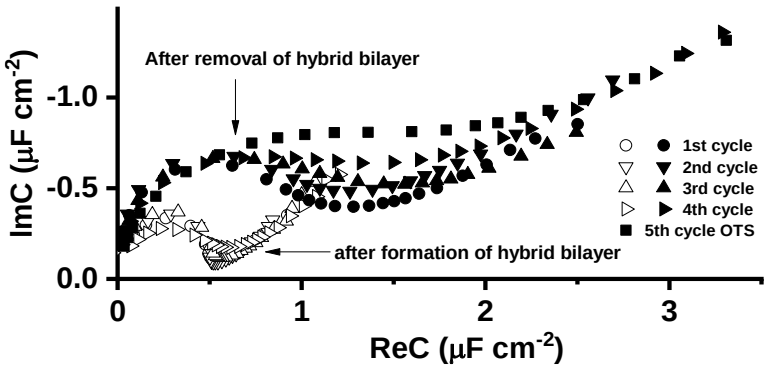

Figure 14. FFT electrochemical impedance spectra of hybrid bilayer regeneration recorded over 4 cycles of vesicle fusion. Electrode potential: 0 V vs $Ag/AgCl/NaCl_{(sat.)}$.

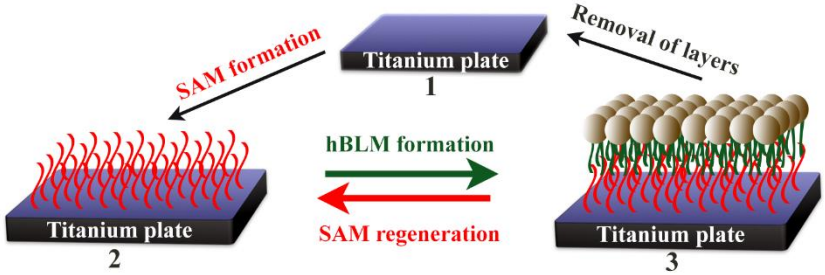

Figure 15. Schematic representation of the metallurgical Ti plate electrode developed for multicycle SAM formation and hBLM regeneration.

3.1.7 Hybrid bilayer interaction with phospholipase A_2

To assess possible utility of the hybrid bilayers as phospholipid biosensor an interaction between the DOPC-Chol (6:4) hybrid bilayer formed and phospholipase A_2 (PLA2) was followed by EIS in real-time. PLA2 is a superfamily of enzymes, which hydrolyzes the fatty acids from *sn2* position of membrane phospholipids, releasing fatty acids and lysophospholipids in the process [105]. Cole-Cole plots in Fig. 16 clearly attests for the capacitance increase with time after the aliquot of the PLA2 was injected into the solution. A significant increase of capacitance from 0.58 μF cm^{-2} to 0.94 μF cm^{-2} was observed within the first minute of injection of 500 nM PLA2 (Fig. 16, A, filled triangles up). Further increase in capacitance approaching 1.12 μF cm^{-2} was observed within next 25 min of interaction. It is worth mentioning that the increase of incubation time results in an evolution of the complex capacitance curve towards the curve of an anchor monolayer on Ti (Fig. 16, A, compare open triangles and filled circles).

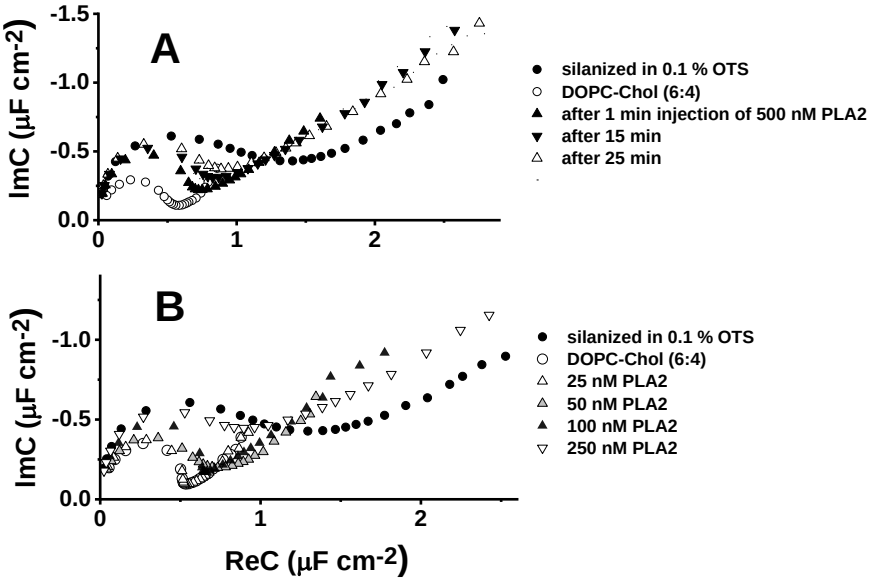

Figure 16. FFT electrochemical impedance spectra of Ti_{hexane} electrode: filled circles – silanized in 0.1 % OTS solution; open circles - neat DOPC(60%)/cholesterol(40%) bilayer; triangles – after the insertion of PLA2. A – time dependent Cole-Cole spectra (PLA2 concentration 500 nM); B – PLA2 concentration dependent Cole-Cole spectra (incubation time 30 min). Electrode potential: 0 V vs $Ag/AgCl/NaCl_{(sat.)}$.

Increase of an incubation time and concentration of PLA2 exhibits similar effects. Fig 16, B demonstrates the effect of PLA2 concentration (25-250 nM range) on evolution of the complex capacitance plots at fixed incubation time, 30 min. At 25 nM PLA2 barely visible effects on the capacitance curve (Fig. 16, B, open triangles up) were observed after 30 min. However, the capacitance noticeably increased after the injection of 50 nM PLA2 (Fig. 16, grey triangles) and 30 min of incubation. Increasing concentration of PLA2 up to 250 nM triggers a major transformation of the capacitance curve (Fig. 16, B, open triangles down) with the resulting complex capacitance values exceeding 1.12 μF cm^{-2}. Further increase in concentration of PLA2 triggers only marginal changes indicating saturation of the effect. Such behavior can be expected because disruption of the hybrid bilayer by the PLA2 results in Ti surface functionalized by the silane monolayer, which is resistant to PLA2.

The sensitivity of the hybrid bilayer to PLA2 can be utilized to construct biosensors sensitive to the enzyme concentration and/or its activity. For this purpose one can choose a singly frequency ac measurement methodology as suggested in ref. [106]. Figure 17 displays the variation of the parameter Y/ω (Y is the admittance of the electrode, and ω is the cyclic frequency) with concentration of the PLA2 at constant time of incubation 30 min. As seen in Fig 17, A the dependence resembles nearly logarithmic shape of the Y/ω function with respect its argument, C_{PLA2}. Indeed, representation of the same data set in semi-logarithmic coordinates returns nearly perfect linear dependence of Y/ω vs log C_{PLA2}. Such dependence can be used for the bioanalytical purposes to assess concentration of the membrane damaging agent, in this case PLA2 or its activity.

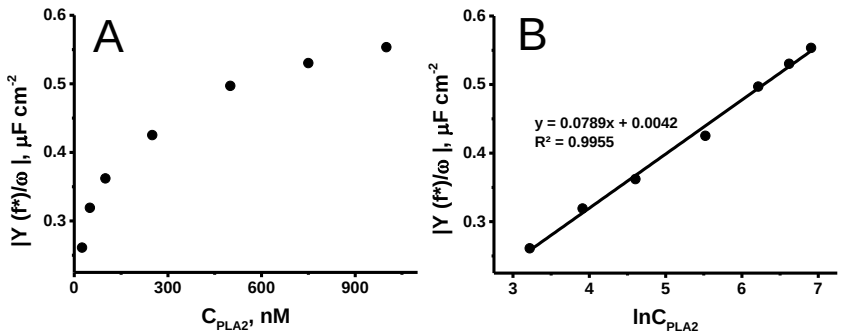

Figure 17. A – dependence of the admittance on the PLA_2 concentration obtained at the specific frequency (f* = 213 Hz); B – the same data on logarithmic x scale. PLA_2 incubation time – 30 min.

3.2 Mixed hybrid bilayer formation on metallurgical titanium surface

In this chapter mixed hybrid bilayer lipid membrane (mhBLM), which resembles the structure of tBLM`s was investigated. mhBLM was formed by forming mixed self-assembled monolayer of MTS and OTS at different molar ratio. The dilution effect of the MTS in a mixed self-assembled monolayer was studied, which should presumably form some polar reservoir between the bilayer and the substrate, needed for integral protein incorporation, relevant biological fluidity, and long-term stability.

3.2.1 Formation of mixed silane self-assembled monolayer

To investigate the hydrophobic properties of a monolayer formation, surface wetting characteristics – contact angles of the water droplets were measured. CA values of titanium surface and functionalized titanium surfaces prepared using silanization solutions of various molar ratios of OTS:MTS are displayed in Fig. 18. Freshly polished and cleaned titanium surface demonstrated hydrophilic properties reaching CA value of 54° ± 3° (Fig. 9, A), while CA increases to 102° ± 2° after the silanization of Ti surface in 2.5 mM (0.1 %) OTS solution (Table 1). A spacer of short alkyl chain MTS molecules and anchoring unit of long alkyl chain OTS molecules were introduced into silanization solution in order to functionalize the Ti surface with mixed self-assembled monolayer. It was determined that the contact angles of titanium surfaces functionalized with mixed OTS:MTS self-assembled monolayers exceeded a threshold of 90°, which is needed for lipid overlayer formation [63]. However, increasing MTS molar ratio causes lower hydrophobicity of the functionalized Ti surface. Similar trend of CA evolution was observed on gold electrodes, using mixture of a short alkyl chain and long alkyl chain thiols [28]. Notably, titanium surface silanized in 100% MTS solution exhibited lowest CA value of 78° ± 3° and did not produce the sufficient hydrophobicity of the SAM suitable for the formation of compact phospholipid overlayer.

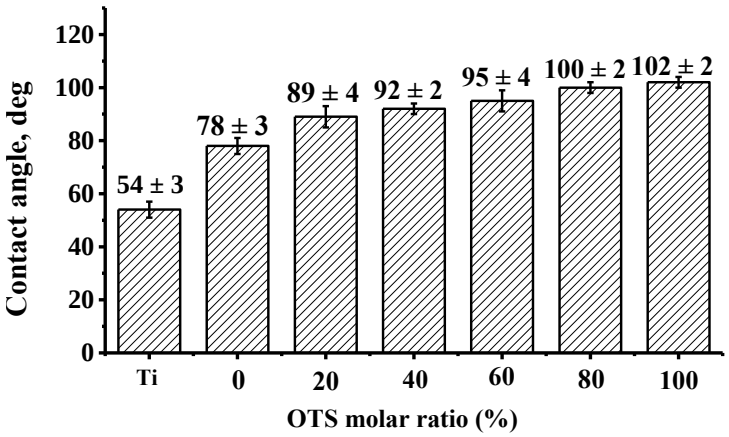

Figure 18. Contact angles of Ti surface before silanization and after silanization using various molar ratios of OTS:MTS. Standard errors were obtained from 6 different samples.

3.2.2 Mixed hybrid bilayer lipid membrane formation

While the CA measurements indicate the surface wetting characteristics, the electrochemical impedance spectroscopy can be applied for investigations of dielectric properties of the functionalized surfaces [28, 69]. Fig. 19 (filled circles) displays EI spectra in Cole – Cole plot of the Ti surfaces after functionalization with SAMs prepared from silanization solutions containing various OTS:MTS molar ratios as well as after formation (open circles) of DOPC:Chol (molar % ratio 6:4) bilayer lipid membrane by vesicle fusion method. The obtained complex capacitance plots exhibited semi-circular shapes which are typical for ideally polarizable interphases showing near ideal capacitive behavior.

Previously, the complex capacitance value of 29 ± 4 μF cm^{-2} was observed for Ti electrode cleaned in hexane (Fig. 10). As expected, functionalization of titanium surface using silanization solutions of various molar ratios of OTS:MTS (Fig. 15, filled circles) causes significant decrease of complex capacitances suggesting formation of dielectric layer on the Ti surface. In particular, the values of complex capacitances decrease considerably from 29 ± 4 μF cm^{-2} (before silanization) to 6.17 ± 1.44 μF cm^{-2} (Fig. 19, A, filled circles) after silanization in the solution consisting only of short alkyl chain MTS molecules. Addition of anchoring units of long alkyl chain OTS molecules into silanization solution positively affects functionalization of Ti

surface, as suggested by the observed gradual decrease of complex capacitances dependently on OTS:MTS molar ratio in silanization solution. Increasing OTS molar ratio in the OTS:MTS silanization solution enables to obtain lower complex capacitance values (Fig. 19, B-E, filled circles), and the lowest value of 1.02 ± 0.17 μF cm^{-2} was observed when Ti surface was silanized in the solution consisting only of long alkyl chain OTS molecules (Fig. 19, F, filled circles). Gradual variation of the complex capacitance values suggests that modification of Ti surface in OTS:MTS silanization solutions leads to the formation of dielectric layers of mixed silane SAMs and the average thickness of the obtained SAMs is dependent on OTS:MTS molar ratio in silanization solution, since capacitance is inversely proportional to the thickness of the dielectric layer on the surface [107]. Similar trends of the complex capacitance dependence on the fraction of molecular anchor were observed on gold surface, modified with thiols mixed self-assembled monolayers [28]. The experimental results in Fig. 16 correlate well with CA data (Fig. 18), which showed that continuously increasing OTS molar ratio in OTS:MTS silanization solution respectively causes higher CA values of silanized Ti surface. In summary, it was concluded that silane-based mixed self-assembled monolayers can be formed on the titanium surface by modifying it in silanization solutions of various molar ratios of OTS:MTS. Furthermore, the obtained EIS and CA data suggest that addition of 20% or 40% of MTS into OTS:MTS silanization solution enables to obtain SAMs which can be tested further for mixed hybrid bilayer lipid membrane formation, since both the values of complex capacitances and contact angles reached the threshold needed for lipid overlayer formation [63].

Therefore, the next series of experiments were carried out in order to form mhBLM of DOPC:Chol (molar % ratio 6:4) by vesicle fusion method using Ti surfaces silanized with SAMs obtained from various molar ratios OTS:MTS silanization solutions. The ability of mixed silane SAMs to immobilize bilayer lipid membrane was monitored by EIS method, which enables to indicate a continuous dielectric sheet of a phospholipid [6] covering the surface, if a significant complex capacitance decrease is observed. EIS data in Fig. 19, A indicates that formation of bilayer lipid membrane on MTS self-assembled monolayer was not successful because only negligible decrease in complex capacitance was observed after vesicle fusion. This result can be explained by taking into consideration the CA values of titanium surface silanized in 100% MTS solution (Fig. 18) which did not exceed the threshold of 90° needed for successful lipid overlayer formation. Hydrophobic properties of the SAM are dependent on the alkyl chain length of molecule

used, because longer alkyl chain molecules are more hydrophobic than shorter alkyl chain molecules [63]. This is due to the density of the non-polar molecules on the surface. The short alkyl chain molecules such as MTS (CH_3SiCl_3) did not exhibit surface with enough hydrophobicity needed for vesicle fusion to produce intact hBLM.

Meanwhile, the EIS data indicate the formation of additional phospholipid layers after DOPC:Chol (molar % ratio 6:4) vesicle fusion on mixed SAMs formed from different silanization solutions (Fig. 19, B-E). This is evident from the decrease of complex capacitance upon exposure of substrates to phospholipid vesicles. However, the EIS response did not displayed complete semi-circular shape after formation of mixed hybrid bilayer lipid membranes on a mixed SAMs prepared from OTS:MTS silanization solution of 2:8 and 4:6 molar ratios (Fig. 19, B, C, open circles) indicating high defectiveness of phospholipid membrane [69]. Formation of mhBLMs on SAMs prepared from OTS:MTS silanization solutions of 6:4 and 8:2 molar ratios (Fig. 19, D and E, open circles) enabled to obtain EIS spectra exhibiting almost complete semi-circular shapes with complex capacitance values of 0.86 ± 0.22 μF cm^{-2} and 0.83 ± 0.18 μF cm^{-2}, respectively, suggesting that the surface coverage of dielectric phospholipid sheet is approximately similar to hybrid bilayer lipid membrane formed on OTS monolayer (Fig. 19, F, open circles) exhibiting slightly lower complex capacitance value of 0.6 ± 0.1 μF cm^{-2}.

All in all, complex capacitance values of mhBLMs (Fig. 19, D, E and F, open circles) on Ti are comparable to the complex capacitances values of tethered bilayer lipid membrane formed on gold surface ($C_{tBLM} = 0.8$ μFcm^{-2}), which was modified with thiols mixed self-assembled monolayers [28], suggesting that silanes mixed SAMs are suitable for mhBLM formation on Ti surface.

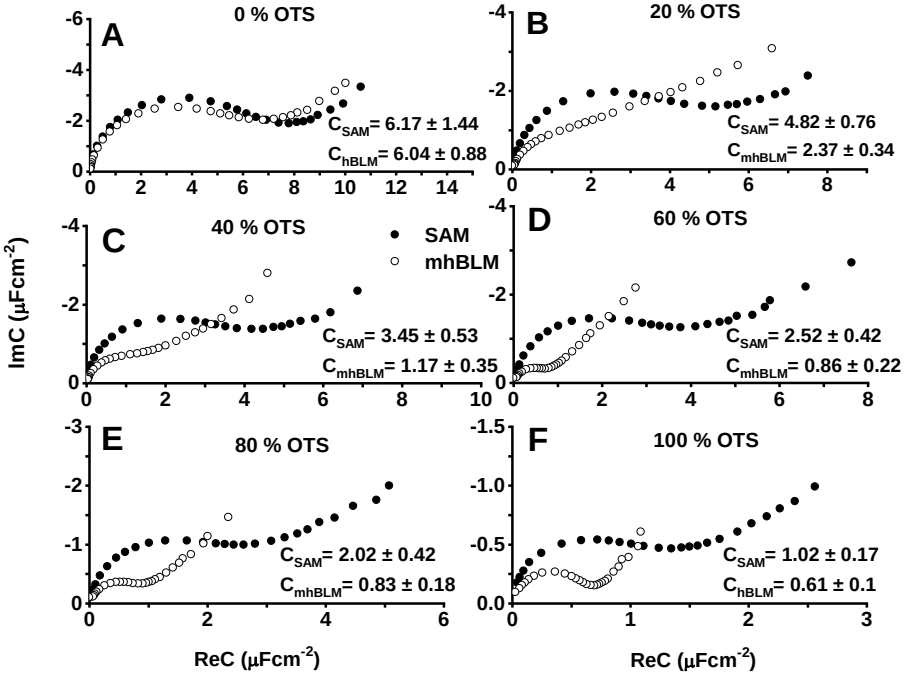

Figure 19. Cole – Cole plots of FFT electrochemical impedance spectra obtained at 0 V potential vs Ag/AgCl/$NaCl_{(sat.)}$ using Ti electrodes after functionalization with SAMs (filled circles) prepared from silanization solutions of various molar ratios of OTS:MTS: A – 0:10, B – 2:8, C – 4:6, D – 6:4, E – 8:2, F – 10:0 and after mixed hybrid bilayer lipid membrane (mhBLM) formation completed with DOPC/Chol (molar ratio 6:4) after 60 min of vesicle fusion (open circles). Values of the complex capacitances after SAM and mhBLM formation in μF cm^{-2} are displayed as well.

3.2.3 Calculation of the surface coverage of mixed hybrid bilayer lipid membrane

The surface coverage of the can be calculated by:

$$\theta = \frac{(C_{SAM} - C_{exp})}{(C_{SAM} - C_{BM})} \qquad (12)$$

where C_{exp} – a capacitance of the mixed hybrid bilayer lipid membrane measured experimentally (the values correspond to C_{mhBLM} in Fig. 19, B, C, D, E), C_{SAM} – a capacitance value of MTS monolayer, 6.17 μF cm^{-2} (Fig. 19, A) and C_{BM} is the specific capacitance of the hybrid bilayer covered patches of the surface, which can be estimated as:

$$C_{BM} = [C_{TiO_2}^{-1} + C_{theor}^{-1}]^{-1} \quad (13)$$

where C_{TiO_2}– the capacitance of the TiO_2, 29 μF cm^{-2} and C_{theor} – theoretical capacitance of the mixed hybrid bilayer construct, which can be calculated using parallel plate capacitor equation eq. (9). The relative dielectric permittivity of the mixed hybrid bilayer, ε, was chosen as the midpoint value between all-DOPC tBLM, 2.8 [108] and the value of the all-C_{18} SAM, 2.3, so that ε for C_{theor} is 2.6. Surface thickness, d, corresponds the hydrophobic slab of bilayer, which according to the neutron reflectometry data is approximately 3.0×10^{-7} cm [28]. Using these parameters, one obtains C_{theor} = 0.77 μF cm^{-2}. Thus, surface coverage of mixed hybrid bilayer lipid membranes on the mixed SAMs were calculated (Table 2) using eq. (12), by taking the values obtained from eq. (13) and (9).

Table 2. The surface coverage of mixed hybrid bilayer lipid membrane on the mixed SAM calculated by eq. (12).

OTS molar % ratio in the silanization solution	θ, surface coverage of mhBLM
20	0.70
40	0.92
60	0.97
80	0.98

To summarize, the surface coverage of mhBLMs based on the EIS data was estimated. Mixed hybrid bilayer lipid membranes formed on SAMs prepared from OTS:MTS silanization solutions of 6:4 and 8:2 molar ratios (Fig. 19, D and E, open circles) displayed surface coverage by lipid 0.97 and 0.98 (Table 2), respectively, indicating that the functionalized titanium surface is almost fully covered with the mixed hybrid bilayer lipid membrane.

3.2.4 Mixed hybrid bilayer lipid membrane regeneration

To test reusability of mixed self-assembled monolayer for the formation of the mhBLM, regeneration experiments were carried out by forming and removing mixed hybrid bilayer lipid membrane multiple times. Firstly, mixed self-assembled monolayer on the Ti was prepared from OTS:MTS silanization solution of 6:4 molar ratio. The molar ratio of 6:4 in OTS:MTS silanization solution was chosen, expecting that the mixed self-assembled monolayer has more spacer units and should exhibit better mhBLM fluidity than mixed SAMs with higher amount of anchoring units. After formation of mixed SAM, bilayer lipid membrane was immobilized via vesicle fusion method and flushed with isopropanol/Milli-Q water (50/50 volume % ratio) to remove the lipid layer. Then, procedure was repeated multiple times and EIS was registered each time after formation and removal of the mhBLM. The obtained EIS data are depicted in Fig. 20. It is observable that complex capacitance values of the mixed SAM increased slightly after mhBLM was removed for the first time. Possible explanation of this phenomenon may be related to an adsorption and retaining of water molecules by reused SAM. After the next five removals of mhBLMs, there were no significant changes in complex capacitance of the mixed SAM (Fig. 20, A). This result suggests that the Ti surface functionalized with the mixed self-assembled monolayer prepared from OTS:MTS silanization solution of 6:4 molar ratio can be used for multiple formations of mhBLMs. As expected, the complex capacitance values remained stable at 0.95 ± 0.03 μF cm^{-2} after multiple formations of the mixed hybrid bilayer lipid membrane (Fig. 20, B), suggesting that exposure to water does not inhibit the repetitive formation of bilayer lipid membrane. Also, these values are in the same range of 0.86 ± 0.22 μF cm^{-2} obtained for mhBLMs formed on 60% OTS SAM as depicted in Fig. 19, D.

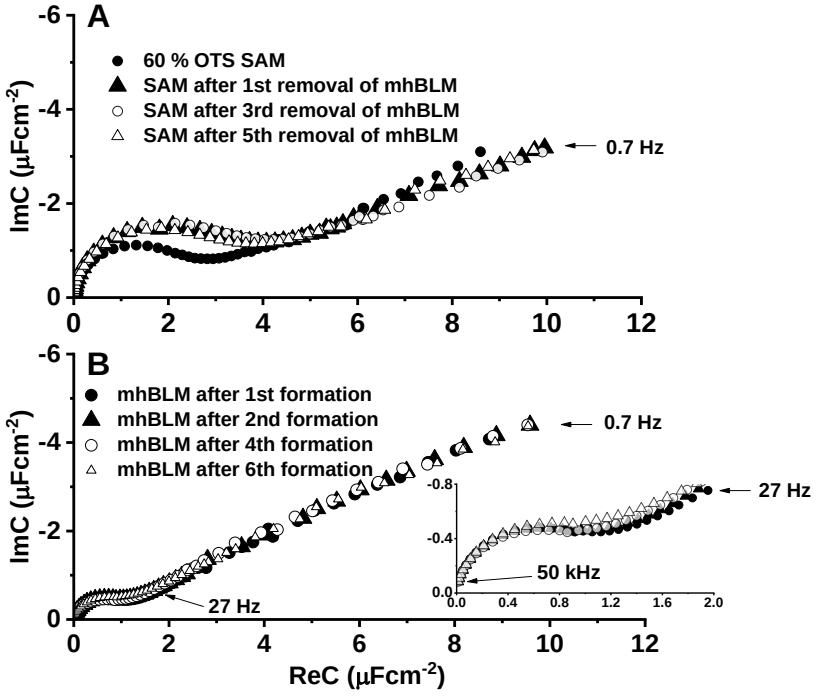

Figure 20. Cole – Cole plots of electrochemical impedance spectra recorded over several times of vesicle fusion and removal of the phospholipid layer; A – a mixed SAM (OTS:MTS molar ratio 6:4) after removals of bilayer lipid membrane; B – mixed hybrid bilayer lipid membrane formation (DOPC/Chol, molar ratio 6:4) after removing the previously formed mhBLM. Electrode potential: 0 V vs $Ag/AgCl/NaCl_{(sat.)}$.

3.2.5 Mixed hybrid bilayer lipid membrane interaction with pore forming toxins pneumolysin and α-hemolysin

To evaluate possible applicability of a mixed hybrid bilayer lipid membrane as a phospholipid biosensor platform, the bilayer lipid membrane containing DOPC:Chol (molar % ratio 6:4) was formed on anchor SAM prepared from OTS:MTS (molar ratio 6:4) silanization solution. The cholesterol containing mhBLMs were challenged with a cholesterol dependent cytolysin pneumolysin (PLY), which action on membrane occurs only in the presence of cholesterol [109-110].

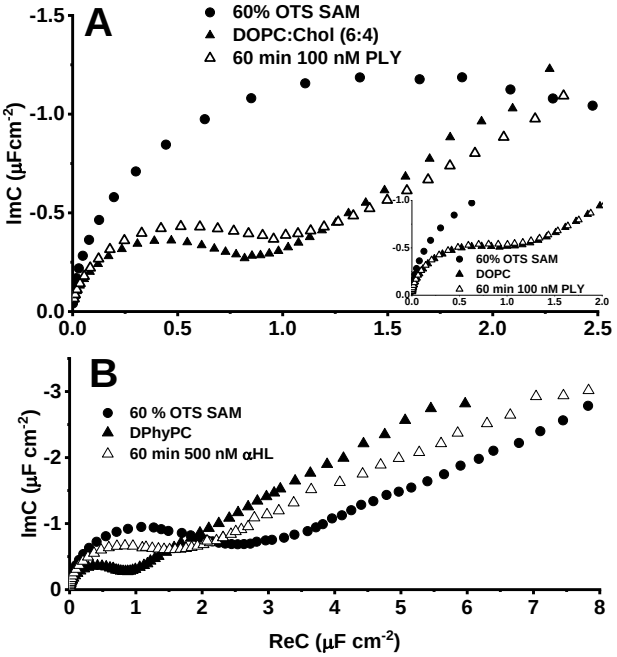

Figure 21. Cole – Cole plots of electrochemical impedance spectra obtained at 0 V potential vs Ag/AgCl/$NaCl_{(sat.)}$ using Ti electrode functionalized with SAM prepared from silanization solution containing OTS:MTS molar ratio of 6:4; A – mixed hybrid bilayer lipid membrane (DOPC:Chol (molar % ratio 6:4)) interaction with 100 nM pneumolysin (PLY), B - mixed hybrid bilayer lipid membrane (DPhyPC) interaction with 500 nM α-hemolysin (αHL). Inset – control experiment - mhBLM (DOPC) interaction with 100 nM of PLY.

The effect of PLY on mhBLMs is seen from the changes of the EIS curves in Fig. 21, A. The addition of 100 nM of PLY to a membrane bathing solution results in a minor increase of the complex capacitance from approximately 0.72 μF cm^{-2} to 0.86 μF cm^{-2}. The process is rather slow, as seen from relatively long time (60 min) necessary to observe the effect. Even though the change of complex capacitance of mhBLM upon exposure to PLY (Fig. 21, A) was quite modest (<0.14 μF cm^{-2}), the phase minimum of argZ = -60.1 deg at lg f_{min} = 0.22 slightly shifted up to argZ = -62.7 towards lower frequencies at lg f_{min} = 1.24 (Fig. 22, A) and resistivity of the mhBLM decreased consistently in the low frequency range (below 10 Hz) (Fig. 22, B). The calculated percentage values of resistivity change of the mhBLM reached 22.83% and 13% at 8 Hz and 0.1 Hz, respectively (Table 3) upon exposure of

mhBLM to PLY. These changes are not observed for cholesterol-free mhBLMs, (Fig. 21, A, inset): no complex capacitance change was observed for DOPC mhBLMs within 1 hour of exposure to 100 nM PLY solution. This allows as to conclude that observed EIS changes are due to a specific interaction between the cholesterol receptor in D4 domain of PLY [110] and cholesterol in phospholipid bilayer.

Taking into account the size of the pore of PLY, which is around 30 nm [111], the EIS response should be in the case of the functional protein pore reconstitution into mixed hybrid bilayer lipid membrane [112]. In the case of such events occurring in tBLMs on gold surface, the EIS phase minimum in the Bode plot (argZ vs. lgf) significantly shifts position of the frequency towards higher frequencies, while also significantly increasing the admittance and decreasing the capacitance of tBLM [69, 95, 112-113]. Such changes were not observed in the current work. Therefore, it was assumed that PLY is not undergoing full oligomerization and pore formation. Instead, the observed capacitance increase and slight decreases of the mhBLM resistance are due to the attachment of the PLY monomer to cholesterol in mhBLMs. The absence of functional reconstitution may be related to the excess density of OTS molecules on the surface. Dense OTS layers prevent pore formation due to the rigidity of the bilayer. To overcome the problem and make bilayers suitable for PLY reconstitution as one a solution may be the reduction of molecular anchor concentration in the silanization solution. Such reduction of the density is presumably possible by using longer-chain unsaturated anchor molecules [101], which however, currently are not available in the silane group terminated form.

Diphytanoyl phosphatidylcholine (DPhyPC) bilayer lipid membranes were also challenged with α-hemolysin expecting spontaneous incorporation of αHL into DPhyPC membrane by the formation of heptameric pores [114]. As it can be seen from Fig. 21, B, the deviation in complex capacitance from 0.71 μF cm^{-2} to 1.32 μF cm^{-2} was observed after 1 hour of injection of 500 nM αHL. The observed change in coefficient value of $C_{bilayer}/C_{bilayer+\ \alpha HL} = 0.54$ is more considerable than in case of PLY ($C_{bilayer}/C_{bilayer+\ PLY} = 0.84$). Also, the change of phase angle and resistivity (Fig. 22, C and D) of the mhBLM in the low frequency range (below 10 Hz) was quite noticeable after introduction of αHL. Particularly, the percentage resistivity change of mhBLM was calculated to be equal to 44.68% and 25.93% for 8 Hz and 0.1 Hz, respectively (Table 3). Also, the coefficient value of $C_{bilayer}/C_{bilayer+\ \alpha HL} = 0.54$ is comparable to $C_{tBLM}/C_{tBLM+\ \alpha HL} = 0.50$, which was obtained on DPhyPC tethered bilayer lipid membrane formed on gold surfaces, where functional reconstitution of αHL

was reported [114]. Therefore, it was assume that such considerable change of the complex capacitance as well as a decrease of the resistance of mhBLM attest for functional reconstitution of αHL into mhBLM [115].

To conclude, both membrane damaging proteins – PLY and αHL – displayed effects on the EIS of mhBLM anchored to a metallurgical Ti surface functionalized with mixed silane self-assembled monolayer. These effects are large enough and can be employed as a signal for the development of electrochemical/electroanalytical biosensor platforms based on modified titanium surface. Schematic representation of the obtained results is depicted in Fig 23. Such substrates are relatively inexpensive compared to gold substrates and exhibit high biocompatibility, mechanical resistance, and non-toxicity.

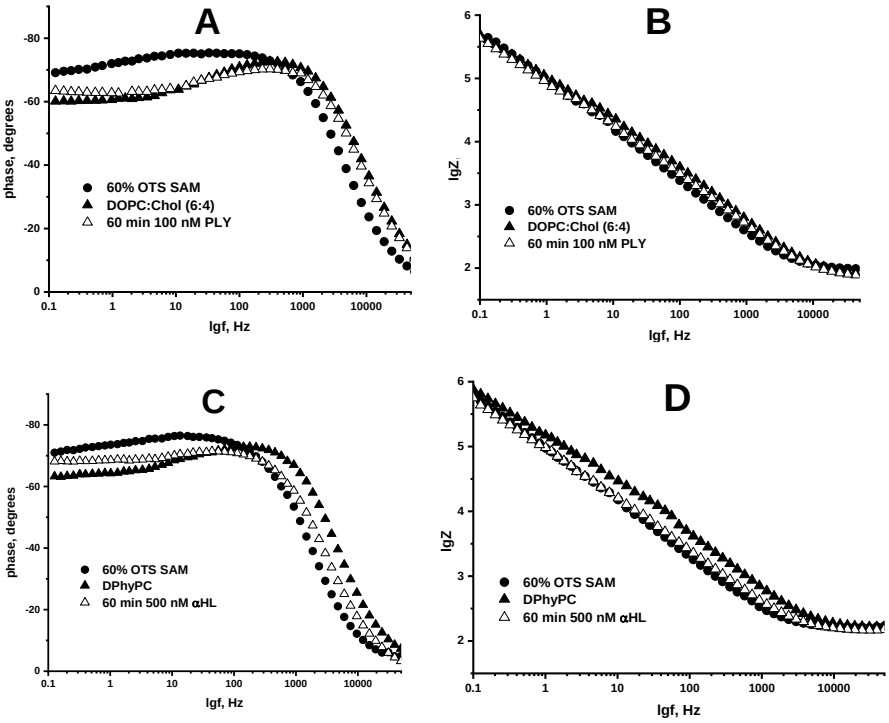

Figure 22. Bode plots of electrochemical impedance spectra obtained at 0 V potential vs Ag/AgCl/NaCl$_{(sat.)}$ using Ti electrode functionalized with SAM prepared from silanization solution containing OTS:MTS molar ratio of 6:4; A, B – mixed hybrid bilayer lipid membrane (DOPC:Chol (molar % ratio 6:4)) interaction with 100 nM pneumolysin (PLY), C, D – mixed hybrid bilayer lipid membrane (DPhypC) interaction with 500 nM α-hemolysin (αHL).

Table 3. The resistivity changes below 10 Hz of mixed hybrid bilayer lipid membrane after introduction of pneumolysin and α-hemolysin.

DOPC:Chol (molar % ratio 6:4) interaction with 100 nM PLY				DPhyPC interaction with 500 nM α-hemolysin			
f, Hz	Z_{mhBLM}, kΩ	$Z_{after\ PLY}$, kΩ	% change of Z	f, Hz	Z_{mhBLM}, kΩ	$Z_{after\ αhl}$, kΩ	% change of Z
8.32	27.53	21.25	22.83	7.70	35.11	19.42	44.68
6.31	33.77	25.77	23.71	5.89	43.97	23.51	46.51
4.79	40.24	31.65	21.32	4.62	55.08	29.30	46.80
3.63	44.47	38.53	13.36	3.54	65.04	34.58	46.84
2.75	53.70	47.62	11.33	2.71	74.68	40.89	45.25
2.09	64.91	52.28	19.46	2.28	84.94	50.33	40.75
1.58	78.15	62.75	19.71	1.81	100.98	60.01	40.57
1.20	91.98	73.87	19.69	1.47	116.24	70.51	39.34
0.91	112.77	92.17	18.26	1.20	135.78	84.90	37.47
0.69	135.73	111.81	17.62	1.01	150.02	96.35	35.77
0.52	163.28	135.42	17.06	0.82	166.45	106.61	35.95
0.40	196.56	164.01	16.56	0.65	197.56	126.78	35.83
0.30	236.46	198.74	15.95	0.52	237.55	152.83	35.66
0.23	284.84	240.96	15.41	0.41	280.05	179.94	35.75
0.17	342.26	292.45	14.55	0.32	328.29	215.54	34.35
0.13	412.38	354.94	13.93	0.26	390.12	255.75	34.44
0.10	494.66	430.17	13.04	0.20	455.98	307.55	32.55
-	-	-	-	0.16	543.58	371.03	31.74
-	-	-	-	0.13	641.58	436.28	32.00
-	-	-	-	0.10	758.61	561.92	25.93

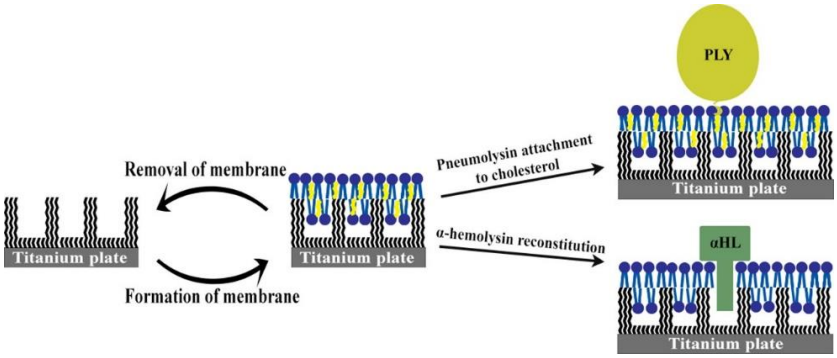

Figure 23. Schematic representation of the repetitive regeneration of the mixed hybrid bilayer lipid membrane on metallurgical titanium surface

3.3 Hybrid bilayer membrane formation on metallurgical aluminum surface

3.3.1 Self-assembled monolayer formation

The formation of the artificial membranes on self-assembled monolayers (SAM) requires sufficient surface free energy [63]. For that reason, the aluminum surface was functionalized with octadecyltrichlorosilane (OTS) monolayer by a simple silanization procedure. The most straightforward way to detect self-assembled monolayer (SAM) is to measure contact angles (CA) before and after silanization of the Al surface. Metallurgical aluminum surface exhibited hydrophilic properties showing CA values of 41.72 ± 3.96° (Fig. 24, A). After the silanization procedure, the values of contact angles increased to 105.13 ± 2.02° (Fig. 24, A) clearly demonstrating hydrophobic properties of the silanized Al surface. The obtained contact angle values of 105.13 ± 2.02° for the silanized Al surface are slightly higher than those obtained on OTS monolayer formed on metallurgical Ti surface (102.27 ± 1.76°) and lower than those obtained on OTS formed on FTO (119 ± 7°) [31] surface. However, the change of the wetting characteristics from hydrophilic to hydrophobic in all cases attests for the formation of the organic OTS monolayer on the surface, and consequently shows that functionalized aluminum surface has sufficient surface free energy, needed for further immobilization of phospholipid layer [63].

Metallurgical Al surface before and after silanization procedure was tested with cyclic voltammetry (CV) in phosphate buffer solution (pH 7.1) in order to determine the potential range of non-Faradaic process needed for further surface evaluation with electrochemical impedance spectroscopy (EIS). The potential range for CV measurements was chosen empirically by measuring the equilibrium potential, which was around -0.65 V vs $Ag/AgCl/NaCl_{(sat.)}$ and increasing the potential to more negative and positive values. Cyclic voltammetry curves showed that Faradaic processes occur on the Al surface over the potential range from -1.1 V to -0.5 V (Fig. 24, B dashed line). Usually, it is expected that aluminum is covered with a naturally occurring Al oxide which at neutral pH (~7) is expected to be electrochemically stable [116]. However, in a presence of the chloride anions the passive oxide film becomes unstable and local corrosion occurs [117]. Therefore, ideal polarizability was not observed on the aluminum surface (Fig. 24, B dashed line), since oxidation and reduction processes take place in the investigated potential range. Nevertheless, after the formation of OTS monolayer on the Al surface, even

in the presence of chloride anions, almost ideal polarizability was observed in the potential range from -1.1 V to -0.65 V (Fig. 24, B solid line). This effect can be attributed to the formation of the self-assembled monolayer resulting in the blockage of the interface aluminum – buffer solution.

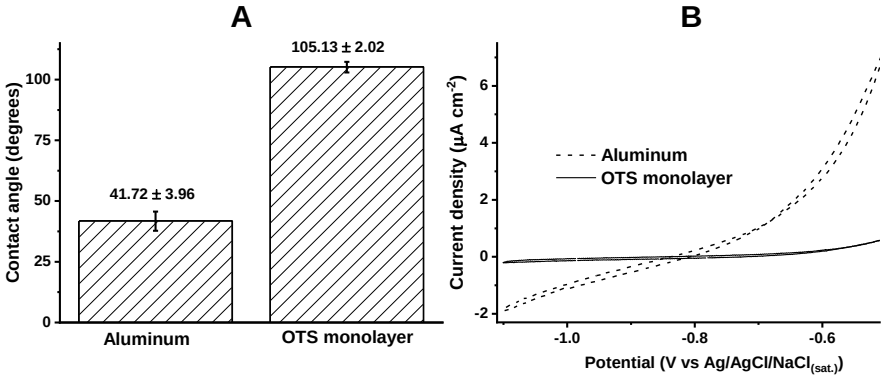

Figure 24. Properties of metallurgical aluminum surface before and after silanization: A – contact angle measurements, B – cyclic voltammograms at the scan rate of 10 mVs^{-1} in phosphate buffer, pH 7.1.

3.3.2 ATR-FTIR analysis of OTS monolayer

OTS monolayer on the Al surface was also analyzed with ATR-FTIR spectroscopy, which allows assessing the order in alkyl chains of the SAM [118-119]. Fig. 25 displays the C-H stretching region where three vibration absorbance bands are observed. The bands at 2852 cm^{-1} and 2923 cm^{-1} can be assigned to C-H symmetric (ν_s(CH2)) and asymmetric (ν_{as}(CH2)) stretching of methylene, respectively. The weak band at 2960 cm^{-1} is assigned to methyl asymmetric stretching ($\nu_{as}(CH_3)$) [118-119]. The position of $\nu_{as}(CH_2)$ band can be used for the evaluation of the order in alkyl chains [119]. For highly ordered octadecanethiol SAMs on the gold surface, the band of $\nu_{as}(CH_2)$ appears at 2917 cm^{-1}, shifting to higher wavenumbers as the gauche conformations along with the methylene chain increases (i.e. disorder) [118-119]. In our case, $\nu_{as}(CH_2)$ appears at 2923 cm^{-1} indicating a disorder of the OTS SAM. Also, the lower band intensity of $\nu_s(CH_3)$ relative to $\nu_s(CH_2)$

shows that the methyl groups are parallel to the surface, as observed in the mixed SAMs with a lower density of the molecular anchors on gold [101].

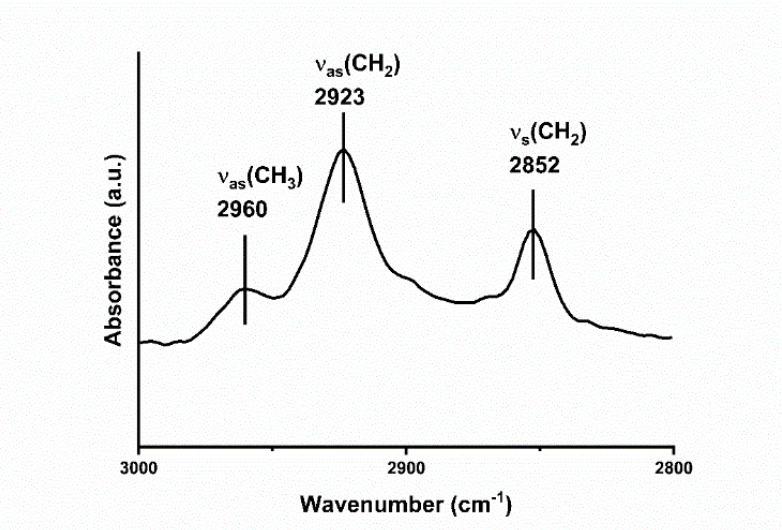

Figure 25. C-H stretching region of ATR-FTIR spectra of OTS self-assembled monolayer formed on the metallurgical aluminum surface.

3.3.3 Hybrid bilayer membrane formation

Contact angle, cyclic voltammetry, and ATR-FTIR measurements (Fig. 24 and Fig. 25) attest for the formation of OTS monolayer needed for immobilization of the hybrid bilayer lipid membrane. Electrochemical impedance spectroscopy (EIS), which is capable of detecting the dielectric properties of the surface, was applied for investigation of the hybrid bilayer formation on the metallurgical aluminum surface.

Fig. 26 shows electrochemical impedance spectra in Cole-Cole plots of the metallurgical Al surface functionalized with OTS monolayer and hybrid bilayer. Initially, the metallurgical aluminum surface exhibited relatively high values of complex capacitance reaching 4.82 ± 0.59 μF cm^{-2} (Fig. 26, open triangles). As expected, the silanization of the aluminum surface causes the "shrinkage" of the semicircle demonstrating the decrease of complex capacitance by approximately four-fold to 1.1 ± 0.11 μF cm^{-2} (Fig. 26, open circles) and indicating the formation of the dielectric layer of OTS monolayer on the Al surface. Meanwhile, OTS analogs – octadecanethiols, which forms compact SAMs on gold surfaces [28, 120], exhibits complex capacitance values well below 1 μF cm^{-2}. This difference in capacitance values is an

indication of void spaces (defects) in the SAM exposing the Al surface and, consequently, these defects increase the complex capacitance of the SAM [121]. Taking into account that OTS functionalized metallurgical titanium and magnetron sputtered titanium [33] surfaces were successfully applied for the formation of bilayer lipid membranes albeit exhibiting complex capacitance values above 1 μF cm^{-2}, the silanized Al surface was also tested for the formation of bilayer lipid membranes via vesicle fusion. After immobilization of hybrid bilayer membrane, the complex capacitance decreased to 0.61 μF cm^{-2} ± 0.07 μF cm^{-2} reaching a value typical for phospholipid bilayers (Fig. 26, filled circles).

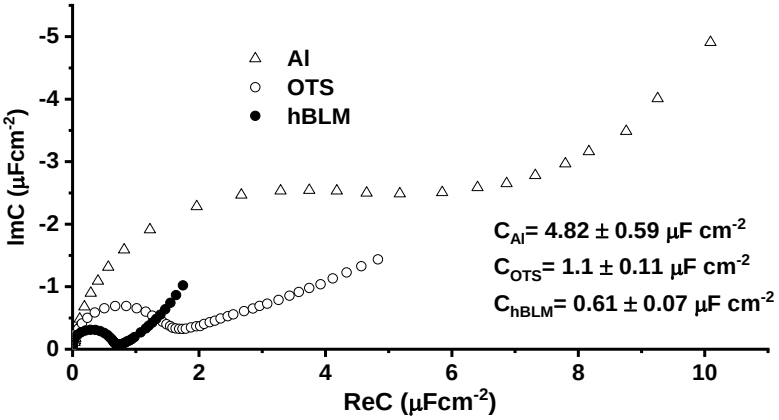

Figure 26. Electrochemical impedance spectra in Cole-Cole plot of Al, OTS and DOPC:Chol (molar % ratio 6:4) hBLM, formed by vesicle fusion method after 30 min incubation time. The applied potential: -0.7 V vs $Ag/AgCl/NaCl_{(sat.)}$. Mean complex capacitance values with standard deviations are displayed as well.

The process of vesicle fusion was monitored in real-time using FFT-EIS method by measuring EIS every 5 s for 40 min. Fig. 27 shows the complex capacitance evolution after injection of DOPC:Chol (molar % ratio 6:4) vesicles on OTS monolayer. The decrease of the complex capacitance was noticeable after 5 s of incubation time indicating that vesicle fusion process was triggered instantaneously (Fig. 27). As incubation time increases, the semicircle in Fig. 27 „shrinks" further indicating the decrease of the complex capacitance from 0.86 μF cm^{-2} (after 5 s) to 0.61 ± 0.07 μF cm^{-2}. The completion of vesicle fusion typically occurred approximately within 500 s. The completion of fusion can be detected by the limit capacitance value of

0.61 ± 0.07 μF cm^{-2} which is comparable to those obtained for the bilayer lipid membranes formed on gold (~0.6 μF cm^{-2}) [27-28] (~0.6 μF cm^{-2}), FTO [31] (0.82 ± 0.10 μF cm^{-2}) and metallurgical Ti surface (0.61 μF ± 0.06 μF cm^{-2}).

The vesicle fusion progression can be observed by following the parameter, θ, which approximately indicates the fraction of the surface covered by the hBLM:

$$\theta = \frac{C_{SAM} - C_{meas}}{C_{SAM} - C_{hBLM}} \quad (14)$$

where C_{SAM} – the magnitude of complex capacitance of self-assembled monolayer, C_{meas} – the magnitude of the complex capacitance measured at a specific time during the vesicle fusion and C_{hBLM} – the magnitude of complex capacitance at 100% coverage by the hybrid bilayer membrane (0.61 μF cm^{-2}).

As observed in Fig. 27 inset, the step-like increase of surface coverage to $\theta = 0.34$ was observed within the first 5 seconds. At 100 s the coverage reached its first plateau at $\theta = 0.42$. The increase resumed at approx. 180 s reaching coverage of $\theta = 0.94$ in 560 s. Then, slow convergence towards $\theta \rightarrow 1$ was observed for the next 350 s. The formation of 100% hBLM was typically observed between 900-1000 s. For the sake of reproducibility, 30 min (1800 s) period of time was typically used of vesicle fusion during which almost defect-free hBLMs was formed.

The trace shown in Fig. 27 inset represents a typical kinetics curve for amphiphilic molecules undergoing two-stage adsorption. During the first stage molecules adsorb onto the surface of adsorbate (in our case SAM) establishing maximal area of contact. In our case this corresponds to a horizontal conformation of the phospholipid molecules on anchor SAMs. Then, as the adsorption proceeds, the molecules rearrange themselves into a more compact arrangement corresponding in our case a monolayer of phospholipid oriented nearly parallel to the normal of a surface.

In conclusion, this finding allows to conclude that the vesicle fusion led to a formation of intact, essentially defect free hBLMs. This leads to a broader conclusion of applicability of the metallurgical Al surface for the formation of hybrid bilayer lipid membrane (hBLM) by the vesicle fusion method.

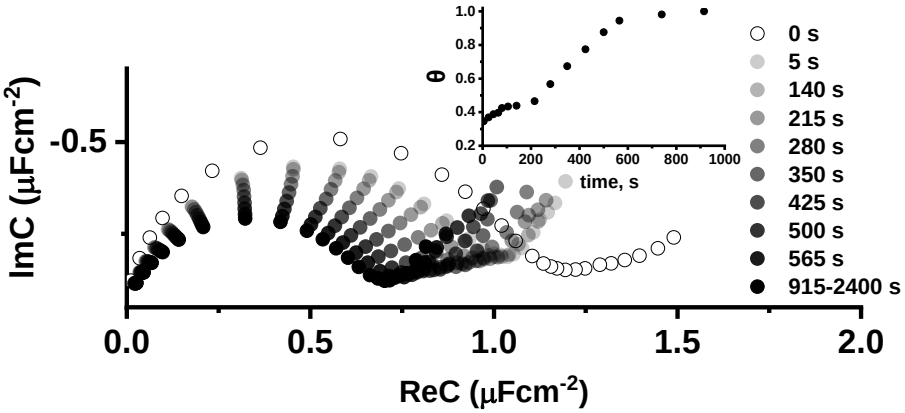

Figure 27. Cole-Cole plots of FFT impedance spectra of the DOPC:Chol (molar % ratio 6:4) vesicle fusion process on silanized aluminum surface. The applied potential: -0.7 V vs Ag/AgCl/$NaCl_{(sat.)}$. Inset – surface coverage, θ, of the lipid layer over time.

3.3.4 Regeneration of self-assembled monolayer for formation of the hybrid bilayer

Regeneration experiments were carried out to explore possible exploitation of the OTS SAM for multiple hybrid bilayer formation. Firstly, OTS SAM was monitored with EIS after the silanization procedure. After that, the hybrid bilayer was formed via the vesicle fusion method, and the formation of hBLM was monitored with EIS technique repeatedly. Fig. 28 displays EIS data obtained after 7 repeating regeneration procedures. It was observed that complex capacitance values of the SAM and hBLM slightly changed after each repetitive formation of hBLM. Initially, OTS complex capacitances were equal to 1.16 μF cm^{-2} (Fig. 28, open circles). Over the course of the regeneration of the SAM, the values of complex capacitance increased and reached 1.42 μF cm^{-2} after the 6th formation of the hBLM (Fig. 28, open diamonds). This feature can be attributed to the loss of the dielectric layer and adsorption of water molecules in the SAM. Hybrid bilayer formation follows the same tendency of an increase in complex capacitance value, however, this tendency was less noticeable. Particularly, the complex capacitance values increased slightly from 0.68 μF cm^{-2} following the first formation of hBLM to 0.74 μF cm^{-2} of the 7th formation of hBLM (Fig. 28, filled diamonds). The apparent transformation of EIS occurs at the end of the semicircle as indicated

by the arrow in Fig. 28, inset. The end of the semicircle shifts consistently towards the "northeast" direction as a number of SAM regeneration increase. Such EIS responses are usually obtained when the size of the defects in the membrane increases [20]. Even though multiple formation of the hBLM on regenerated SAM increases its defectiveness, the metallurgical aluminum surface functionalized with OTS self-assembled monolayer can be regenerated up to 6 times and used for multiple formations of the hybrid bilayer lipid membrane.

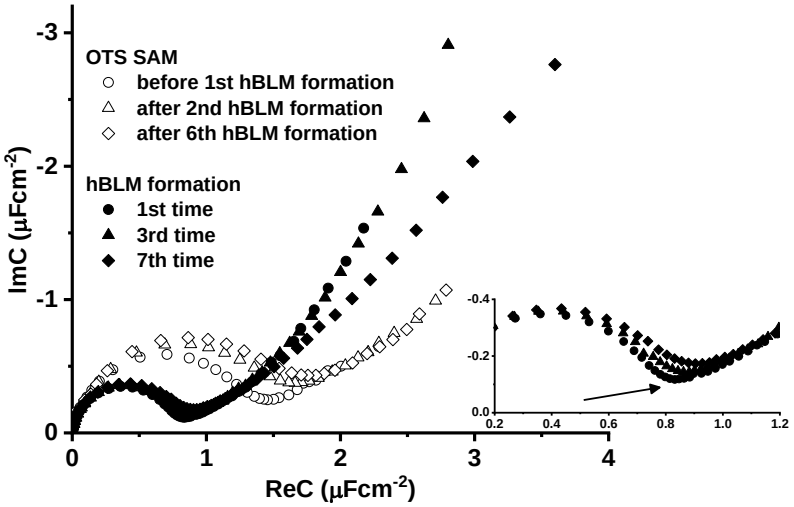

Figure 28. Cole-Cole plots of electrochemical impedance spectroscopy of the OTS SAM regeneration for DOPC:Chol (molar % ratio 6:4) hybrid bilayer formation on the metallurgical aluminum surface. The applied potential for EI measurements: –0.7 V vs Ag/AgCl/$NaCl_{(sat.)}$. Inset shows an enlarged part of the complex capacitance plot of the hBLM formations.

3.3.5 Hybrid bilayer lipid membrane interaction with melittin

In order to test biological relevance of hBLMs formed on the Al surface DOPC:Chol (molar % ratio 6:4) interaction with 500 nM melittin solution was investigated. Melittin, one of the major components of the bee venom [122], is 26 amino acid cationic peptide existing as a monomer in an aqueous environment [123-124]. As amphipathic peptide it easily associates with the structures like the lipid bilayers. When bound to lipid bilayers melittin adopts α-helical conformation and disrupts the bilayer lipid membrane by the pore formation process. Fig. 29 displays Cole-Cole plots of the hybrid bilayers after

60 min interaction with solutions containing various amounts of melittin. In all cases exposure of hBLM to melittin triggers EIS spectral changes consistent with the disruption of the phospholipid insulating layer and increases of a complex capacitance. The effect of melittin was found to be dependent on concentration and lipid composition. After exposure of DOPC:Chol (molar % ratio 6:4) hBLM to 200 nM melittin solution, the EI spectra (Fig. 29, A) remained almost unchanged. An increase of melittin concentration to 400 nM results in a significant increase of the complex capacitance of DOPC:Chol hBLM from 0.64 μF cm^{-2} to 0.94 μF cm^{-2} (Fig. 29, C). Further increase in melittin concentration to 500 nM results in a disintegration of the hBLM which is evident from the complex capacitance increase to 1.06 μF cm^{-2} (Fig. 30), a value close to the complex capacitance value of the bare anchor SAM with no phospholipid overlayer.

In cholesterol-free hBLMs (100 % DOPC hybrid bilayer) the melittin effect on membrane capacitance is quite significant even at low melittin concentrations. At 100 nM, the complex capacitance of DOPC bilayer slightly increased from 0.8 μF cm^{-2} to 0.88 μF cm^{-2} (Fig. 29, B). However, at 400 nM of melittin cholesterol-free DOPC hBLM was fully disrupted as indicated by a large complex capacitance increase from 0.8 μF cm^{-2} to 1.16 μF cm^{-2} (Fig. 29, D).

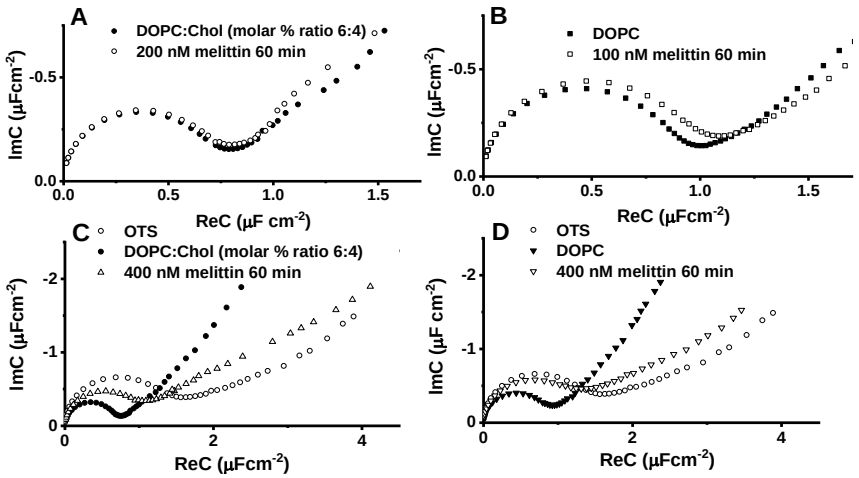

Figure 29. Electrochemical impedance spectra in Cole-Cole plot of melittin interaction: A and C – with DOPC:Chol (molar % ratio 6:4), B and D – with DOPC hybrid bilayer lipid membranes. The applied potential: -0.7 V vs $Ag/AgCl/NaCl_{(sat.)}$.

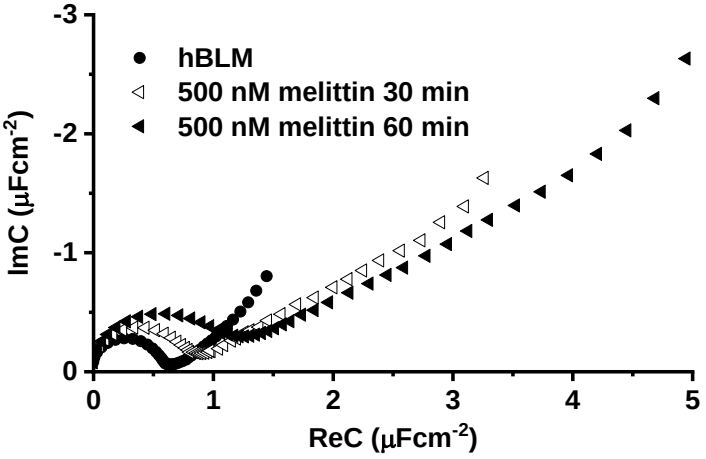

Figure 30. Electrochemical impedance spectra in Cole-Cole plot of 500 nM melittin interaction with DOPC:Chol (molar % ratio 6:4) hybrid bilayer lipid membrane. The applied potential: –0.7 V vs $Ag/AgCl/NaCl_{(sat.)}$.

Our findings indicate an inhibitory effect of cholesterol towards melittin induced damage of the bilayer [125-126]. Actually, the membrane-bound melittin can exist in two orientations: parallel, where only interaction with lipid head group occurs, and perpendicular, where it reconstitutes into hydrophobic core of the membrane, leading to pore formation [127]. These orientations highly depend on melittin concentration. At lower concentration (approximately below 0.5 μM [128], however it must be noted that exact concentration depends on the many factors e.g. lipids [129], ionic strength [130], pH [131]), peptide binds to the surface of the bilayer in parallel conformation. However, as concentration of the peptide increases, melittin shifts to perpendicular orientation. The major difference between cholesterol-free and cholesterol-loaded hBLMs on aluminum surface was observed at low melittin concentrations, therefore, it was speculated that melittin conformers oriented parallel to the membrane are mostly affected by the cholesterol, while at concentrations above 400 nM, the peptide form is vertical and less affected by the cholesterol content of the membrane.

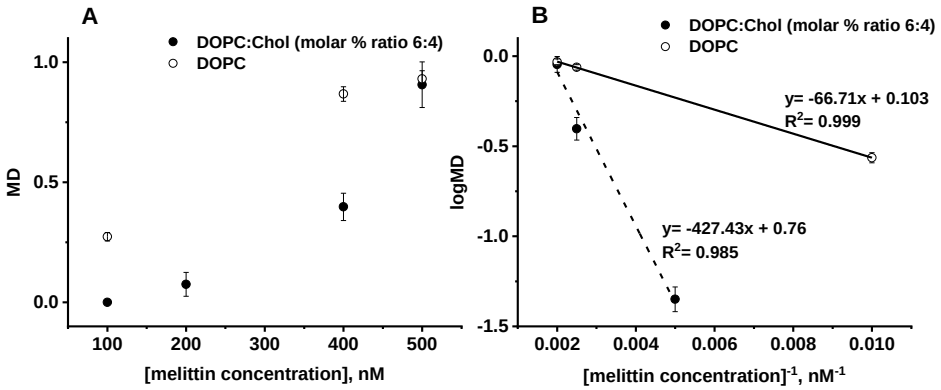

Figure 31. A – dependence of the membrane damage, MD, on melittin concentration, B – same data depicted in logMD vs inverse of melittin concentration

The disruptive effect of the peptide on the hybrid bilayers can be utilized to design impedimetric biosensors for the detection of membrane damaging toxins such as melittin. For this purpose, the extent of damage can be quantified as follows:

$$MD = 1 - \left(\frac{C_{SAM} - C_{melittin}}{C_{SAM} - C_{hBLM}}\right) \quad (15)$$

where MD denotes the membrane damage, C_{SAM} – is the complex capacitance value of OTS monolayer, $C_{melittin}$ – the complex capacitance of hBLM after 60 min of exposure to melittin solution, C_{hBLM} – the complex capacitance value of hBLM. Fig. 31, A displays the dependence of MD vs melittin concentration. The curve indicates non-linear dependence. Therefore, for analytical purposes, semi logarithmic inverse concentration plot (Fig. 31, B) is better suited, which was found empirically, and exhibits relatively good linear dependence in the concentration range from 100 nM to 500 nM. This interval of melittin concentration can be extended by properly adjusting phospholipid composition of hBLMs which possibly requires further investigation.

To summarize, artificial bilayer lipid membrane was successfully formed metallurgical aluminum. Such bilayer exhibited biological relevance evident by the interaction with membrane damaging peptide – melittin. The self-

assembled monolayer can be reused for artificial membrane formation. The designed system is depicted in Fig. 32.

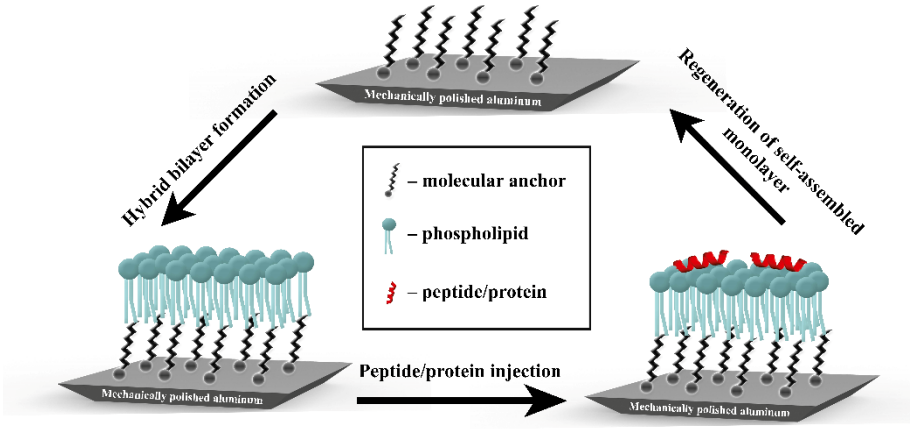

Figure 32. Schematic representation of the regenerable hybrid bilayers on the metallurgical aluminum surface.

CONCLUSIONS

1. Simple surface preparation technique was developed resulting in highly reproducible self-assembled monolayer formation on metallurgical titanium and aluminum surfaces. The optimal concentration of OTS monolayer formation on titanium and aluminum surfaces was determined to be 0.1 % (2.5 mM).

2. Hybrid bilayer lipid membrane of DOPC:Chol (molar % ratio 6:4) was formed on metallurgical titanium surface, exhibiting complex capacitance value of 0.61 ± 0.06 μF cm^{-2}. Surface thickness of the hybrid bilayer calculated from EIS data was found to be 3.57 nm. Phospholipid biosensor utility was displayed, which showed that interaction between phospholipase A_2 and hybrid bilayer can be used both for the real-time monitoring and for biosensor application.

3. Mixed hybrid bilayer lipid membranes were formed on metallurgical titanium surface. The optimal molar ratio of the MTS in the silanization solution was determined to be 40 %, which provides the surface coverage of phospholipid bilayer 0.97. Phospholipid biosensor utility was tested, which showed functional reconstitution of α-hemolysin and attachment of large pore-forming toxin – pneumolysin.

4. Hybrid bilayer lipid membrane of DOPC:Chol (molar % ratio 6:4) was formed on the metallurgical aluminum surface, exhibiting excellent insulating ability. The designed hybrid bilayers were tested with membrane damaging peptide – melittin, which showed biological relevance of hBLMs on polished aluminum surfaces.

5. Hybrid bilayers on the aluminum and titanium surfaces as well as mixed hybrid bilayer lipid membranes on titanium surface can be used for multiple formation of DOPC:Chol (molar % ratio 6:4) lipid membranes reusing regenerated self-assembled monolayer.

PUBLICATION LIST

PUBLICATIONS INCLUDED IN THE THESIS

1. **Tomas Sabirovas**, Aušra Valiūnienė and Gintaras Valincius, Mechanically Polished Titanium Surface for Immobilization of Hybrid Bilayer Membrane, Journal of the Electrochemical Society, 2018, 165: G109-G115. DOI: https://doi.org/10.1149/2.0101810jes
2. **Tomas Sabirovas**, Aušra Valiūnienė, Inga Gabriunaite, Gintaras Valincius, Mixed hybrid bilayer lipid membranes on mechanically polished titanium surface, Biochimica et Biophysica Acta (BBA) – Biomembranes, 2020, 1862. DOI: https://doi.org/10.1016/j.bbamem.2020.183232

PUBLICATIONS NOT INCLUDED IN THE THESIS

1. Aušra Valiūnienė, **Tomas Sabirovas**, Jūratė Petronienė, Arūnas Ramanavičius, Towards the application of fast Fourier transform - scanning electrochemical impedance microscopy (FFT-SEIM), Journal of Electroanalytical Chemistry, 2020, 864. DOI: https://doi.org/10.1016/j.jelechem.2020.11

REFERENCES

[1] E. Sackmann, Supported membranes: scientific and practical applications, Science, 271 (1996) 43-48. https://doi.org/10.1126/science.271.5245.43

[2] K. Seifert, K. Fendler, E. Bamberg, Charge transport by ion translocating membrane proteins on solid supported membranes, Biophys. J., 64 (1993) 384-391. https://doi.org/10.1016/S0006-3495(93)81379-1

[3] C. Steinem, A. Janshoff, K. von dem Bruch, R. Karsten, J. Goossens, H.-J. Galla, Valinomycin-mediated transport of alkali cations through solid supported membranes, Bioelectrochem. Bioenerg., 45 (1998) 17-26. https://doi.org/10.1016/S0302-4598(98)00073-7

[4] Y. Murakami, Z. Zhang, T. Taniguchi, M. Sohgawa, K. Yamashita, M. Noda, A High-Sensitive Detection of Several Tens of nM of Amyloid-Beta by Cantilever-Type Biosensor Immobilized DPPC Liposome Incorporated with Cholesterol, Procedia Eng., 168 (2016) 565-568. https://doi.org/10.1016/j.proeng.2016.11.526

[5] M.B. Fritzen-Garcia, V.C. Zoldan, I.R.W.Z. Oliveira, V. Soldi, A.A. Pasa, T.B. Creczynski-Pasa, Peroxidase immobilized on phospholipid bilayers supported on au (111) by DTT self-assembled monolayers: Application to dopamine determination, Biotechnol. Bioeng., 110 (2013) 374-382. https://doi.org/10.1002/bit.24721

[6] H.I. Ingólfsson, O.S. Andersen, Screening for small molecules' bilayer-modifying potential using a gramicidin-based fluorescence assay, ASSAY DRUG DEV TECHN., 8 (2010) 427-436. https://doi.org/10.1089/adt.2009.0250

[7] D. Tadaki, D. Yamaura, S. Araki, M. Yoshida, K. Arata, T. Ohori, K.-i. Ishibashi, M. Kato, T. Ma, R. Miyata, Y. Tozawa, H. Yamamoto, M. Niwano, A. Hirano-Iwata, Mechanically stable solvent-free lipid bilayers in nano- and micro-tapered apertures for reconstitution of cell-free synthesized hERG channels, Sci. Rep., 7 (2017) 17736. https://doi.org/10.1038/s41598-017-17905-x

[8] H. Guan, F. Zhang, J. Yu, D. Chi, The novel acetylcholinesterase biosensors based on liposome bioreactors–chitosan nanocomposite film for detection of organophosphates pesticides, Food Res. Int., 49 (2012) 15-21. https://doi.org/10.1016/j.foodres.2012.07.014

[9] D.P. Nikolelis, V.G. Andreou, Electrochemical transduction of interactions of atrazine with bilayer lipid membranes, Electroanalysis, 8 (1996) 643-647. https://doi.org/10.1002/elan.1140080708

[10] P. Mueller, D.O. Rudin, H. Ti Tien, W.C. Wescott, Reconstitution of Cell Membrane Structure in vitro and its Transformation into an Excitable System, Nature, 194 (1962) 979-980. https://doi.org/10.1038/194979a0

[11] P. Mueller, D.O. Rudin, H.T. Tien, W.C. Wescott, Methods for the formation of single bimolecular lipid membranes in aqueous solution, J. Phys. Chem., 67 (1963) 534-535. https://doi.org/10.1021/j100796a529
[12] L.K. Tamm, H.M. McConnell, Supported phospholipid bilayers, Biophys. J., 47 (1985) 105-113. https://doi.org/10.1016/S0006-3495(85)83882-0
[13] Y. Jing, H. Trefna, M. Persson, B. Kasemo, S. Svedhem, Formation of supported lipid bilayers on silica: relation to lipid phase transition temperature and liposome size, Soft Matter, 10 (2014) 187-195. https://doi.org/10.1039/C3SM50947H
[14] J.A. Zasadzinski, C.A. Helm, M.L. Longo, A.L. Weisenhorn, S.A. Gould, P.K. Hansma, Atomic force microscopy of hydrated phosphatidylethanolamine bilayers, Biophys. J., 59 (1991) 755-760. https://doi.org/10.1016/S0006-3495(91)82288-3
[15] J.A. Jackman, S.R. Tabaei, Z. Zhao, S. Yorulmaz, N.-J. Cho, Self-Assembly Formation of Lipid Bilayer Coatings on Bare Aluminum Oxide: Overcoming the Force of Interfacial Water, ACS Appl. Mater. Interfaces, 7 (2015) 959-968. https://doi.org/10.1021/am507651h
[16] N.-J. Cho, C.W. Frank, Fabrication of a Planar Zwitterionic Lipid Bilayer on Titanium Oxide, Langmuir, 26 (2010) 15706-15710. 10.1021/la101523f
[17] C.A. Keller, B. Kasemo, Surface specific kinetics of lipid vesicle adsorption measured with a quartz crystal microbalance, Biophys. J., 75 (1998) 1397-1402. https://doi.org/10.1016/S0006-3495(98)74057-3
[18] M.-P. Mingeot-Leclercq, M. Deleu, R. Brasseur, Y.F. Dufrêne, Atomic force microscopy of supported lipid bilayers, Nat. Protoc., 3 (2008) 1654-1659. https://doi.org/10.1038/nprot.2008.149
[19] E. Reimhult, M. Zäch, F. Höök, B. Kasemo, A Multitechnique Study of Liposome Adsorption on Au and Lipid Bilayer Formation on SiO2, Langmuir, 22 (2006) 3313-3319. https://doi.org/10.1021/la0519554
[20] G. Valincius, T. Meškauskas, F. Ivanauskas, Electrochemical Impedance Spectroscopy of Tethered Bilayer Membranes, Langmuir, 28 (2012) 977-990. https://doi.org/10.1021/la204054g
[21] S.G. Boxer, Molecular transport and organization in supported lipid membranes, Curr. Opin. Chem. Biol., 4 (2000) 704-709. https://doi.org/10.1016/S1367-5931(00)00139-3
[22] J.Y. Wong, J. Majewski, M. Seitz, C.K. Park, J.N. Israelachvili, G.S. Smith, Polymer-cushioned bilayers. I. A structural study of various preparation methods using neutron reflectometry, Biophys. J., 77 (1999) 1445-1457. https://doi.org/10.1016/S0006-3495(99)76992-4
[23] H. Hillebrandt, G. Wiegand, M. Tanaka, E. Sackmann, High Electric Resistance Polymer/Lipid Composite Films on Indium−Tin−Oxide Electrodes, Langmuir, 15 (1999) 8451-8459. https://doi.org/10.1021/la990341u

[24] M. Hausch, R. Zentel, W. Knoll, Synthesis and characterization of hydrophilic lipopolymers for the support of lipid bilayers, Macromol. Chem. Phys., 200 (1999) 174-179. https://doi.org/10.1002/(SICI)1521-3935(19990101)200:1<174::AID-MACP174>3.0.CO;2-C
[25] R.G. Nuzzo, D.L. Allara, Adsorption of bifunctional organic disulfides on gold surfaces, J. Am. Chem. Soc., 105 (1983) 4481-4483. https://doi.org/10.1021/ja00351a063
[26] R. Naumann, S.M. Schiller, F. Giess, B. Grohe, K.B. Hartman, I. Kärcher, I. Köper, J. Lübben, K. Vasilev, W. Knoll, Tethered Lipid Bilayers on Ultraflat Gold Surfaces, Langmuir, 19 (2003) 5435-5443. https://doi.org/10.1021/la0342060
[27] L.J.C. Jeuken, N.N. Daskalakis, X. Han, K. Sheikh, A. Erbe, R.J. Bushby, S.D. Evans, Phase separation in mixed self-assembled monolayers and its effect on biomimetic membranes, Sens. Actuators B Chem., 124 (2007) 501-509. https://doi.org/10.1016/j.snb.2007.01.014
[28] D.J. McGillivray, G. Valincius, D.J. Vanderah, W. Febo-Ayala, J.T. Woodward, F. Heinrich, J.J. Kasianowicz, M. Löscheb, Molecular-scale structural and functional characterization of sparsely tethered bilayer lipid membranes, Biointerphases, 2 (2007) 21-33. https://doi.org/10.1116/1.2709308
[29] H.M. Keizer, B.R. Dorvel, M. Andersson, D. Fine, R.B. Price, J.R. Long, A. Dodabalapur, I. Köper, W. Knoll, P.A.V. Anderson, R.S. Duran, Functional Ion Channels in Tethered Bilayer Membranes—Implications for Biosensors, ChemBioChem, 8 (2007) 1246-1250. https://doi.org/10.1002/cbic.200700094
[30] H. Hillebrandt, M. Tanaka, Electrochemical Characterization of Self-Assembled Alkylsiloxane Monolayers on Indium−Tin Oxide (ITO) Semiconductor Electrodes, J. Phys. Chem. B, 105 (2001) 4270-4276. https://doi.org/ 10.1021/jp004062n
[31] I. Gabriūnaitė, A. Valiūnienė, G. Valincius, Formation and properties of phospholipid bilayers on fluorine doped tin oxide electrodes, Electrochim. Acta, 283 (2018). https://doi.org/10.1016/j.electacta.2018.04.160
[32] A. Valiūnienė, Ž. Margarian, I. Gabriūnaitė, V. Matulevičiūtė, T. Murauskas, G. Valinčius, Cadmium Stannate Films for Immobilization of Phospholipid Bilayers, J. Electrochem. Soc., 163 (2016) H762-H767. https://doi.org/10.1149/2.0331609jes
[33] A. Valiūnienė, T. Petrulionienė, I. Balevičiūtė, L. Mikoliūnaitė, G. Valinčius, Formation of hybrid bilayers on silanized thin-film Ti electrode, Chem. Phys. Lipids, 202 (2017) 62-68. https://doi.org/10.1016/j.chemphyslip.2016.12.001
[34] D. Marchal, J. Pantigny, J.M. Laval, J. Moiroux, C. Bourdillon, Rate Constants in Two Dimensions of Electron Transfer between Pyruvate Oxidase, a Membrane Enzyme, and Ubiquinone (Coenzyme Q8), Its Water-

Insoluble Electron Carrier, Biochemistry, 40 (2001) 1248-1256. https://doi.org/ 10.1021/bi002325y
[35] R.F. Roskamp, I.K. Vockenroth, N. Eisenmenger, J. Braunagel, I. Köper, Functional Tethered Bilayer Lipid Membranes on Aluminum Oxide, ChemPhysChem, 9 (2008) 1920-1924. https://doi.org/ 10.1002/cphc.200800248
[36] T.D. Lazzara, C. Carnarius, M. Kocun, A. Janshoff, C. Steinem, Separating Attoliter-Sized Compartments Using Fluid Pore-Spanning Lipid Bilayers, ACS Nano, 5 (2011) 6935-6944. https://doi.org/ 10.1021/nn201266e
[37] J. Drexler, C. Steinem, Pore-Suspending Lipid Bilayers on Porous Alumina Investigated by Electrical Impedance Spectroscopy, J. Phys. Chem. B, 107 (2003) 11245-11254. https://doi.org/ 10.1021/jp030762r
[38] S. Saraf, C.J. Neal, S. Park, S. Das, S. Barkam, H.J. Cho, S. Seal, Electrochemical study of nanoporous gold revealing anti-biofouling properties, RSC Advances, 5 (2015) 46501-46508. https://doi.org/ 10.1039/C5RA05043J
[39] E.F. Bowden, F.M. Hawkridge, H.N. Blount, Interfacial electrochemistry of cytochrome c at tin oxide, indium oxide, gold, and platinum electrodes, Journal of Electroanalytical Chemistry and Interfacial Electrochemistry, 161 (1984) 355-376. https://doi.org/10.1016/S0022-0728(84)80193-X
[40] M. Long, H.J. Rack, Titanium alloys in total joint replacement—a materials science perspective, Biomaterials, 19 (1998) 1621-1639. https://doi.org/10.1016/S0142-9612(97)00146-4
[41] L. Picard, P. Phalip, E. Fleury, F. Ganachaud, Chemical adhesion of silicone elastomers on primed metal surfaces: A comprehensive survey of open and patent literatures, Prog. Org. Coat., 80 (2015) 120-141. https://doi.org/10.1016/j.porgcoat.2014.11.022
[42] S.J. Singer, G.L. Nicolson, The Fluid Mosaic Model of the Structure of Cell Membranes, Science, 175 (1972) 720-731. https://doi.org/10.1126/science.175.4023.720
[43] K. Simons, E. Ikonen, Functional rafts in cell membranes, Nature, 387 (1997) 569-572. https://doi.org/10.1038/42408
[44] D.A. Brown, E. London, FUNCTIONS OF LIPID RAFTS IN BIOLOGICAL MEMBRANES, Annu. Rev. Cell Dev. Biol., 14 (1998) 111-136. https://doi.org/10.1146/annurev.cellbio.14.1.111
[45] T. Harayama, H. Riezman, Understanding the diversity of membrane lipid composition, Nature Reviews Molecular Cell Biology, 19 (2018) 281-296. https://doi.org/10.1038/nrm.2017.138
[46] D. Casares, P.V. Escribá, C.A. Rosselló, Membrane Lipid Composition: Effect on Membrane and Organelle Structure, Function and Compartmentalization and Therapeutic Avenues, Int J Mol Sci, 20 (2019) 2167. https://doi.org/10.3390/ijms20092167
[47] M. Sud, E. Fahy, D. Cotter, A. Brown, E.A. Dennis, C.K. Glass, A.H. Merrill, Jr., R.C. Murphy, C.R. Raetz, D.W. Russell, S. Subramaniam, LMSD:

LIPID MAPS structure database, Nucleic Acids Res., 35 (2007) D527-532. https://doi.org/10.1093/nar/gkl838
[48] G. van Meer, D.R. Voelker, G.W. Feigenson, Membrane lipids: where they are and how they behave, Nature Reviews Molecular Cell Biology, 9 (2008) 112-124. https://doi.org/10.1038/nrm2330
[49] T. Berry, D. Dutta, R. Chen, A. Leong, H. Wang, W.A. Donald, M. Parviz, B. Cornell, M. Willcox, N. Kumar, C.G. Cranfield, Lipid Membrane Interactions of the Cationic Antimicrobial Peptide Chimeras Melimine and Cys-Melimine, Langmuir, 34 (2018) 11586-11592. https://doi.org/10.1021/acs.langmuir.8b01701
[50] O. Gutiérrez-Sanz, D. Olea, M. Pita, A.P. Batista, A. Alonso, M.M. Pereira, M. Vélez, A.L. De Lacey, Reconstitution of Respiratory Complex I on a Biomimetic Membrane Supported on Gold Electrodes, Langmuir, 30 (2014) 9007-9015. https://doi.org/10.1021/la501825r
[51] G. Krishna, J. Schulte, B.A. Cornell, R.J. Pace, P.D. Osman, Tethered Bilayer Membranes Containing Ionic Reservoirs: Selectivity and Conductance, Langmuir, 19 (2003) 2294-2305. https://doi.org/10.1021/la026238d
[52] X. Zhang, W. Fu, C.G. Palivan, W. Meier, Natural channel protein inserts and functions in a completely artificial, solid-supported bilayer membrane, Sci. Rep., 3 (2013) 2196. https://doi.org/10.1038/srep02196
[53] F.J. Martin, Liposomes: From biophysics to therapeutics. Edited by Marc Ostro. Marcel Dekker: New York. 1987. xiv + 393 pp. 24 × 16 cm. ISBN 0-8247-7762-x. $85.00, J. Pharm. Sci., 78 (1989) 181-182. https://doi.org/10.1002/jps.2600780223
[54] A. Samad, Y. Sultana, M. Aqil, Liposomal drug delivery systems: an update review, Curr Drug Deliv, 4 (2007) 297-305. https://doi.org/10.2174/156720107782151269
[55] L. Sercombe, T. Veerati, F. Moheimani, S.Y. Wu, A.K. Sood, S. Hua, Advances and Challenges of Liposome Assisted Drug Delivery, Frontiers in pharmacology, 6 (2015) 286-286. https://doi.org/10.3389/fphar.2015.00286
[56] S. Vemuri, C.T. Rhodes, Encapsulation of a Water Soluble Drug in a Liposome Preparation: Removal of Free Drug by Washing, Drug Dev. Ind. Pharm., 21 (1995) 1329-1338. https://doi.org/10.3109/03639049509063021
[57] R.A. Schwendener, H. Schott, Liposome formulations of hydrophobic drugs, Methods Mol Biol, 605 (2010) 129-138. https://doi.org/10.1007/978-1-60327-360-2_8
[58] J. Jass, T. Tjärnhage, G. Puu, From liposomes to supported, planar bilayer structures on hydrophilic and hydrophobic surfaces: an atomic force microscopy study, Biophys. J., 79 (2000) 3153-3163. https://doi.org/10.1016/s0006-3495(00)76549-0
[59] H.-L. Wu, P.-Y. Chen, C.-L. Chi, H.-K. Tsao, Y.-J. Sheng, Vesicle deposition on hydrophilic solid surfaces, Soft Matter, 9 (2013) 1908-1919. https://doi.org/10.1039/C2SM27450G

[60] J. Swaminathan, C. Ehrhardt, Liposomes for Pulmonary Drug Delivery, in: H.D.C. Smyth, A.J. Hickey (Eds.) Controlled Pulmonary Drug Delivery, Springer New York, New York, NY, 2011, pp. 313-334. https://doi.org/10.1007/978-1-4419-9745-6_14
[61] M. Montal, P. Mueller, Formation of bimolecular membranes from lipid monolayers and a study of their electrical properties, Proc Natl Acad Sci U S A, 69 (1972) 3561-3566. https://doi.org/10.1073/pnas.69.12.3561
[62] E.T. Castellana, P.S. Cremer, Solid supported lipid bilayers: From biophysical studies to sensor design, Surf. Sci. Rep., 61 (2006) 429-444. https://doi.org/10.1016/j.surfrep.2006.06.001
[63] V.I. Silin, H. Wieder, J.T. Woodward, G. Valincius, A. Offenhausser, A.L. Plant, The role of surface free energy on the formation of hybrid bilayer membranes, J. Am. Chem. Soc., 124 (2002) 14676-14683. https://doi.org/10.1021/ja026585+
[64] N.A. Anderson, L.J. Richter, J.C. Stephenson, K.A. Briggman, Characterization and control of lipid layer fluidity in hybrid bilayer membranes, J. Am. Chem. Soc., 129 (2007) 2094-2100. https://doi.org/10.1021/ja066588c
[65] A.L. Plant, Self-assembled phospholipid/alkanethiol biomimetic bilayers on gold, Langmuir, 9 (1993) 2764-2767. https://doi.org/10.1021/la00035a004
[66] A.L. Plant, Supported Hybrid Bilayer Membranes as Rugged Cell Membrane Mimics, Langmuir, 15 (1999) 5128-5135. 10.1021/la981662t
[67] J.A. Jackman, W. Knoll, N.-J. Cho, Biotechnology Applications of Tethered Lipid Bilayer Membranes, Materials, 5 (2012) 2637-2657. https://doi.org/10.3390/ma5122637
[68] J. Andersson, I. Köper, Tethered and Polymer Supported Bilayer Lipid Membranes: Structure and Function, Membranes, 6 (2016) 30. https://doi.org/10.3390/membranes6020030
[69] G. Valincius, M. Mickevicius, Chapter Two - Tethered Phospholipid Bilayer Membranes: An Interpretation of the Electrochemical Impedance Response, in: A. Iglič, C.V. Kulkarni, M. Rappolt (Eds.) Advances in Planar Lipid Bilayers and Liposomes, vol. 21, Academic Press, 2015, pp. 27-61. https://doi.org/10.1016/bs.adplan.2015.01.003
[70] J. Sagiv, Organized monolayers by adsorption. 1. Formation and structure of oleophobic mixed monolayers on solid surfaces, J. Am. Chem. Soc., 102 (1980) 92-98. https://doi.org/10.1021/ja00521a016
[71] N.K. Chaki, K. Vijayamohanan, Self-assembled monolayers as a tunable platform for biosensor applications, Biosens. Bioelectron., 17 (2002) 1-12. https://doi.org/10.1016/S0956-5663(01)00277-9
[72] C.E.D. Chidsey, D.N. Loiacono, Chemical functionality in self-assembled monolayers: structural and electrochemical properties, Langmuir, 6 (1990) 682-691. https://doi.org/10.1021/la00093a026
[73] D.O. Hutchins, T. Weidner, J. Baio, B. Polishak, O. Acton, N. Cernetic, H. Ma, A.K.Y. Jen, Effects of self-assembled monolayer structural order,

surface homogeneity and surface energy on pentacene morphology and thin film transistor device performance, Journal of Materials Chemistry C, 1 (2013) 101-113. https://doi.org/10.1039/C2TC00378C
[74] C. Vericat, M.E. Vela, G. Corthey, E. Pensa, E. Cortés, M.H. Fonticelli, F. Ibañez, G.E. Benitez, P. Carro, R.C. Salvarezza, Self-assembled monolayers of thiolates on metals: a review article on sulfur-metal chemistry and surface structures, RSC Advances, 4 (2014) 27730-27754. https://doi.org/10.1039/C4RA04659E
[75] R.K. Smith, P.A. Lewis, P.S. Weiss, Patterning self-assembled monolayers, Prog. Surf. Sci., 75 (2004) 1-68. https://doi.org/10.1016/j.progsurf.2003.12.001
[76] S.R. Wasserman, Y.T. Tao, G.M. Whitesides, Structure and reactivity of alkylsiloxane monolayers formed by reaction of alkyltrichlorosilanes on silicon substrates, Langmuir, 5 (1989) 1074-1087. https://doi.org/10.1021/la00088a035
[77] N. Tillman, A. Ulman, J.S. Schildkraut, T.L. Penner, Incorporation of phenoxy groups in self-assembled monolayers of trichlorosilane derivatives. Effects on film thickness, wettability, and molecular orientation, J. Am. Chem. Soc., 110 (1988) 6136-6144. https://doi.org/10.1021/ja00226a031
[78] D.K. Aswal, S. Lenfant, D. Guerin, J.V. Yakhmi, D. Vuillaume, Self assembled monolayers on silicon for molecular electronics, Anal. Chim. Acta, 568 (2006) 84-108. https://doi.org/10.1016/j.aca.2005.10.027
[79] D.L. Angst, G.W. Simmons, Moisture absorption characteristics of organosiloxane self-assembled monolayers, Langmuir, 7 (1991) 2236-2242. https://doi.org/10.1021/la00058a043
[80] C.P. Tripp, M.L. Hair, An infrared study of the reaction of octadecyltrichlorosilane with silica, Langmuir, 8 (1992) 1120-1126. https://doi.org/10.1021/la00040a018
[81] M.E. McGovern, K.M.R. Kallury, M. Thompson, Role of Solvent on the Silanization of Glass with Octadecyltrichlorosilane, Langmuir, 10 (1994) 3607-3614. https://doi.org/10.1021/la00022a038
[82] U. Srinivasan, M.R. Houston, R.T. Howe, R. Maboudian, Alkyltrichlorosilane-based self-assembled monolayer films for stiction reduction in silicon micromachines, Journal of Microelectromechanical Systems, 7 (1998) 252-260. https://doi.org/10.1109/84.679393
[83] R. Helmy, A.Y. Fadeev, Self-Assembled Monolayers Supported on TiO2: Comparison of C18H37SiX3 (X = H, Cl, OCH3), C18H37Si(CH3)2Cl, and C18H37PO(OH)2, Langmuir, 18 (2002) 8924-8928. https://doi.org/10.1021/la0262506
[84] N. Faucheux, R. Schweiss, K. Lützow, C. Werner, T. Groth, Self-assembled monolayers with different terminating groups as model substrates for cell adhesion studies, Biomaterials, 25 (2004) 2721-2730. https://doi.org/10.1016/j.biomaterials.2003.09.069

[85] H. Hähl, F. Evers, S. Grandthyll, M. Paulus, C. Sternemann, P. Loskill, M. Lessel, A.K. Hüsecken, T. Brenner, M. Tolan, K. Jacobs, Subsurface Influence on the Structure of Protein Adsorbates as Revealed by in Situ X-ray Reflectivity, Langmuir, 28 (2012) 7747-7756. https://doi.org/10.1021/la300850g
[86] A.Z. Summers, C.R. Iacovella, P.T. Cummings, C. McCabe, Investigating Alkylsilane Monolayer Tribology at a Single-Asperity Contact with Molecular Dynamics Simulation, Langmuir, 33 (2017) 11270-11280. https://doi.org/10.1021/acs.langmuir.7b02479
[87] C.R. Kessel, S. Granick, Formation and characterization of a highly ordered and well-anchored alkylsilane monolayer on mica by self-assembly, Langmuir, 7 (1991) 532-538. https://doi.org/10.1021/la00051a020
[88] F. Deflorian, S. Rossi, L. Fedrizzi, Silane pre-treatments on copper and aluminium, Electrochim. Acta, 51 (2006) 6097-6103. https://doi.org/10.1016/j.electacta.2006.02.042
[89] E. Ajami, K.-F. Aguey-Zinsou, Functionalization of electropolished titanium surfaces with silane-based self-assembled monolayers and their application in drug delivery, J. Colloid Interface Sci., 385 (2012) 258-267. https://doi.org/10.1016/j.jcis.2012.07.005
[90] G.K. Toworfe, S. Bhattacharyya, R.J. Composto, C.S. Adams, I.M. Shapiro, P. Ducheyne, Effect of functional end groups of silane self-assembled monolayer surfaces on apatite formation, fibronectin adsorption and osteoblast cell function, J Tissue Eng Regen Med, 3 (2009) 26-36. https://doi.org/10.1002/term.131
[91] L. Miozzo, A. Yassar, G. Horowitz, Surface engineering for high performance organic electronic devices: the chemical approach, J. Mater. Chem., 20 (2010) 2513-2538. https://doi.org/10.1039/B922385A
[92] A. Khaskhoussi, L. Calabrese, E. Proverbio, Superhydrophobic Self-Assembled Silane Monolayers on Hierarchical 6082 Aluminum Alloy for Anti-Corrosion Applications, Applied Sciences, 10 (2020) 2656. https://doi.org/10.3390/app10082656
[93] A.J. Bard, Electrochemical methods : fundamentals and applications / Allen J. Bard, Larry R. Faulkner, Wiley, New York, 1980.
[94] M. Itagaki, S. Suzuki, I. Shitanda, K. Watanabe, Electrochemical Impedance and Complex Capacitance to Interpret Electrochemical Capacitor, Electrochemistry, 75 (2007) 649-655. https://doi.org/10.5796/electrochemistry.75.649
[95] T. Ragaliauskas, M. Mickevicius, B. Rakovska, T. Penkauskas, D.J. Vanderah, F. Heinrich, G. Valincius, Fast formation of low-defect-density tethered bilayers by fusion of multilamellar vesicles, Biochim Biophys Acta Biomembr., 1859 (2017) 669-678. https://doi.org/10.1016/j.bbamem.2017.01.015

[96] G.S. Popkirov, R.N. Schindler, A new impedance spectrometer for the investigation of electrochemical systems, Rev. Sci. Instrum., 63 (1992) 5366-5372. https://doi.org/10.1063/1.1143404
[97] M.J. Eslamibidgoli, Gro, M. Eikerling, Surface configuration and wettability of nickel(oxy)hydroxides: a first-principles investigation, Physical Chemistry Chemical Physics, 19 (2017) 22659-22669. https://doi.org/10.1039/C7CP03396F
[98] G. Valincius, V. Reipa, V. Vilker, J.T. Woodward, M. Vaudin, Electrochemical Properties of Nanocrystalline Cadmium Stannate Films, J. Electrochem. Soc., 148 (2001) E341. https://doi.org/10.1149/1.1379742
[99] J.B. Brzoska, I.B. Azouz, F. Rondelez, Silanization of Solid Substrates: A Step Toward Reproducibility, Langmuir, 10 (1994) 4367-4373. https://doi.org/10.1021/la00023a072
[100] P. Diao, D. Jiang, X. Cui, D. Gu, R. Tong, B. Zhong, Unmodified supported thiol/lipid bilayers: studies of structural disorder and conducting mechanism by cyclic voltammetry and AC impedance, Bioelectrochemistry and bioenergetics (Lausanne, Switzerland), 48 (1999) 469-475. https://doi.org/10.1016/s0302-4598(99)00038-0
[101] R. Budvytyte, G. Valincius, G. Niaura, V. Voiciuk, M. Mickevicius, H. Chapman, H.-Z. Goh, P. Shekhar, F. Heinrich, S. Shenoy, M. Lösche, D.J. Vanderah, Structure and Properties of Tethered Bilayer Lipid Membranes with Unsaturated Anchor Molecules, Langmuir, 29 (2013) 8645-8656. https://doi.org/10.1021/la401132c
[102] P. Krysiński, A. Żebrowska, B. Pałys, Z. Łotowski, Spectroscopic and Electrochemical Studies of Bilayer Lipid Membranes Tethered to the Surface of Gold, Journal of The Electrochemical Society, 149 (2002) E189-E194. https://doi.org/10.1149/1.1473779
[103] L. Ringstad, A. Schmidtchen, M. Malmsten, Effect of Peptide Length on the Interaction between Consensus Peptides and DOPC/DOPA Bilayers, Langmuir, 22 (2006) 5042-5050. https://doi.org/10.1021/la060317y
[104] M.L. Fernández, G. Marshall, F. Sagués, R. Reigada, Structural and Kinetic Molecular Dynamics Study of Electroporation in Cholesterol-Containing Bilayers, J. Phys. Chem. B, 114 (2010) 6855-6865. https://doi.org/10.1021/jp911605b
[105] J.E. Burke, E.A. Dennis, Phospholipase A2 structure/function, mechanism, and signaling, J. Lipid Res., 50 Suppl (2009) S237-S242. https://doi.org/10.1194/jlr.R800033-JLR200
[106] G. Valincius, D.J. McGillivray, W. Febo-Ayala, D.J. Vanderah, J.J. Kasianowicz, M. Lösche, Enzyme Activity to Augment the Characterization of Tethered Bilayer Membranes, The Journal of Physical Chemistry B, 110 (2006) 10213-10216. https://doi.org/10.1021/jp0616516
[107] Allen J. Bard and Larry R. Faulkner, Electrochemical Methods: Fundamentals and Applications, New York: Wiley, 2001, 2nd ed, Russ. J.

Electrochem., 38 (2002) 1364-1365. https://doi.org/10.1023/A:1021637209564
[108] G. Valincius, F. Heinrich, R. Budvytyte, D.J. Vanderah, D.J. McGillivray, Y. Sokolov, J.E. Hall, M. Lösche, Soluble amyloid beta-oligomers affect dielectric membrane properties by bilayer insertion and domain formation: implications for cell toxicity, Biophys. J., 95 (2008) 4845-4861. https://doi.org/10.1529/biophysj.108.130997
[109] D.R. Neill, T.J. Mitchell, A. Kadioglu, Chapter 14 - Pneumolysin, in: J. Brown, S. Hammerschmidt, C. Orihuela (Eds.) Streptococcus Pneumoniae, Academic Press, Amsterdam, 2015, pp. 257-275. https://doi.org/10.1016/B978-0-12-410530-0.00014-4
[110] J. Rossjohn, R.J.C. Gilbert, D. Crane, P.J. Morgan, T.J. Mitchell, A.J. Rowe, P.W. Andrew, J.C. Paton, R.K. Tweten, M.W. Parker, The molecular mechanism of pneumolysin, a virulence factor from Streptococcus pneumoniae11Edited by J. Thornton, J. Mol. Biol., 284 (1998) 449-461. https://doi.org/10.1006/jmbi.1998.2167
[111] S.L. Lawrence, S.C. Feil, C.J. Morton, A.J. Farrand, T.D. Mulhern, M.A. Gorman, K.R. Wade, R.K. Tweten, M.W. Parker, Crystal structure of Streptococcus pneumoniae pneumolysin provides key insights into early steps of pore formation, Sci. Rep., 5 (2015) 14352. https://doi.org/10.1038/srep14352
[112] T. Raila, T. Penkauskas, M. Jankunec, G. Dreižas, T. Meškauskas, G. Valincius, Electrochemical impedance of randomly distributed defects in tethered phospholipid bilayers: Finite element analysis, Electrochim. Acta, 299 (2019) 863-874. https://doi.org/10.1016/j.electacta.2018.12.148
[113] G. Valincius, R. Budvytyte, T. Penkauskas, M. Pleckaityte, A. Zvirbliene, Phospholipid Sensors for Detection of Bacterial Pore-Forming Toxins, ECS Transactions, 64 (2014) 117-124. https://doi.org/10.1149/06401.0117ecst
[114] I.K. Vockenroth, P.P. Atanasova, A.T.A. Jenkins, I. Köper, Incorporation of α-Hemolysin in Different Tethered Bilayer Lipid Membrane Architectures, Langmuir, 24 (2008) 496-502. https://doi.org/10.1021/la7030279
[115] D.J. McGillivray, G. Valincius, F. Heinrich, J.W.F. Robertson, D.J. Vanderah, W. Febo-Ayala, I. Ignatjev, M. Lösche, J.J. Kasianowicz, Structure of functional Staphylococcus aureus alpha-hemolysin channels in tethered bilayer lipid membranes, Biophys. J., 96 (2009) 1547-1553. https://doi.org/10.1016/j.bpj.2008.11.020
[116] M.H. Pournaghi-Azar, H. Razmi-Nerbin, Voltammetric behaviour and electrocatalytic activity of the aluminum electrode modified with nickel and nickel hexacyanoferrate films, prepared by electroless deposition, J. Electroanal. Chem., 456 (1998) 83-90. https://doi.org/10.1016/S0022-0728(98)00284-8

[117] P.M. Natishan, W.E. O'Grady, Chloride Ion Interactions with Oxide-Covered Aluminum Leading to Pitting Corrosion: A Review, J. Electrochem. Soc., 161 (2014) C421-C432. https://doi.org/10.1149/2.1011409jes
[118] M.D. Porter, T.B. Bright, D.L. Allara, C.E.D. Chidsey, Spontaneously organized molecular assemblies. 4. Structural characterization of n-alkyl thiol monolayers on gold by optical ellipsometry, infrared spectroscopy, and electrochemistry, J. Am. Chem. Soc., 109 (1987) 3559-3568. https://doi.org/10.1021/ja00246a011
[119] P.E. Laibinis, G.M. Whitesides, D.L. Allara, Y.T. Tao, A.N. Parikh, R.G. Nuzzo, Comparison of the structures and wetting properties of self-assembled monolayers of n-alkanethiols on the coinage metal surfaces, copper, silver, and gold, J. Am. Chem. Soc., 113 (1991) 7152-7167. https://doi.org/10.1021/ja00019a011
[120] T. Ragaliauskas, M. Mickevicius, R. Budvytyte, G. Niaura, B. Carbonnier, G. Valincius, Adsorption of β-amyloid oligomers on octadecanethiol monolayers, J. Colloid Interface Sci., 425 (2014) 159-167. https://doi.org/10.1016/j.jcis.2014.03.042
[121] D.J. Vanderah, J. Arsenault, H. La, R.S. Gates, V. Silin, C.W. Meuse, G. Valincius, Structural Variations and Ordering Conditions for the Self-Assembled Monolayers of HS(CH2CH2O)3-6CH3, Langmuir, 19 (2003) 3752-3756. https://doi.org/10.1021/la026580q
[122] T.C. Terwilliger, D. Eisenberg, The structure of melittin. II. Interpretation of the structure, J. Biol. Chem., 257 (1982) 6016-6022.
[123] J. Bello, H.R. Bello, E. Granados, Conformation and aggregation of melittin: dependence of pH and concentration, Biochemistry, 21 (1982) 461-465. https://doi.org/10.1021/bi00532a007
[124] G. Schwarz, G. Beschiaschvili, Kinetics of melittin self-association in aqueous solution, Biochemistry, 27 (1988) 7826-7831. https://doi.org/10.1021/bi00420a036
[125] L.-Y. Chen, C.-W. Cheng, J.-J. Lin, W.-Y. Chen, Exploring the effect of cholesterol in lipid bilayer membrane on the melittin penetration mechanism, Anal. Biochem., 367 (2007) 49-55. https://doi.org/10.1016/j.ab.2007.04.039
[126] T. Benachir, M. Monette, J. Grenier, M. Lafleur, Melittin-induced leakage from phosphatidylcholine vesicles is modulated by cholesterol: a property used for membrane targeting, European Biophysics Journal, 25 (1997) 201-210. https://doi.org/10.1007/s002490050032
[127] G. van den Bogaart, J.V. Guzmán, J.T. Mika, B. Poolman, On the Mechanism of Pore Formation by Melittin, J. Biol. Chem., 283 (2008) 33854-33857. https://doi.org/10.1074/jbc.M805171200
[128] C. Humbert, B. Busson, Chapter 10 - Sum-frequency generation spectroscopy of biointerfaces, in: C.M. Pradier, Y.J. Chabal (Eds.) Biointerface Characterization by Advanced IR Spectroscopy, Elsevier,

Amsterdam, 2011, pp. 279-321. https://doi.org/10.1016/B978-0-444-53558-0.00010-2
[129] G. Klocek, T. Schulthess, Y. Shai, J. Seelig, Thermodynamics of Melittin Binding to Lipid Bilayers. Aggregation and Pore Formation, Biochemistry, 48 (2009) 2586-2596. https://doi.org/10.1021/bi802127h
[130] H. Raghuraman, A. Chattopadhyay, Effect of ionic strength on folding and aggregation of the hemolytic peptide melittin in solution, Biopolymers, 83 (2006) 111-121. https://doi.org/10.1002/bip.20536
[131] A. Kashiwada, M. Mizuno, J. Hashimoto, pH-Dependent membrane lysis by using melittin-inspired designed peptides, Org. Biomol. Chem., 14 (2016) 6281-6288. https://doi.org/10.1039/C6OB01002D

SANTRAUKA

ĮVADAS

Plazminė membrana yra viena iš svarbiausių ląstelės struktūros elementų, kuri atskiria ląstelės vidinę dalį nuo išorinės. Plazminę membraną sudaro įvairūs fosfolipidai ir baltymai. Baltymai ląstelės membranoje yra atsakingi už įvairias funkcijas: apsauginę, molekulių pernašą iš ląstelės ir į ją, molekulių atpažinimą ir kt. Siekiant supaprastinti plazminės membranos sistemą, moksliniams tyrimams buvo sukurti biologinės membranos modeliai, kurie yra naudojami biofiziniams ir biocheminiams tyrimams pvz., baltymų-lipidų sąveikoms, jonų pernašoms. Medicininės diagnostikos ir vaistų patikros technologijos bei aplinkai kenksmingų medžiagų nustatymas taip pat yra paremti dirbtinių membranų modeliais.

Membranos modeliai gali būti įvairūs, tačiau dažniausiai yra naudojamos dirbtinės membranos suformuotos ant kietų paviršių. Dvisluoksnių lipidinių membranų formavimui ant kietų paviršių yra naudojama keletas skirtingų būdų. Vienas iš jų – tai tiesioginis dvisluoksnės membranos suformavimas ant kieto paviršiaus, pvz. ant oksiduoto silicio, žėručio, aliuminio, titano. Lipidinės membranos suformuotos ant kietų paviršių pasižymi didesniu patvarumu ir stabilumu, o taip pat galimybė taikyti tokius analitinius tyrimo metodus, kaip kvarco kristalo mikrogravimetrija, atominės jėgos mikroskopija, paviršiaus plazmonų rezonansas, elektrocheminio impedanso spektroskopija. Nepaisant to, dvisluoksnių membranų, suformuotų ant kietų paviršių, pagrindinis trūkumas yra plonas vandens sluoksnis tarp lipidinės membranos ir kieto paviršiaus, todėl integraliniai baltymai, įterpti į dvisluoksnę membraną, nepalankiai sąveikauja su substratu, t. y. gali būti stebimas integralinio baltymo funkcijos ir/ar mobilumo praradimas lipidinėje membranoje.

Kitas būdas yra formuoti dvisluoksnę membraną ant kieto paviršiaus, kuris yra funkcionalizuotas polimeru ar savitvarkiu monosluoksniu. Taip suformuotos dvisluoksnės membranos yra atskirtos nuo kieto paviršiaus ir leidžia integraliniams baltymams išlaikyti savo funkcijas. Kietą paviršių galima modifikuoti pasinaudojant tiolo-metalo ar silano-metalo oksido paviršiaus chemijos reakcijomis. Plačiausiai ištirtas yra aukso paviršius, tačiau kiti paviršiai, tokie kaip: indžio alavo oksidas (angl. ITO), fluoru legiruotas alavo oksidas (angl. FTO), kadmio alavo oksidas (angl. CTO), titano oksidas (Ti/TiO2), aliuminis ir kt. taip pat gali būti naudojami dvisluoksnių membranų formavimui. Daugumos substratų paruošimui reikia

naudoti sudėtingas metodikas, tokias kaip magnetroninis dulkinimas, ir tai padidina bendrą membraninių procesų tyrimų ar elektrocheminių/elektroanalitinių prietaisų kūrimo kainą. Viena iš alternatyvų aukso paviršiams gali būti metalurginiai paviršiai, nereikalaujantis sudėtingų paviršiaus paruošimo metodų. Pavyzdžiui, Ti ar jo lydiniai pasižymi puikiomis mechaninėmis ir antikorozinėmis savybėmis bei dideliu biologiniu suderinamumu, todėl fosfolipidinių membranų formavimas ant Ti ar jo lydinių gali būti pritaikytas implantuose. Nepaisant to, lipidinių membranų modelių kūrimas gali būti apribotas dėl Ti ar jo lydinių kainos ir dėl metalo kietumo, nes titano paviršiaus paruošimas pvz., poliravimas, yra laikui imlus procesas. Todėl minkšti bei pigūs metalai tokie kaip aliuminis, taip pat gali būti panaudojami fosfolipidinių membranų formavimui. Vienas iš aliuminio privalumų, lyginant su titano paviršiumi, yra lengvas paviršiaus paruošimas dėl metalo minkštumo bei didesnis afiniškumas alkilsilano molekulėms. Dėl šių priežasčių, lipidinės membranos suformuotos ant metalurginio aliuminio paviršiaus gali sumažinti bendrą membraninių procesų tyrimų ir/ar bioanalitinių prietaisų kūrimo kainą.

Darbo tikslas: suformuoti ir ištirti fosfolipidinių dvisluoksnių membranų modelius ant metalurginių titano ir aliuminio paviršių.

Darbo uždaviniai:

1. Parengti tinkamą paviršiaus paruošimo procedūrą oktadeciltrichlorosilano (OTS) savitvarkių monosluoksnių formavimui ant metalurginių titano ir aliuminio paviršių.
2. Ant metalurginio titano paviršiaus suformuoti hibridinę bisluoksnę membraną bei ištirti jos funkcionalumą, naudojant membranos pažaidą sukeliantį toksiną – fosfolipazę A2.
3. Ant metalurginio titano paviršiaus suformuoti mišrią hibridinę membraną, ir ištirti jos funkcionalumą, naudojant membranos pažaidą sukeliančius toksinus – pneumoliziną ir α-hemoliziną.
4. Ant metalurginio aliuminio paviršiaus suformuoti hibridinę membraną bei ištirti jos funkcionalumą, naudojant membranos pažaidą sukeliantį toksiną – melitiną.
5. Ištirti savitvarkių monosluoksnių daugkartinio panaudojimo galimybes dirbtinių fosfolipidinių membranų formavimui ant metalurginių titano ir aliuminio paviršių.

Mokslinis naujumas

Dirbtinės membranos ant kietų paviršių buvo plačiai tiriamos per pastaruosius dešimtmečius. Dirbtinių fosfolipidinių membranų formavimui dažniausiai yra naudojamas aukso substratas. Tačiau aukso substrato paruošimas yra brangus procesas, reikalaujantis specialių paviršiaus paruošimo metodų (pvz., magnetroninio dulkinimo). Taip pat molekulinių „inkarų“ formavimas ant aukso paviršiaus yra laikui imlus procesas. Be to, savitvarkiai monosluoksniai suformuoti ant aukso paviršiaus yra linkę į struktūrinius persitvarkymus, todėl Au paviršius yra tinkamas tik vienkartiniam fosfolipidinių membranų formavimui. Šiame darbe, pirmą kartą, dirbtinių fosfolipidinių membranų formavimui buvo naudojami metalurginiai aliuminio ir titano paviršiai, funkcionalizuoti oktadeciltrichlorosilano savitvarkiais monosluoksniais. Darbe buvo nustatyta, jog fosfolipidinės membranos gali būti formuojamos keletą kartų ant oktadeciltrichlorosilano savitvarkiu monosluoksniu funkcionalizuotų aliuminio ir titano paviršių. Taip pat, buvo ištirtos dirbtinių membranų biologinio pritaikymo galimybės, naudojant membranos pažaidą sukeliančius baltymus/peptidus. Visi rezultatai, pristatyti šiame darbe, rodo, jog metalurginiai titano ir aliuminio paviršiai gali būti sėkmingai pritaikyti dirbtinių fosfolipidinių membranų formavimui bei gali būti pritaikyti fosfolipidinių biologinių jutiklių kūrimui.

EKSPERIMENTŲ METODIKA

Titano ir aliuminio paviršiaus paruošimas. Metalurginio titano (25 × 55 mm, storis 0,125 mm, > 99,0 %) ir metalinio aliuminio (25 × 55 mm, storis 0,125 mm, > 99,0 %) plokštelės buvo nupoliruotos deimantine pasta, kurios grūdėtumas 200,000, iki veidrodinio atspindžio paviršiaus. Nupoliruotos plokštelės buvo valomos skirtingomis procedūromis. Titano plokštelė buvo plaunama ultragarso vonelėje skirtinguose tirpikliuose/tirpaluose po 10 min: heksane arba acetone, 2 % “MICRO®-90“ ploviklio tirpale, 2-propanolyje ir dejonizuotame vandenyje. Aliuminio plokštele taip pat buvo plaunama ultagarso vonelėje: 10 min heksano tirpiklyje, 10 min 2-propanolio tirpiklyje ir 2 min dejonizuotame vandenyje. Po nuplovimo, plokštelės buvo nudžiovinamos azoto dujų srove.

Savitvarkių monosluoksnių formavimas. Nupoliruoti ir nuplauti titano ir aliuminio paviršiai buvo naudojami octadeciltrichlorosilano (OTS) savitvarkių monosluoksnių formavimui. Metiltrichlorosilanas (MTS) kartu su OTS buvo naudojamas mišrių savitvarkių monosluoksnių formavimui ant

titano paviršiaus. Silanizavimo tirpalas buvo paruošiamas taip: į cheminę stiklinę įpilamas heptano tirpalas, kuris kaitinimas iki 60-65 °C temperatūros ir įdedamas 2,5 mM koncentracijos oktadeciltrichlorosilanas (nebent nurodyta kitaip). Tada, titano arba aliuminio plokštelė buvo įmerkiama į silanizavimo tirpalą 45 min. Po to, funkcionalizuoti paviršiai buvo išimami iš cheminės stiklinės, nuplaunami dideliu kiekiu heptano tirpikliu ir nudžiovinami azoto dujų srove. Nudžiovinti paviršiai buvo kaitinami krosnyje 100 °C temperatūroje vieną valandą, siekiant pašalinti adsorbuotas vandens ar tirpiklio molekules.

Dirbtinės membranos formavimas. Dvisluoksnės lipidinės membranos buvo formuojamos vezikulių liejimo metodu. Vezikulių tirpalas buvo paruoštas iš 1,2 – difitanoil-sn-glicerolio-3-fosfocholino (DPhyPC), 1,2-dioleoil-sn-glicerolio-3-fosfocholino (DOPC) ar lipidų mišinio sudaryto iš DOPC ir cholesterolio (Chol). Visuose eksperimentuose naudota 1,5 mM vezikulių tirpalo koncentracija.

Elektrocheminiai matavimai. Elektrocheminio impedanso spektroskopijos (EIS) ir ciklinės voltamperometrijos (CV) matavimai buvo atlikti fosfatiniame buferiniame tirpale, kurio pH 7,1. Buvo naudojama standartinė trijų elektrodų sistema, kur darbinis elektrodas – titano arba aliuminio plokštelė, palyginamasis elektrodas – Ag/AgCl elektrodas sočiame NaCl tirpale ir pagalbinis elektrodas – platinos viela. CV matavimai buvo atlikti naudojant 10 mVs^{-1} skleidimo greitį su μAutolab potenciostatu. EIS matavimai buvo atlikti su μAutolab dažnių diapozone tarp 0,1 Hz ir 50 kHz arba su greitosios Furje transformacijos elektrocheminio impedanso spektrometru (FFT-EIS) dažnių diapozone tarp 0,7 Hz ir 50 kHz (nebent nurodyta kitaip). Papildoma platinos viela buvo naudojama FFT-EIS matavimams kaip kvazi-palyginamasis elektrodas, siekiant sumažinti impedansą aukštų kintamosios srovės dažnių intervale. Gauti EIS duomenys buvo normalizuoti į geometrinį darbinio elektrodo paviršiaus plotą – 0,32 cm^2.

Drėkinimo kampo matavimai. Drėkinimo kampo matavimai buvo atlikti naudojant „Theta Lite“ optinį tensiometrą užlašinant 6-8 distiliuoto 10 μL vandens lašus ant tiriamo paviršiaus. Standartiniai nuokrypiai gauti įvertinant 5 skirtingus tiriamuosius paviršius.

Savitvarkio monosluoksnio formavimas ant titano paviršiaus

Savitvarkio monosluoksnio formavimas ant mechaniškai nupoliruoto metalurginio titano paviršiaus buvo stebimas drėkinimo kampo, ciklinės voltamperometrijos ir elektrocheminio impedanso spektroskopijos metodais. Buvo pastebėta, jog paviršiaus savybės skiriasi, naudojant skirtingus organinius tirpiklius (acetoną arba heksaną) paviršiaus plovimo stadijoje. Naudojant heksaną, toliau $Ti_{heksanas}$, drėkinimo kampų vertės buvo gautos didesnės (8°), nei naudojant acetoną, toliau $Ti_{acetonas}$ (9A pav., 25 psl). Remiantis ciklinės voltamperometrijos duomenimis, idealiai poliarizuojamos srities intervalas $Ti_{acetonas}$ atveju buvo tarp -0,4 V iki -0,2 V Ag/AgCl palyginamojo elektrodo atžvilgiu. Tačiau, $Ti_{heksanas}$ atveju, idealiai poliarizuojama sritis padidėjo per -0,05 V anodinėje srityje (9B pav., 25 p.). Taip pat, abiejų paviršių elektrocheminio impedanso spektrai, pateikti Cole-Cole koordinatėse, skyrėsi (10 pav., 26 p.). $Ti_{acetonas}$ atveju kompleksinių talpų vertės ($23,78 \pm 4,50$ μF cm^{-2}) buvo mažesnės, nei $Ti_{heksanas}$ atveju ($29,18 \pm 4,24$ μF cm^{-2}). Didesnės kompleksinių talpų vertės, gautos ant $Ti_{heksanas}$ paviršiaus, parodo esant plonesnį dielektrinio oksido sluoksnio storį. Taigi, Ti elektrodų skirtingas paviršiaus paruošimas daro įtaką paviršiaus savybėms. Visų pirma, didesnis hidrofiliškumas buvo gautas ant $Ti_{acetonas}$ paviršiaus. Antra, $Ti_{acetonas}$ paviršius, sprendžiant iš EIS duomenų, pasižymėjo didesniu homogeniškumu dėl mažesnių kompleksinių talpų verčių bei taisyklingesnės pusapskritimio formos Cole-Cole koordinatėse (10 pav., 26 p.). Tačiau platesnis idealiai poliarizuojamos srities intervalas buvo gautas ant $Ti_{heksanas}$ paviršiaus. Todėl buvo nuspręsta savitvarkius monosluoksnius bei dirbtines fosfolipidines membranas formuoti ant abiejų paviršių.

Siekiant nustatyti optimalias OTS savitvarkio monosluoksnio formavimo sąlygas, buvo tiriama OTS koncentracijos įtaka savitvarkio monosluoksnio formavimui. Buvo parinktos trys koncentracijos: 2,5 mM, 25 mM, 125 mM. Remiantis padidėjusiomis drėkinimo kampų vertėmis (1 lentelė, 27 p.) bei kompleksinių talpų sumažėjimu (12 pav., 29 p.), galima teigti, kad savitvarkiai monosluoksniai susiformavo ir ant $Ti_{acetonas}$, ir ant $Ti_{heksanas}$ paviršių. Būtina paminėti, jog savitvarkiai monosluoksniai buvo tiriami prieš ir po kaitinimo krosnyje 1 h, esant 100 °C temperatūrai. Kaitinant savitvarkį monosluoksnį pasišalina prisiadsorbavusios vandens molekulės bei susidaro tvarkingesnis savitvarkis monosluoksnis. Po savitvarkio monosluoksnio kaitinimo, ant $Ti_{heksanas}$ paviršiaus buvo gautos didžiausios kontaktinių kampų vertės ir mažiausios kompleksinių talpų vertės, atitinkamai $102,27 \pm 1,76°$ ir $1,02 \pm$

0,17 µF cm^{-2}, todėl tolimesniems tyrimams buvo pasirinktas naudoti $Ti_{heksanas}$ paviršius.

Hibridinės bisluoksnės membranos formavimas ant titano paviršiaus

Hibridinės bisluoksnės membranos formavimas buvo tiriamas EIS metodu. Membrana ant OTS funkcionalizuoto titano paviršiaus buvo formuojama vezikulių liejimo metodu. Iš EIS duomenų yra matoma, jog po DOPC:Chol (lipidų molinis santykis % 6:4) vezikulių liejimo, kompleksinės talpos vertės sumažėja nuo 1,02 ± 0,17 µF cm^{-2} iki 0,61 ± 0,06 µF cm^{-2} (13 pav., 31 p.), kas parodo papildomo dielektrinio sluoksnio t.y., hibridinės bisluoksnės membranos susidarymą. Taip pat buvo nustatytas hibridinės bisluoksnės membranos susiformavimo laikas – 20 min, per kurį yra pasiekiama mažiausia kompleksinės talpos vertė. Pagal plokščiojo kondensatoriaus formulę (9 formulė, 29 p.) buvo apskaičiuotas hibridinės membranos storis, kuris lygus 3,57 nm ir atitinka literatūroje pateiktas vertes.

Hibridinės bisluoksnės membranos regeneracija

Siekiant išsiaiškinti OTS savitvarkio monosluoksnio daugkartinį panaudojimą hibridinėms bisluoksnėms membranoms formuoti, buvo atlikti savitvarkio monosluoksnio regeneracijos eksperimentai. T.y., suformavus hibridinę membraną vezikulių liejimo metodu ant OTS savitvarkio monosluoksnio, membrana buvo nuplauta izopropanolio/distiliuoto vandens tirpalu (tūrinis santykis, 1:1). Nustatyta, jog po kiekvienos hibridinės bisluoksnės membranos nuplovimo, savitvarkio monosluoksnio kompleksinė talpa didėjo (14 pav., 32 p.), kas parodo dielektrinio sluoksnio (OTS) nusiplovimą nuo paviršiaus. Nepaisant to, hibridinės membranos kompleksinė talpa išliko beveik pastovi. Tik po ketvirtos hibridinės bisluoksnės membranos formavimo, kompleksinių talpų vertės padidėjo. Todėl galima teigti, jog hibridinę bisluoksnę membraną ant Ti paviršiaus galima regeneruoti 3 kartus.

Hibridinės bisluoksnės lipidinės membranos sąveika su fosfolipaze A_2

Siekiant įvertinti hibridinės membranos panaudojimą kaip fosfolipidinį biologinį jutiklį, FFT-EIS metodu realiu laiku buvo tiriama sąveika tarp DOPC:Chol (molinis santykis %, 6:4) hibridinės bisluoksnės membranos ir membranos pažaidą sukeliančio baltymo – fosfolipazės A_2 (PLA2). Injekavus į elektrocheminę celę 500 nM PLA2 jau pirmomis minutėmis buvo matomas kompleksinės talpos padidėjimas nuo 0,58 µF cm^{-2} iki 0,94 µF cm^{-2} (16A pav., 33 p.), kas rodo dielektrinio sluoksnio (hibridinės dvisluoksnės membranos) destrukciją. Tolimesnis kompleksinės talpos padidėjimas iki 1,12 µF cm^{-2}

buvo pastebėtas po 25 min PLA2 injekcijos į elektrocheminę celę. Didinant PLA2 inkubacijos laiką, buvo pastebėta, jog kompleksinių talpų vertės atitinka savitvarkio monosluoksnio kompleksinių talpų vertes (16A pav., 33 p.), t.y., hibridinė membrana yra pilnai suardoma.

PLA2 poveikis hibridinei bisluoksnei membranai buvo tiriamas ir koncentracijų intervale tarp 25-250 nM (16B pav., 33 p.). Esant 25 nM PLA2 koncentracijai, hibridinės membranos kompleksinės talpų vertės nepakito. Tačiau, esant 50 nM PLA2 koncentracijai buvo gautas aiškiai matomas kompleksinės talpos padidėjimas iki 0,77 μF cm^{-2}. Toliau didinant PLA2 koncentraciją iki 250 nM buvo užfiksuotas kompleksinės talpos padidėjimas iki 1,12 μF cm^{-2}.

Hibridinės membranos jautrumas PLA2 baltymui gali būti panaudotas kuriant biologinius jutiklius, jautrius baltymo koncentracijai ir/arba jo aktyvumui. Tuo tikslu, 17 paveikslėlyje, 25 p. buvo atvaizduotas parametro Y/ω, esant 213 Hz dažniui, (Y yra elektrodo admitansas, o ω yra kampinis dažnis) priklausomybė nuo PLA2 koncentracijos (25-500 nM). Logaritminėse koordinatėse (Y/ω vs $\log C_{PLA2}$) (17B pav., 25 p.) buvo gauta tiesinė priklausomybė. Ši priklausomybė gali būti panaudota siekiant įvertinti membranos pažaidą sukeliančio baltymo, PLA2, koncentraciją ir/ar jo aktyvumą.

Mišrių savitvarkių monosluoksnių formavimas ant metalurginio titano paviršiaus

Siekiant suformuoti mišrias hibridines bisluoksnes membranas, ant mechaniškai nupoliruoto titano paviršiaus buvo formuojami mišrūs savitvarkiai monosluoksniai. Mišrių savitvarkių monosluoksnių formavimas ant Ti paviršiaus, naudojant įvairius OTS ir MTS molinius santykius silanizavimo tirpale, buvo tiriamas drėkinimo kampo ir elektrocheminio impedanso spektroskopijos metodais. Kaip prieš tai buvo nustatyta, švaraus ir nupoliruoto titano paviršiaus drėkinimo kampų vertės siekė 54° ± 3° (9 pav., 25 p.). Po silanizavimo reakcijos, OTS savitvarkiu monosluoksniu funkcionalizuoto titano paviršiaus drėkinimo kampų vertės padidėjo iki 102° ± 2° (1 lentelė, 27 p.). Nustatyta, jog didinant MTS molinį santykį silanizavimo tirpale, drėkinimo kampų vertės nuosekliai mažėja (18 pav., 36 p.). Visais atvejais, (išskyrus MTS funkcionalizuotą titano paviršių), drėkinimo kampų vertės viršijo 90° ribą, kuri yra reikalinga fosfolipidinių membranų formavimui.

Funkcionalizavus mišriais savitvarkiais monosluoksniais titano paviršių įvairiais OTS:MTS moliniais santykiais, kompleksinių talpų vertės visais

atvejais sumažėjo. MTS funkcionalizuoto titano paviršiaus kompleksinių talpų vertės sumažėjo nuo 29 ± 4 μF cm^{-2} (prieš silanizavimo reakciją) iki 6,17 ± 1,44 μF cm^{-2} (19A pav., 39 p.). Didinat OTS molinį santykį silanizavimo tirpale (19B-E pav., 39 p.), kompleksinių talpų vertės tolygiai mažėjo. Mažiausia kompleksinės talpos vertė buvo gauta 1,02 ± 0,17 μF cm^{-2}, kai titano paviršius buvo funkcionalizuotas tik OTS savitvarkiu monosluoksniu. Palaipsniui kintančios kompleksinių talpų vertės, gautos naudojant skirtingus OTS ir MTS molinius santykius silanizavimo tirpale, rodo skirtingą savitvarkių monosluoksnių paviršiaus storį. Be to, EIS eksperimentiniai rezultatai koreliuoja su drėkinimo kampo matavimo rezultatais (18 pav., 36 p.), kurie parodė, jog drėkinimo kampų vertės didėja, didinant OTS molinį santykį silanizavimo tirpale. Taigi, mišrūs savitvarkiai monosluoksniai buvo suformuoti ant titano paviršiaus, keičiant OTS ir MTS molinius santykius silanizavimo tirpale.

Mišrios hibridinės bisluoksnės membranos formavimas

Mišri hibridinė bisluoksnė membrana buvo formuojama vezikulių liejimo metodu ant titano paviršiaus, funkcionalizuoto įvairiais OTS ir MTS moliniais santykiais. Remiantis EIS duomenimis, po vezikulių liejimo metodo, MTS funkcionalizuoto titano paviršiaus elektrocheminio impedanso spektras Cole-Cole koordinatėse beveik nepakito t.y., hibridinė membrana nesusiformavo (19A pav., 39 p.). Tačiau, esant net ir mažam OTS molekulių kiekiui OTS:MTS silanizavimo tirpale, buvo nustatytas kompleksinės talpos sumažėjimas. Be to kompleksinės talpos sumažėjimas buvo užfiksuotas didinant OTS molinę dalį silanizavimo tirpale (19B-E pav., 39 p.). Tačiau naudojant 2:8 ir 4:6 OTS:MTS moliniu santykiu suformuotus mišrius savitvarkius monosluoksnius, gauta mišrių hibridinių bisluoksnių membranų EI spektrų forma Cole-Cole koordinatėse nepasižymėjo taisyklinga pusapskritimio forma ir tai gali būti siejama su padidėjusiu fosfolipidinių membranų defektiškumu. Nepaisant to, beveik taisyklingos pusapskritimio formos EIS atsakas buvo gautas formuojant fosfolipidines membranas ant mišrių savitvarkių monosluoksnių, gautų naudojant 6:4 ir 8:2 OTS:MTS molinius santykius. Šių mišrių bisluoksnių lipidinių membranų kompleksinių talpų vertės buvo gautos atitinkamai 0,86 ± 0.22 μF cm^{-2} bei 0,83 ± 0,18 μF cm^{-2} ir yra artimos toms, kurios buvo gautos tiriant hibridines membranas, suformuotas ant 100 % OTS savitvarkio monosluoksnio (0,61 ± 0,06 μF cm^{-2}). Panaši kompleksinių talpų tendencija yra matoma formuojant paviršiuje imobilizuotas fosfolipidines membranas ant aukso paviršių.

Mišrios hibridinės bisluoksnės membranos sąveika su pneumolizinu ir α-hemolizinu

Mišrios hibridinės membranos funkcionalumas buvo tiriamas naudojant pneumoliziną (PLY) ir α-hemoliziną (αHL). Šių toksinų, sukeliančių membranos pažaidą, veikimas buvo nagrinėjamas EIS metodu. Pneumolizino sąveika buvo tiriama naudojant DOPC:Chol (molinis santykis % 6:4) hibridinę bisluoksnę membraną. Buvo nustatyta, jog injekavus į celę 100 nM PLY, mišrios hibridinės membranos kompleksinės talpos vertės po 1 valandos pakito nežymiai, nuo 0,72 μF cm^{-2} iki 0,86 μF cm^{-2} (21A pav., 43 p.). Tačiau tokios pačios koncentracijos PLY efektas nebuvo užfiksuotas ant DOPC mišrios hibridinės bisluoksnės membranos. Tai parodo PLY specifinę sąveiką su cholesteroliu. Be to, membranos varžos pokytis <10 Hz dažnių srityje buvo mažesnis nei 24 % (2 lentelė, 46 p.) po toksino sąveikos su membrana. Remiantis literatūros duomenimis, tiek kompleksinės talpos vertės, tiek hibridinės membranos varžos pokytis tūrėtų būti didesnis po 100 nM PLY sąveikos. Dėl to galime daryti prielaidą, jog šiuo atveju PLY neįsiterpimas į membraną, tačiau PLY sąveikauja su cholesteroliu esančiu mišrioje hibridinėje bisluoksnėje membranoje.

Kita vertus, skirtingas poveikis buvo stebimas naudojant αHL toksiną su DPhyPC mišria hibridine bisluoksne membrana. Po vienos valandos sąveikos su 500 nM αHL, mišrios hibridinės membranos kompleksinės talpos vertė ženkliai padidėjo nuo 0,71 μF cm^{-2} iki 1,32 μF cm^{-2} (21B pav., 43 p.). Be to, žemesnių dažių srityje varžos pokytis išreikštas procentais buvo didesnis (<45 %)(2 lentelė, 46 p.), nei PLY atveju. Lyginant su literatūroje esančiais duomenimis, tokį αHL efektą galima sieti su jo įsiterpimu į fosfolipidinę mišrią hibridinę membraną.

Savitvarkio monosluoksnio formavimas ant metalurginio aliuminio paviršiaus

Mechaniškai nupoliruoto aliuminio paviršiaus nustatytos drėkinimo kampo vertės buvo lygios 41,72 ± 3,96° (24A pav., 48 p.). Po silanizavimo reakcijos Al paviršius tapo hidrofobiškas, ir drėkinimo kampų vertės padidėjo iki 105,13 ± 2.02° (24A pav., 48 p.). Paviršiaus drėkinimo savybių pasikeitimas iš hidrofilinių į hidrofobines parodo organinio OTS monosluoksnio susiformavimą.

Siekiant išsiaiškinti, kokiame elektrodo potencialo intervale nevyksta oksidacijos ir redukcijos reakcijos, buvo atlikti CV matavimai. Iš ciklinės voltamperometrijos duomenų (24B pav., 48 p.) buvo nustatyta, jog Al

paviršius fosfatiniame buferiniame tirpale (pH 7,1), skleidžiant potencialią intervale nuo -1,1 V iki -0,5 V Ag/AgCl palyginamojo elektrodo atžvilgiu, neturi idealiai poliarizuojamos srities. Remiantis literatūros duomenis, aliuminio paviršius turėtų būti elektrochemiškai inertiškas tirpaluose, pasižyminčiuose neutraliu pH (~7). Tačiau šiuo atveju, dėl fosfatiniame buferiniame tirpale esančių chlorido anijonų, vyko lokali (pitingo) Al korozija. Nepaisant to, suformavus ant aliuminio paviršiaus OTS savitvarkį monosluoksnį, idealiai poliarizuojama sritis jau buvo stebima skleidžiant potencialą intervale nuo -1,1 V iki -0,65 V Ag/AgCl palyginamojo elektrodo atžvilgiu, net ir esant chlorido anijonų fosfatiniame buferiniame tirpale (24B pav., 48 p.). Tai parodo, jog suformuotas OTS savitvarkis monosluoksnis apsaugo Al paviršių nuo chlorido anijonų įtakos.

Hibridinės bisluoksnės membranos formavimas ant metalurginio aliuminio paviršiaus

OTS monosluoksnio ir hibridinės bisluoksnės membranos formavimas buvo stebimas EIS metodu. Nustatyta, jog aliuminio paviršiaus kompleksinių talpų vertės buvo $4,82 \pm 0,59$ μF cm^{-2} (26 pav., 50 p.). Po silanizavo reakcijos, kompleksinės talpų vertės sumažėjo iki $1,1 \pm 0,11$ μF cm^{-2} (26 pav., 50 p.), kas parodo dielektrinio sluoksnio susidarymą.

Vezikulių liejimo procesas buvo stebimas realiu laiku naudojant FFT-EIS metodą. Lipidinio sluoksnio adsorbcijos kinetika buvo įvertinta pagal lipidinio sluoksnio paviršiaus užpildymo laipsnį – θ (14 lygtis, 51 p.) – tam tikru laiko momentu (27 pav., intarpas, 52 p.). Iš kinetinės kreivės buvo pastebėta dviejų pakopų adsorbcija, būdinga ampifilinėms molekulėms. Pirmoje pakopoje, lipidai adsorbuojasi horizontaliai prie savitvarkio monosluoksnio. Toliau vykstant adsorbcijai, lipidų molekulės persitvarko paraleliai paviršiaus atžvilgiu.

Hibridinės bisluoksnės membranos suformuotos ant aliuminio paviršiaus sąveika su melitinu

Hibridinės dvisluoksnės membranos, suformuotos ant aliuminio paviršiaus, funkcionalumas buvo tiriamas naudojant membranos pažaidą sukeliantį toksiną – melitiną. Buvo nustatyta, jog melitino poveikis hibridinei bisluoksnei membranai priklauso nuo peptido koncentracijos bei hibridinės bisluoksnės membranos lipidinės sudėties. Naudojant 200 nM melitino, DOPC:Chol (molinis santykis %, 6:4) hibridinės bisluoksnės membranos EI spektras nepasikeitė (29A pav., 55 p.). Tačiau padidinus melitino koncentraciją iki 500 nM, DOPC:Chol (molinis santykis %, 6:4) hibridinės

bisluoksnės membranos kompleksinių talpų vertės stipriai pasikeitė nuo 0,64 μF cm^{-2} iki 1,06 μF cm^{-2} (30 pav., 55 p.), kas parodo pilną membranos suardymą.

Melitino sąveika su cholesterolio neturinčiomis hibridinėmis bisluoksnėmis membranomis buvo skirtinga. Esant 100 nM melitino koncentracijai, sąveika buvo pastebėta pagal kompleksinių talpų verčių padidėjimą nuo 0,8 μF cm^{-2} iki 0,88 μF cm^{-2} (29B pav., 55 p.), o esant 400 nM melitino koncentracijai, DOPC hibridinė membrana yra visiškai suardoma (29D pav., 55 p.).

Šie tyrimai parodo, jog hibridinė bisluoksnė membrana, suformuota ant aliuminio paviršiaus, yra funkcionali. Melitino sąveika su hibridine bisluoksne membrana atitinka literatūroje esančius šaltinius, kur parodoma, jog melitino poveikis yra slopinamas, kai hibridinėje bisluoksnėje membranoje yra cholesterolio.

IŠVADOS

1. Ant mechaniškai nupoliruotų metalurginių titano ir aliuminio paviršių gali būti formuojami oktadeciltrichloro savitvarkiai monosluoksniai. Nustatyta, kad optimali oktadeciltrichlorosilano koncentracija savitvarkių monosluoksnių formavimui lygi 2,5 mM.
2. EIS metodu nustatyta, kad ant metalurginio titano paviršiaus suformuotos hibridinės bisluoksnės membranos kompleksinės talpos vertė lygi 0,61 ± 0,06 μF cm^{-2}, o hibridinės bisluoksnės membranos storis – 3,57 nm. Suformuota hibridinė bisluoksnė membrana gali būti naudojama fosfolipazės A_2 detekcijai realiu laikui.
3. Ant metalurginio titano paviršiaus gali būti formuojamos mišrios hibridinės bisluoksnės membranos. Nustatyta, kad optimalus OTS ir MTS molinis santykis mišrių hibridinių membranų formavimui yra 6:4. Suformuota mišri bisluoksnė hibridinė membrana gali būti naudojama biologinių jutiklių kūrimui.
4. Ant mechaniškai nupoliruoto metalurginio aliuminio paviršiaus gali būti formuojama hibridinė bisluoksnė membrana, pasižyminti puikiomis izoliacinėmis savybėmis ir tinkama biologinių jutiklių kūrimui.
5. Hibridinės bisluoksnės membranos suformuotos ant metalurginių titano ir aliuminio paviršių bei mišri hibridinė bisluoksnė membrana suformuota ant titano paviršiaus gali būti formuojamos keletą kartų ant to pačio savitvarkio monosluoksnio.

ACKNOWLEDGEMENTS

I would like to thank to a lot of people who so generously contributed in one way or another to the work presented in this thesis.

First of all, I would like to express my deep gratitude to my supervisor assoc. prof. dr. Aušra Valiūnienė and consultant prof. dr. Gintaras Valinčius who have guided and supported me with their brilliant ideas, wisdom, guidance and patience. I don't think I could have asked for a better mentors. They have inspired me to strive for excellence, and to keep a high standard throughout my future career and life.

I would also like to thank the members of the Department of the Physical chemistry at Vilnius University as well as the administration personnel for their help and support.

I would also like to acknowledge my lab mates, Inga, Asta, Povilas, Modestas, Ramūnas, Edita, Tomas and Tadas for their amazing work environment, energy, and good sense of humor.

Finally, I would like to thank my family, who have given me moral and emotional support. Also, I would like to especially thank Elena for her support, motivation, and patience.

ARTICLE I

Mechanically Polished Titanium Surface for Immobilization of Hybrid Bilayer Membrane

T.Sabirovas, A. Valiūnienė, G. Valincius

Journal of The Electrochemical Society, 165 (10) G109-G115 (2018)

Journal of The Electrochemical Society, **165** (10) G109-G115 (2018)
0013-4651/2018/165(10)/G109/7/$37.00 © The Electrochemical Society

Mechanically Polished Titanium Surface for Immobilization of Hybrid Bilayer Membrane

Tomas Sabirovas,[1] Aušra Valiūnienė,[1,z] and Gintaras Valincius[2]

[1]*Department of Physical Chemistry, Faculty of Chemistry and Geosciences, Vilnius University, Vilnius LT-03225, Lithuania*
[2]*Institute of Biochemistry, Life Sciences Center, Vilnius University, Vilnius LT- 10257, Lithuania*

In this work, hybrid bilayer lipid membrane (hBLM) was assembled on a mechanically polished metallurgical titanium plate. Hydrophobic molecular anchors needed for phospholipid overlayers were obtained by silanization of the Ti surface with octadecyltrichlorosilane (OTS). The formation of hBLM was accomplished by fusion of the multilamellar vesicles containing of 1, 2-dioleoyl-sn-glycero-3-phosphocholine (DOPC) and cholesterol (Chol) at molar % ratio 60/40. The fusion process was monitored in real-time by the dynamic fast Fourier transformation (FFT) electrochemical impedance spectroscopy. We found that the repetitive regeneration of hBLM can be performed up to 4 times with no major loss of the electrochemical properties. Also, we showed that the electric barrier function of hBLMs is disrupted by phospholipase A_2 (PLA2) – an enzyme, which hydrolyzes the fatty acid bonds at *sn2* position in membrane phospholipids. Such effect may be used to design biosensors sensitive to both concentration and activity of the membrane damaging proteins, and possibly other agents.
 [DOI: 10.1149/2.0101810jes]

Manuscript submitted April 26, 2018; revised manuscript received June 11, 2018. Published June 30, 2018.

Plasma membrane is one of the most essential structures in the cell which separates cell interior from the environment and/or extracellular matrix. Wide range of proteins is incorporated in the lipid bilayer. These proteins are responsible for a number of functions: compartmentalization of life components, cell-to-cell electric and/or chemical communications, recognition and biosignaling, and others. To simplify this complex system, various lipid bilayer models were developed and used for biochemical and biophysical studies involving protein-lipid interaction,[1] ion transportation,[2,3] immunology,[4] drug screening,[5] biosensor development[6–8] and others.

One of the models is solid-supported lipid bilayer. This model has been intensively studied on various substrates such as gold[9,10] glass[11,12] or other supports.[13–17] The deposition of lipid membrane on the surface allows probing the surface with techniques that are surface specific (e.g. quartz crystal microbalance, atomic force microscopy, surface plasmon resonance, electrochemical impedance spectroscopy, etc.). However, such model system is still relatively unstable, and the small space between the membrane and solid support hinders protein incorporation, since incorporated proteins most likely interacts with solid supports.[18] Such unwanted interactions also may interfere with protein mobility and function.[19]

An alternative approach to study lipid membranes, which includes engineering a hydrophilic space between the lipid membrane and substrate is a hybrid bilayer lipid membranes. Typically, such model is more robust and has higher stability than suspended on a surface lipid bilayers due to the strong bond between the self-assembled monolayer (SAM) and substrate.[20] This system has a separated inner leaflet from the solid support through a spacer unit, which anchors a lipid membrane.[21] Also, these systems are generally easy to form through self-assembly methods and can be characterized by a variety of surface science techniques. Mostly, gold as a substrate have been used, since it can be easily modified by thiol and sulfur based anchoring units.[22] Also, there have been examples for the formation of hybrid lipid bilayers on hafnium oxide substrate,[23] silicon,[24] alumina,[25] etc. For oxide surfaces, such as alumina, glass, tin oxide, titanium oxide and others silanes are a viable choice for forming SAMs, because silane-based SAMs are less mobile and hence less prone to structural rearrangements upon annealing, in comparison with thiol-Au systems.[26] Titanium is the most interesting one, because it has been used in biomedical devices and components, it has high chemical stability, mechanical resistance, non-toxicity and most important – biocompatibility.[27,28] Main drawback is that the quality of these SAMs is very sensitive to the conditions, such as preparation of the substrate, solvent used in silanization, the amount of water present in the system, the temperature and most important, the substrate.[29]

Magnetron sputtered titanium surfaces are associated with significant cost for specimen and in most cases they are disposed after single use. Therefore, we aimed at formation of hybrid bilayer lipid membranes on a mechanically polished titanium surface with its native oxide layer. Octadecyltrichlorosilane (OTS) was formed on titanium as an anchoring layer for hybrid bilayer formation. The surface properties as well as vesicle fusion which was used to transfer phospholipids to a surface were investigated by the contact angle (CA) methodology and Fast-Fourier transform electrochemical impedance spectroscopy (FFT EIS). Accomplished hybrid bilayers were challenged with the Phospholipase A_2 (PLA2) capable of hydrolyzing phospholipid in cell membranes.

Experimental

Preparation of titanium plate electrode.—Commercially produced metallurgical titanium plate (99% purity, Alfa Aesar GmbH & Co KG) was polished using diamond lapidary paste 200,000 grit 0/0.1 micron, 50% concentration of diamond powder at 1000 rpm until mirror like surface was achieved. Polished titanium plate was sonicated for 15 min each in acetone or hexane, 2% MICRO-90/Mili-Q water solution, 2-propanol and Mili-Q water. After sonication, titanium plate was dried under N_2 stream.

Silanization.—Formation of octadecyltrichlorosilane (OTS) (Sigma-Aldrich) self-assembled monolayer was formed on cleanly washed titanium plate. Titanium plate was immersed vertically in a small beaker in OTS in heptane (Sigma-Aldrich) solution. The temperature was kept between 60–65°C without stirring or stirring solution at 500 rpm for 45 min. After 45 min, silanized titanium plate was rinsed in heptane and dried under nitrogen stream. Then, functionalized titanium plates were kept under 100°C for 1 h.

Hybrid bilayer formation.—Hybrid bilayer was formed using multilamellar vesicle-fusion method described in the ref. 30. Vesicle solution consisting of 1, 2-dioleoyl-sn-glycero-3-phosphocholine (DOPC) (Avanti Lipids Alabaster, USA) and cholesterol (Avanti Lipids Alabaster, USA) in chloroform at molar % ratio 60/40 was prepared by gently drying mixed lipids solution under N_2 stream until formation of lipid film. Then vesicle film was re-suspended gently by phosphate buffer (0.1 M NaCl, 0.01 M NaH_2PO_4) pH 4.6 to total 1.5 mM concentration. Phospholipase A_2 from bee venom (Sigma-Aldrich) was diluted in working buffer (PBS, 0.1 M NaCl, 0.01 M NaH_2PO_4) to 68.96 μM.

[z]E-mail: ausra.valiuniene@chf.vu.lt

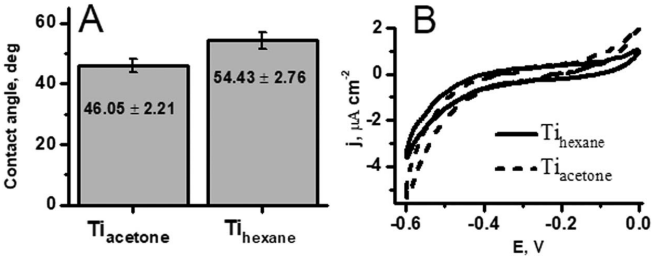

Figure 1. Properties of Ti surface cleaned by using different solvents detected A – by measuring contact angles; B – by recording cyclic voltammograms in phosphate buffer solution pH 7.1.

Electrochemical measurements.—All measurements were carried out in phosphate buffer (0.1 M NaCl and 0.01 M NaH_2PO_4) pH 7.1 at 0 V. Electrochemical impedance spectra were measured using fast Fourier transform impedance spectrometer EIS-128/16[31] (University of Kiel, Germany) and selected frequency range was between 1.5 Hz and 50 kHz, using four-electrode configuration. A saturated silver-silver chloride (Ag/AgCl/NaCl (sat.)) microelectrode (M-401F, Bedford, USA) was used as a reference. Two platinum (99.99% purity, Aldrich) wires were used. One as a quasi-reference electrode, which was connected to 1 μF capacitor to reduce the impedance of the reference electrode at higher frequencies and another one as auxiliary, which was coiled around the barrel of the reference electrode. Titanium plate was used as a working electrode. The working volume of the electrochemical cell was 300 μL and the surface area of the cell was 0.32 cm^2. Throughout this paper the specific capacitance refereeing to a 1 cm^2 of the geometric area of the working electrodes are presented and discussed.

Cyclic voltammetry was measured using μAUTOLAB from ECO-Chemie (Utrecht, The Netherlands), which was performed in conventional three-electrode configuration (same as for electrochemical impedance measurements, except quasi-reference electrode). All the potentials given in this article are referred to the Ag/AgCl/NaCl (sat.) electrode.

Contact angle measurements.—Theta Lite Optical Tensiometer from Biolin Scientific (Finland) was used for contact angle measurements. CA was measured by placing eight droplets of 10 μL each Mili-Q water on different spots on the surface. Measurements were performed on freshly cleaned titanium plate at ambient conditions.

Results and Discussion

Properties of titanium plate electrode cleaned by using different solvents.—The first step in assembling hybrid bilayers is preparation of substrate on which SAM will be formed. In our study we used commercially produced metallurgical titanium plate, surface of which was cleaned and polished to mirror-like appearance. The polished surface exhibited hydrophilicity and was ready for functionalization by octadecyltrichlorosilane. After the silanization, the surface became hydrophobic as determined by the contact angle measurements. In our experiments, polished Ti surface was rather hydrophilic exhibiting contact angles of approx. 50° ± 5° (Fig. 1A). This value is comparable to the value reported earlier for the magnetron sputtered thin-film Ti electrode.[32] However these contact angles are higher than those obtained for gold[33] or cadmium stannate[34] described in our previous research. To obtain more hydrophilic Ti surfaces the effect of the cleaning solvent was investigated. Figure 1A shows that replacing hexane with acetone causes consistently lower values of the contact angle. Different contact angles may reflect different chemical compositions of the oxide covered surfaces. For example, according to Eslamibidgoli et al.[35] the surfaces of NiOOH and $Ni(OH)_2$ have different wettability parameters. Water interacts weakly with $Ni(OH)_2$ due to a weak dipole moment of the surface. Surface of NiOOH have strong interaction with water because of its high dipole moment, moreover unsaturated O atoms form hydrogen bonds with water which leads to a stronger interaction with water molecules. Based on consistently higher contact angle values we presume that the hexane cleaned titanium surface have more hydroxyl surface groups.

Ti electrodes treated using different cleaning solutions were analyzed by the cyclic voltammetry. Fig. 1B compares cyclic voltammograms from Ti electrodes cleaned with acetone ($Ti_{acetone}$) and Ti electrodes cleaned with hexane (Ti_{hexane}). $Ti_{acetone}$ electrode exhibited nearly ideal polarizability in the potential interval (Fig. 1B, dashed line) from −0.4 V to −0.2 V (vs Ag/AgCl/NaCl (sat.)). Ti_{hexane} surface exhibited wider ideal polarizability interval extending to the anodic range up to −0.05 V (Fig. 1B, solid line).

The method of electrochemical impedance spectroscopy is capable of testing ideally polarizable interfaces. Fig. 2 displays electrochemical impedance spectra obtained on Ti_{hexane} and $Ti_{acetone}$ electrodes plotted in the complex capacitance format.[36] Independently on the type of electrode, the obtained complex capacitance plots exhibit semi-circular shape similar to ones observed earlier for sputtered Ti thin-film electrodes.[32] Such a shape is typical for ideally polarizable interphases exhibiting near ideal capacitive behavior.[37] The diameter of the semicircle is equal to capacitance of the double layer of the surface. The values of specific capacitances were calculated from the complex capacitance plots, by taking the maximum point of the semicircular curve, which represents the radius of the semicircle and multiplying it by two. The specific capacitances of the $Ti_{acetone}$ and Ti_{hexane} electrodes were found to be 23.78 ± 4.50 μFcm^{-2} and 29.18 ± 4.24 μFcm^{-2} respectively. Slightly higher capacitances observed for Ti_{hexane}. This may attest for the thinner dielectric oxide layer on Ti_{hexane} interface, which though exhibits slightly less polar environment as deduced from the contact angle data in Fig. 1A.

Formation of the layer of octadecyltrichlorosilane on titanium surface.—*Influence of cleaning solvent of Ti substrate and effect of heating on the properties of SAM.*—Preparation of Ti plate electrodes by using different cleaning solutions resulted in subtle differences in their surface properties. First, higher hydrophilicity was obtained for $Ti_{acetone}$ electrode (Fig. 1A). This feature is an important reason for selecting this type of the electrode for further

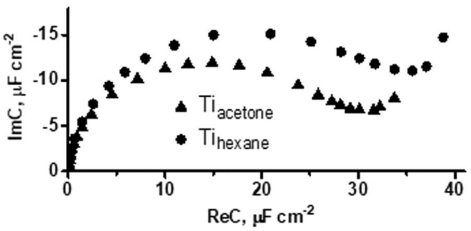

Figure 2. Electrochemical impedance spectra (Cole-Cole plots) of titanium electrode cleaned with different solvents. Electrode potential is −0.3 V vs Ag/AgCl/NaCl (sat.) Solution is the phosphate buffer pH 7.1.

Table I. Comparison of contact angles of the $Ti_{acetone}$ and Ti_{hexane} electrodes, unheated and heated after the silanization in OTS solution of different concentrations.

Cleaning solvent of Ti surface	Concentration of OTS, %	Contact angles, degrees (without heating)	Contact angles, degrees (after heating at 100°C for 1 hour)
Acetone	0.1	95.31 ± 1.81	95.84 ± 1.86
	1	98.01 ± 1.86	101.90 ± 1.94
	5	98.82 ± 1.86	101.45 ± 2.27
Hexane	0.1	99.87 ± 0.98	102.27 ± 1.76
	1	101.84 ± 1.53	100.24 ± 1.92
	5	96.27 ± 1.47	103.81 ± 5.60

modification with OTS SAM. Second, by testing the electrodes using EIS (Fig. 2) it was found that surface of $Ti_{acetone}$ electrode exhibits higher homogeneity compared to Ti_{hexane} electrode, because i) it exhibits smaller value of specific capacitance and ii) it exhibits more complete semicircle in Cole-cole plot (Fig. 2). However, the cyclic voltammogram of $Ti_{acetone}$ electrode (Fig. 1B) showed narrower ideally polarizable interval of potentials than Ti_{hexane} electrode. These were the reasons to continue experiments using both types of Ti electrodes.

Table I summarizes CA data obtained in the course of silanization of $Ti_{acetone}$ and Ti_{hexane} electrodes by using different concentrations of OTS. As expected, a clear increase of CA's was observed for both types of electrodes after the silanization. An increase was OTS concentration dependent reaching maximal values of 98.82° ± 1.86° upon silanization in 5% OTS solution for $Ti_{acetone}$ electrode, and values of 101.84° ± 1.53° for Ti_{hexane} electrode in 1% OTS solution. In all the cases the values of the CA exceeded threshold of 90°, indicated earlier as a threshold at which compact lipid overlayers can be formed.[38,39]

The next series of experiments were carried out using heated for 1 h at 100°C Ti electrodes. Electrodes were heated to remove adsorbed water which is known impedes formation of uniform and stable monolayer.[40] CA values increase slightly (Table I) in all the cases exceeding 100° except $Ti_{acetone}$ electrode silanized in 0.1 % OTS solution (95.84° ± 1.86°). Also, the positive effect of the heating was observed analyzing cyclic voltammetry curves (Fig. 3). The potential interval of ideal polarizability was obtained wider in the anodic range of CV (vs Ag/AgCl, NaCl (sat.) electrode) for the silanized and heated Ti_{hexane} electrode compared to that obtained for the silanized and unheated Ti_{hexane} electrode.

Electrochemical impedance spectroscopy and evaluation of specific capacitances.—Formation of OTS monolayer was monitored by the EIS. For both acetone and hexane incubated electrodes the decrease of the electrode capacitance was observed. Comparison of the specific capacitances of $Ti_{acetone}$ and Ti_{hexane} electrodes before and after silanization followed by heating at 100°C for 1 hour is presented in Figure 4. The lowest values of capacitance with the smallest parameter scatter (Fig. 4, gray columns) were observed when 0.1 % OTS concentration solution was used during silanization procedure. Increase in OTS concentration to 5 % results in much higher value of specific capacitances. These features attest for the formation of a more defective and possibly inhomogeneous OTS monolayer. The increase of measured capacitance that follows the increase of the defectiveness is well documented in SAMs on gold.[41] Such increase occurs because the defects present in organic dielectric layer expose high capacitance metal, in the current case - metaloxide patches of surface. As a result the observed electrode capacitance increase. It is interesting to note that the differential capacitances of both $Ti_{acetone}$ and Ti_{hexane} electrodes always decrease upon silanization, however, lower values were consistently observed for Ti_{hexane} electrodes silanized in 0.1 % OTS solution (1.02 ± 0.17 μF cm^{-2}) and in 1 % OTS solution (1.08 ± 0.22 μF cm^{-2}). Higher values of specific capacitances were obtained for the $Ti_{acetone}$ electrode (from 1.26 ± 0.16 μF cm^{-2} to 1.96 ± 0.38 μF cm^{-2}), indicating hexane to be a more efficient as a cleaning solvent for Ti surface than acetone. This finding parallels contact angle measurements showing lower CA values in case of $Ti_{acetone}$ electrodes (Fig. 1A) suggesting higher hydrophilicity of $Ti_{acetone}$ surfaces,

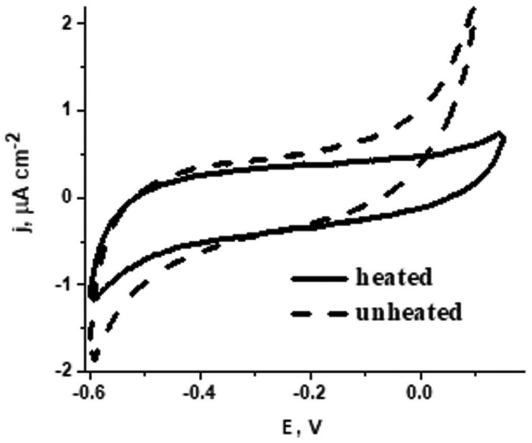

Figure 3. Cyclic voltammograms of unheated (dashed line) and heated at 100°C for 1 hour (solid line) Ti_{hexane} electrode after the silanization in 0.1% OTS solution.

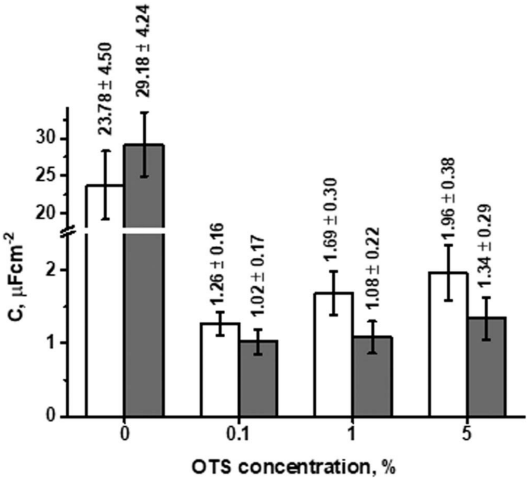

Figure 4. Specific capacitances of Ti_{hexane} (gray columns) and $Ti_{acetone}$ (white columns) electrodes, silanized using various OTS concentrations.

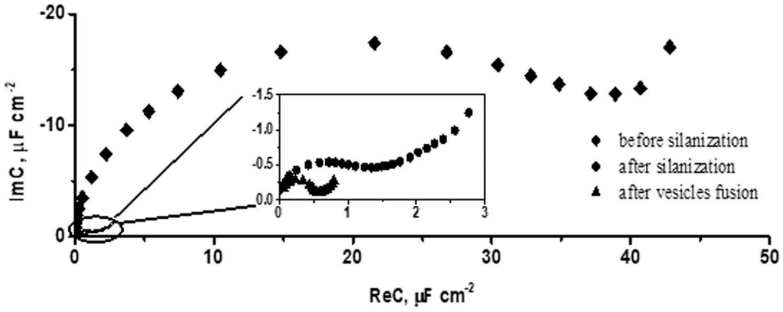

Figure 5. Electrochemical impedance spectra of Ti_{hexane} electrode: diamonds – neat Ti_{hexane} electrode; circles – after silanization in 0.1 % OTS solution with following heating; triangles – after 20 min of DOPC(60 %)/Cholesterol(40 %) vesicles fusion. Electrode potential: 0 V vs Ag/AgCl/NaCl (sat.).

and relatively higher hydrophobicity of Ti_{hexane}. These observations possibly confirm the assumption that Ti_{hexane} may have higher density of the surface hydroxyl groups than $Ti_{acetone}$. Because hydroxyl groups are essential for forming silane bonds, Ti_{hexane} exhibited consistently denser OTS monolayers as deducted from the capacitance OTS modified Ti_{hexane} electrode. The obtained values of specific capacitance are comparable to the ones of the thiolate self-assembled monolayers on gold.[33,42] This indicates the formation of a relatively compact and reproducible anchor monolayer of OTS on Ti_{hexane} surface.

Calculation of the thickness of OTS monolayer.—EIS data obtained for silanized Ti electrode (Fig. 4) gave possibility to estimate the value of thickness of OTS layer. Taking into account that capacitance of the SAM modeled as a parallel plate capacitor can be easily calculated using the following equation:

$$C = (\varepsilon\varepsilon_0)/d \qquad [1]$$

In our case the thickness of OTS SAM, d (cm), can be calculated by using ε – dielectric permittivity of OTS monolayer (2.3), ε_0 – vacuum permittivity (8.85×10^{-14} F cm^{-1}) and C - specific capacitance of silanized Ti electrode, $C_{Ti/OTS}$ (F cm^{-2}), which can be expressed as a sum of two terms:

$$C_{Ti/OTS}^{-1} = C_{Ti}^{-1} + C_{OTS}^{-1} \qquad [2]$$

where C_{Ti} – specific capacitance of Ti plate electrode before silanization, C_{OTS} – specific capacitance of OTS monolayer.

The specific capacitance of OTS film (C_{OTS}) for the Ti_{hexane} electrode silanized in 0.1% OTS solution was calculated to be equal to 1.05 μF cm^{-2} according to Equation 2 by using the experimental data in Fig. 2 (C_{Ti} = 29.18 μF cm^{-2}) and Fig. 4 ($C_{Ti/OTS}$ = 1.02 μF cm^{-2}). By inserting the obtained C_{OTS} value into Eq. 1 the thickness of OTS film was estimated to be 1.94 nm. For Ti_{hexane} electrode silanized in 1% OTS solution it does not changes significantly and was calculated equal to 1.69 nm. These values of thickness are comparable to those obtained for OTS monolayer on thin-film Ti electrode when measured with spectroscopic ellipsometry method and calculated theoretically, which were found to be approximately 2.0 – 2.3 nm.[32] In our case, we conclude that nearly 90 % of the surface of Ti_{hexane} electrode silanized in 0.1 % or in 1 % OTS solution is covered by compact OTS monolayer.

Summarizing, CA data (Figs. 1A) together with the electrochemical experiments using CV and EIS methods (Figs. 3, 4) indicate the formation of a compact hydrophobic OTS monolayer occurs on Ti_{hexane} surface which can be further used for phospholipid hybrid bilayer formation.

Formation of hybrid bilayer by DOPC-Chol vesicles fusion.— In case if the surface is covered by a continuous dielectric sheet of a phospholipid a significant capacitance decrease should be obtained for the electrode.[33] Such modification of the surface can be tested by using EIS. The effect of capacitance decrease of OTS functionalized Ti_{hexane} electrode triggered by the interaction with DOPC-Chol vesicles are shown in Cole-Cole plot (Fig. 5). It was found out that 20 minutes of vesicle fusion were needed to reach values of specific capacitance (0.61 ± 0.06 μF cm^{-2}). Such values are very close to those observed for hybrid bilayer on silanized thin-film Ti electrode[32] and on thiolipid molecular anchors.[43] Consequently, these results show that silanized Ti surface is completely covered by phospholipid film.

Capacitance of the hybrid bilayer, C_{HB}, which can be considered as a composite of OTS and DOPC-Chol layer, can be evaluated using the following equation:

$$C_{hBLM}^{-1} = C_{Ti}^{-1} + C_{HB}^{-1} \qquad [3]$$

in which C_{hBLM} = 0.61 μF cm^{-2} (from EIS data in Fig. 5). By using the calculated value of C_{HB} = 0.62 μF cm^{-2} and assuming the average relative dielectric constant as 2.5, the thickness of the composite of OTS and DOPC-CHOL layer was found to be 3.57 nm. This value is similar for covered by DOPC-Chol bilayer tethered on gold surface.[33,44] The obtained quantitative data of DOPC-Chol layer similar with those proposed previously by other authors,[45,46] enable us to conclude that hybrid bilayer on OTS anchors can be formed on metallurgical Ti substrate. As we show in further experiments (Fig. 6), the obtained OTS monolayer exhibits proper features for phospholipid membrane formation and even has an advantage to be reusable for multiple cycles of vesicles fusion.

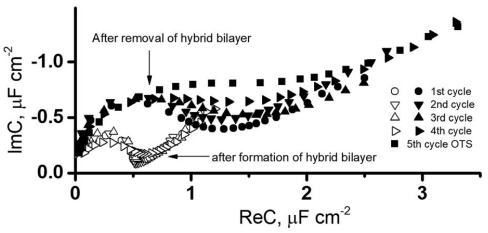

Figure 6. Electrochemical impedance spectra of hybrid bilayer regeneration recorded over 4 cycles of vesicle fusion. Electrode potential: 0 V vs Ag/AgCl/NaCl (sat.).

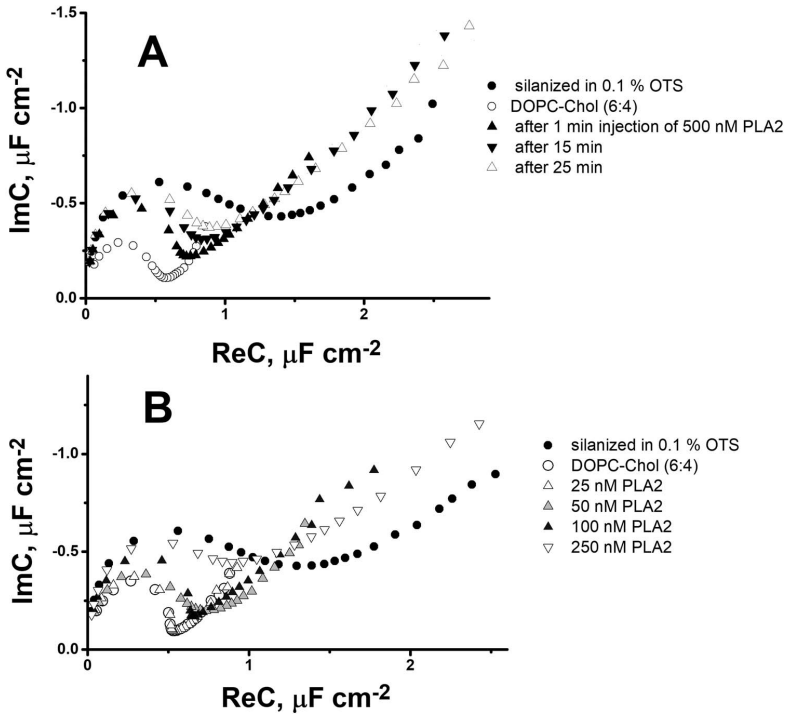

Figure 7. Electrochemical impedance spectra of Ti_{hexane} electrode: filled circles – silanized in 0.1 % OTS solution; open circles - neat DOPC(60%)/cholesterol(40%) bilayer; triangles – after the insertion of PLA2. A – time dependent Cole-Cole spectra (PLA2 concentration 500 nM); B – PLA2 concentration dependent Cole-Cole spectra (incubation time 30 min). Electrode potential: 0 V vs Ag/AgCl, NaCl (sat.).

Hybrid bilayer regeneration.—In order to determine the reusability of the OTS SAM for hybrid bilayer formation, the EIS data were collected by repeating the processes of vesicle fusion and monitoring changes of electrochemical impedance spectra. In the first cycle of measurements, OTS monolayer was formed and EIS was measured (Fig. 6, filled circles), then DOPC-Chol membrane was formed and EIS was measured again (Fig. 6, open circles). Afterward, the membrane was flushed with isopropanol/water mixture (50:50 %) and the second cycle of measurements was carried out by measuring EIS of residual OTS monolayer (Fig. 6, filled circles) and of bilayer (Fig. 6, filled triangles) formed on it. It is seen from EIS data in Fig. 6 that despite some loss of OTS monolayer after every cycle, as many

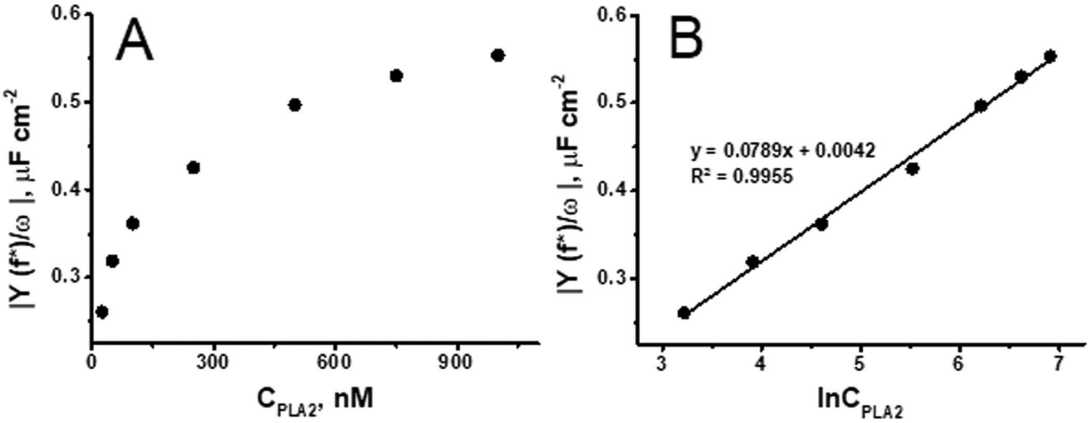

Figure 8. (A) - dependence of the admittance on the PLA2 concentration obtained at the the specific frequency ($f^* = 213$ Hz); (B) – the same data on logarithmic x scale. PLA2 incubation time – 30 min.

as 3 cycles were achieved with almost identical capacitance value of silanized T_{hexane} electrode. Only on the 4th cycle a slight increase in capacitance was observed.

Hybrid bilayer interaction with phospholipase A₂.—To assess possible utility of the hybrid bilayers as phospholipid biosensor an interaction between the DOPC-Chol (6:4) hybrid bilayer formed and phospholipase A_2 was followed by EIS in real-time. PLA2 is a superfamily of enzymes, which hydrolyzes the fatty acids from *sn2* position of membrane phospholipids releasing fatty acids and lysophospholipids in the process.[47] Cole-Cole plots in Fig. 7 clearly attests for the capacitance increase with time after the aliquote of the PLA2 was injected into the solution. A significant increase of capacitance from 0.58 $\mu F\ cm^{-2}$ to 0.94 $\mu F\ cm^{-2}$ is observed within the first minute of injection of 500 nM PLA2 (Fig. 7A, filled triangles up). Further increase in capacitance approaching 1.12 $\mu F\ cm^{-2}$ was observed within next 25 min of interaction. It is worth mentioning that the increase of incubation time results in an evolution of the complex capacitance curve toward the curve of an anchor monolayer on Ti (Fig. 7A, compare open triangles and filled circles).

We found that increase of an incubation time and concentration of PLA2 exhibits similar effects. Fig 7B demonstrates the effect of PLA concentration (25–250 nM range) on evolution of the complex capacitance plots at fixed incubation time, 30 min. At 25 nM PLA2 barely visible effects on the capacitance curve (Fig. 7B, open triangles up) were observed after 30 min. However, the capacitance noticeably increased after the injection of 50 nM PLA2 (Fig. 7, gray triangles) and 30 min of incubation. Increasing concentration of PLA2 up to 250 nM triggers a major transformation of the capacitance curve (Fig. 7B, open triangles down) with the resulting specific capacitance values exceeding 1.12 $\mu F\ cm^{-2}$. Further increase in concentration of PLA2 triggers only marginal changes indicating saturation of the effect. Such behavior can be expected because disruption of the hybrid bilayer by the PLA2 results in Ti surface functionalized by the silane monolayer, which is resistant to PLA2.

The sensitivity of the hybrid bilayer to PLA2 can be utilized to construct biosensors sensitive to the enzyme concentration and/or its activity. For this purpose one can choose a singly frequency ac measurement methodology as suggested in ref. 48. Figure 8 displays the variation of the parameter Y/ω (Y is the admittance of the electrode, and ω is the cyclic frequency) with concentraion of the PLA2 at constant time of incubation 30 min. As seen in Fig 8A the dependence resembles nearly logarithmic shape of the Y/ω function with respect its argument, C_{PLA2}. Indeed, representation of the same data set in semi-logarithmic coordinates returns nearly perfect linear dependence of Y/ω vs. log C_{PLA2}. Such dependence can be used for the bioanalytical purposes to assess concentration of the membrane damaging agent, in this case PLA2 or its activity.

Conclusions

In this study we described the process of formation of hybrid bilayer on metallurgical Ti plate electrode. We showed that surface of metallurgical Ti can be used for the formation of a compact and reproducible anchor monolayer of OTS via simple silanization procedure. The experimental data suggests hexane to be a more efficient cleaning solvent prior silanization than acetone. The origin of this effect remained elusive, though surface density of the hydroxyl groups can be a primary reason for this effect. Silanization of Ti surface results in hydrophobic cushion for vesicle fusion. Upon exposure of silanized Ti surface to a multilammelar vesicle solution led to vesicle fusion and formation of a dielectric phospholipid layer atop of the anchoring monolayer. We showed that the process of OTS functionalization and hybrid bilayer formation was monitored by the FFT EIS techniques. Every stage of the hybrid bilayer formation can be assigned certain values of the specific capacitance. OTS monolayer was found to be $1.02 \pm 0.17\ \mu F\ cm^{-2}$ while DOPC-Chol bilayer $0.61 \pm 0.06\ \mu F\ cm^{-2}$. Assuming the relative dielectric constant value is 2.3 for OTS and 2.5 for DOPC-Chol bilayer, one may estimate physical thickness of surface layers which were 1.94 nm and 3.57 nm for OTS and DOPC-Chol layers respectively. We found that OTS anchor monolayer can be reused multiple times as a vesicle fusion substrate. Every time, the reassembled hybrid bilayer exhibited similar dielectric properties, making such construct advantageous over the tethered bilayer on gold, which can be used only once.[49]

We showed that the hybrid bilayer on metallurgic Ti exhibits phospholipid biosensor utility. In particular the interaction between Phospholipase A_2 can be used both for the real-time monitoring of the interaction as well as for biosensing of the phospholipid layer damaging protein interactions.

ORCID

Aušra Valiūnienė https://orcid.org/0000-0003-0535-023X

References

1. E. Sackmann, *Science*, **271**(5245), 43 (1996).
2. K. Seifert, K. Fendler, and E. Bamberg, *Biophysical Journal*, **64**(2), 384 (1993).
3. C. Steinem, A. Janshoff, K. von dem Bruch, R. Karsten, J. Goossens, and H.-J. Galla, *Bioelectrochemistry and Bioenergetics*, **45**(1), 17 (1998).
4. K. Mossman and J. Groves, *Chemical Society Reviews*, **36**(1), 46 (2007).
5. A. Lueking, D. J. Cahill, and S. Müllner, *Drug Discovery Today*, **10**(11), 789 (2005).
6. M. Keizer Henk, R. Dorvel Brian, M. Andersson, D. Fine, B. Price Rebecca, R. Long Joanna, A. Dodabalapur, I. Köper, W. Knoll, A. V. Anderson Peter, and S. Duran Randolph, *ChemBioChem*, **8**(11), 1246 (2007).
7. P. Yin, C. J. Burns, P. D. J. Osman, and B. A. Cornell, *Biosensors and Bioelectronics*, **18**(4), 389 (2003).
8. V. Atanasov, N. Knorr, R. S. Duran, S. Ingebrandt, A. Offenhäusser, W. Knoll, and I. Köper, *Biophysical Journal*, **89**(3), 1780 (2005).
9. Z. Peng, J. Tang, X. Han, E. Wang, and S. Dong, *Langmuir*, **18**(12), 4834 (2002).
10. B. A. Cornell, V. L. B. Braach-Maksvytis, L. G. King, P. D. J. Osman, B. Raguse, L. Wieczorek, and R. J. Pace, *Nature*, **387** 580 (1997).
11. S. G. Boxer, *Current Opinion in Chemical Biology*, **4**(6), 704 (2000).
12. P. S. Cremer and S. G. Boxer, *The Journal of Physical Chemistry B*, **103**(13), 2554 (1999).
13. Z. Salamon and G. Tollin, *Biophysical Journal*, **71**(2), 848 (1996).
14. F. Roskamp Robert, K. Vockenroth Inga, N. Eisenmenger, J. Braunagel, and I. Köper, *ChemPhysChem*, **9**(13), 1920 (2008).
15. E. Reimhult, F. Höök, and B. Kasemo, *Langmuir*, **19**(5), 1681 (2003).
16. G. Csúcs and J. J. Ramsden, *Biochimica et Biophysica Acta (BBA) - Biomembranes*, **1369**(2), 304 (1998).
17. G. Puu and I. Gustafson, *Biochimica et Biophysica Acta (BBA) - Biomembranes*, **1327**(2), 149 (1997).
18. E. T. Castellana and P. S. Cremer, *Surface Science Reports*, **61**(10), 429 (2006).
19. B. W. Koenig, S. Krueger, W. J. Orts, C. F. Majkrzak, N. F. Berk, J. V. Silverton, and K. Gawrisch, *Langmuir*, **12**(5), 1343 (1996).
20. C. W. Meuse, S. Krueger, C. F. Majkrzak, J. A. Dura, J. Fu, J. T. Connor, and A. L. Plant, *Biophysical Journal*, **74**(3), 1388 (1998).
21. A. L. Plant, *Langmuir*, **15**(15), 5128 (1999).
22. C. Vericat, M. E. Vela, G. Corthey, E. Pensa, E. Cortes, M. H. Fonticelli, F. Ibanez, G. E. Benitez, P. Carro, and R. C. Salvarezza, *RSC Advances*, **4**(53), 27730 (2014).
23. H. Chen, N. Cheng, W. Ma, M. Li, S. Hu, L. Gu, S. Meng, and X. Guo, *ACS Nano*, **10**(1), 436 (2016).
24. A. N. Parikh, J. D. Beers, A. P. Shreve, and B. I. Swanson, *Langmuir*, **15**(16), 5369 (1999).
25. D. Marchal, C. Bourdillon, and B. Demé, *Langmuir*, **17**(26), 8313 (2001).
26. S. Casalini, C. A. Bortolotti, F. Leonardi, and F. Biscarini, *Chemical Society Reviews*, **46**(1), 40 (2017).
27. M. Abdel-Hady Gepreel and M. Niinomi, *Journal of the Mechanical Behavior of Biomedical Materials*, **20**, 407 (2013).
28. A. Yamamoto, R. Honma, and M. Sumita, *Journal of Biomedical Materials Research*, **39**(2), 331 (1998).
29. X. Liu, P. K. Chu, and C. Ding, *Materials Science and Engineering: R: Reports*, **47**(3), 49 (2004).
30. T. Ragaliauskas, M. Mickevicius, B. Rakovska, T. Penkauskas, D. J. Vanderah, F. Heinrich, and G. Valincius, *Biochimica et Biophysica Acta (BBA) - Biomembranes*, **1859**(5), 669 (2017).
31. G. S. Popkirov and R. N. Schindler, *Review of Scientific Instruments*, **63**(11), 5366 (1992).
32. A. Valiūnienė, T. Petrulionienė, I. Balevičiūtė, L. Mikoliūnaitė, and G. Valinčius, *Chemistry and Physics of Lipids*, **202**, 62 (2017).
33. D. J. McGillivray, G. Valincius, D. J. Vanderah, W. Febo-Ayala, J. T. Woodward, F. Heinrich, J. J. Kasianowicz, and M. Lösche, *Biointerphases*, **2**(1), 21 (2007).
34. A. Valiūnienė, Ž. Margarian, I. Gabriūnaitė, V. Matulevičiūtė, T. Murauskas, and G. Valinčius, *Journal of The Electrochemical Society*, **163**(9), H762 (2016).
35. M. J. Eslamibidgoli Gro and M. Eikerling, *Physical Chemistry Chemical Physics*, **19**(34), 22659 (2017).
36. M. Itagaki, S. Suzuki, I. Shitanda, and K. Watanabe, *Electrochemistry*, **75**(8), 649 (2007).

37. G. Valincius, V. Reipa, V. Vilker, J. T. Woodward, and M. Vaudin, *Journal of The Electrochemical Society*, **148**(8), E341 (2001).
38. L. K. Tamm and H. M. McConnell, *Biophysical Journal*, **47**(1), 105 (1985).
39. V. I. Silin, H. Wieder, J. T. Woodward, G. Valincius, A. Offenhausser, and A. L. Plant, *J Am Chem Soc*, **124**(49), 14676 (2002).
40. J. B. Brzoska, I. B. Azouz, and F. Rondelez, *Langmuir*, **10**(11), 4367 (1994).
41. D. J. Vanderah, J. Arsenault, H. La, R. S. Gates, V. Silin, C. W. Meuse, and G. Valincius, *Langmuir*, **19**(9), 3752 (2003).
42. P. Diao, D. Jiang, X. Cui, D. Gu, R. Tong, and B. Zhong, *Bioelectrochemistry and Bioenergetics*, **48**(2), 469 (1999).
43. R. Budvytyte, G. Valincius, G. Niaura, V. Voiciuk, M. Mickevicius, H. Chapman, H.-Z. Goh, P. Shekhar, F. Heinrich, S. Shenoy, M. Lösche, and D. J. Vanderah, *Langmuir*, **29**(27), 8645 (2013).
44. P. Krysiński, A. Żebrowska, B. Pałys, and Z. Łotowski, *Journal of The Electrochemical Society*, **149**(6), E189 (2002).
45. L. Ringstad, A. Schmidtchen, and M. Malmsten, *Langmuir*, **22**(11), 5042 (2006).
46. M. L. Fernández, G. Marshall, F. Sagués, and R. Reigada, *The Journal of Physical Chemistry B*, **114**(20), 6855 (2010).
47. J. E. Burke and E. A. Dennis, *Journal of Lipid Research*, **50**(Suppl), S237 (2009).
48. G. Valincius, D. J. McGillivray, W. Febo-Ayala, D. J. Vanderah, J. J. Kasianowicz, and M. Lösche, *The Journal of Physical Chemistry B*, **110**(21), 10213 (2006).
49. B. Rakovska, T. Ragaliauskas, M. Mickevicius, M. Jankunec, G. Niaura, D. J. Vanderah, and G. Valincius, *Langmuir*, **31**(2), 846 (2015).

ARTICLE II

Mixed hybrid bilayer lipid membranes on mechanically polished titanium surface

T.Sabirovas, A. Valiūnienė, I. Gabriunaite, G. Valincius

Biochimica et Biophysica Acta (BBA) - Biomembranes, 1862 (6) (2020)

BBA - Biomembranes 1862 (2020) 183232

Contents lists available at ScienceDirect

BBA - Biomembranes

journal homepage: www.elsevier.com/locate/bbamem

Mixed hybrid bilayer lipid membranes on mechanically polished titanium surface

Tomas Sabirovas[a], Aušra Valiūnienė[a], Inga Gabriunaite[a], Gintaras Valincius[b,*]

[a] Department of Physical Chemistry, Faculty of Chemistry and Geosciences, Vilnius University, Naugarduko 24, Vilnius LT-03225, Lithuania
[b] Vilnius University, Institute of Biochemistry, Life Sciences Center, Sauletekio ave. 7, Vilnius LT-10257, Lithuania

ARTICLE INFO

Keywords:
Titanium
Self-assembled monolayer
Octadecyltrichlorosilane
Methyltrichlorosilane
Phospholipid bilayer membrane
Electrochemical impedance spectroscopy

ABSTRACT

Mixed self-assembled monolayers of octadecyltrichlorosilane (OTS) and methyltrichlorosilane (MTS) were deposited via simple silanization procedure on a mechanically polished titanium surface. The monolayers act as molecular anchors for mixed hybrid bilayer lipid membranes (mhBLM) which were accomplished via vesicle fusion. A variation of the MTS concentration in silanization solutions significantly affects properties of mhBLMs composed of a 1,2-dioleoyl-sn-glycero-3-phosphocholine (DOPC) and cholesterol (Chol). The bilayers become less insulating following an increase of the MTS content. On the other hand, an increase of the MTS concentration provides flexibility of the mhBLM membranes necessary for the functional reconstitution of membrane proteins. The optimal molar ratio of MTS in silanization solution is 40% providing anchors for intact mhBLMs as confirmed by their specific capacitance of 0.86 μF cm^{-2}. We found that the bilayers containing 40% (mol) of cholesterol bind cholesterol dependent pneumolysin (PLY). However, we did not observe functional reconstitution of PLY. While α-hemolysin almost fully disrupts mhBLMs assembled from 100% diphytanoyl. An important advantage of the titanium/OTS/MTS molecular anchor systems is their ability of repetitive regeneration of phospholipid bilayers without losing functional properties as demonstrated in the current study. This creates a possibility for the multiple-use phospholipid membrane biosensors which have a potential of decreasing the cost of such electrochemical/electroanalytical devices.

1. Introduction

Tethered bilayer lipid membranes (tBLM) are self-assembled systems, which mimic phospholipid bilayer of the cell. tBLMs are suitable for the investigation of different membrane proteins with various characteristics such as redox reactions [1,2], ion permeability [3,4], protein-membrane interactions [5], etc. Generally, tBLM system consists of mixed self-assembled monolayer (SAM) on the electro-conductive surface and a phospholipid bilayer on top of it [6]. Mixed SAM is typically composed of short and long alkyl chain hydrocarbons. Long alkyl chain molecules, usually having an end group of lipid or sterol moiety [7,8] act as an anchor for the phospholipids and a short alkyl chain molecule acts as a spacer. Surface architecture of short and long alkyl chain molecules generates an ionic reservoir between phospholipid membrane and solid surface, which is the main characteristic of tBLMs [9]. Therefore, tethered bilayer lipid membranes are exceptional model of bilayer lipid membranes, which has a desirable biological fluidity, an ionic reservoir, needed for transmembrane protein reconstitution, and long-term stability. For these reasons, tBLMs are more advantageous than other membrane lipid models such as hybrid bilayer lipid membrane [10].

In the last couple of decades, gold as a substrate has been extensively studied for formation of tethered bilayer lipid membrane, since it can be examined by surface sensitive techniques (e.g. surface plasmon resonance, electrochemical impedance spectroscopy, quartz crystal microbalance etc.) and easily modified by thiol group anchoring units, based on sulphur-gold chemistry [11–14]. Tethered bilayer lipid membranes formed on gold modified with thiol anchors usually exhibit low number of defects density [15] and high sensitivity towards membrane damaging toxins [16]. However, gold as a substrate is associated with high cost and mostly is disposed after single use. Furthermore, gold substrates have propensity to denature proteins which leads to biofouling of the surface [17,18]. In contrast, widely used titanium alloys exhibit good biocompatibility [19] therefore, tailoring titanium surfaces by the phospholipid membranes may expand their utility in implant/replacement medicine. For these reasons, a promising choice is metal oxide substrates, for example, fluorine doped tin oxide (FTO) [20], cadmium tin oxide (CTO) [10], indium tin oxide (ITO)

* Corresponding author.
E-mail address: gintaras.valincius@gmc.vu.lt (G. Valincius).

https://doi.org/10.1016/j.bbamem.2020.183232
Received 3 November 2019; Received in revised form 7 February 2020; Accepted 20 February 2020
Available online 28 February 2020
0005-2736/

[21,22], aluminum [23], magnetron sputtered titanium [24] or mechanically polished metallurgical titanium surface which is naturally coated by stable TiO_2 oxide film [25] and others. Formation of SAM on metal oxide surfaces can be accomplished by the silane-oxide based chemistry. Nonetheless, achieving desired and reproducible properties of silane SAMs are challenging, since it is highly dependent on preparation of substrate, type of solvent used in silanization, presence of water and temperature [10,24–26].

It was shown in our previous study that successful formation of hybrid bilayer can be accomplished on mechanically polished metallurgical titanium surface [25], which exhibits greater advantages compared to gold surfaces because (i) titanium is distinguished as highly biocompatible and non-toxic material, (ii) octadecyltrichlorosilane (OTS) anchor monolayer formed on the surface of Ti can be reused multiple times for bilayer lipid membrane formation. Also, it was shown that the hybrid bilayer on metallurgical Ti exhibits phospholipid biosensor utility. However, the developed hybrid bilayer lipid membrane does not have an aqueous reservoir, which in tethered bilayer lipid membranes enables functional reconstitution of membrane-associated proteins [27].

The aim of this work was to explore the formation of mixed hybrid bilayer lipid membrane (mhBLM), which resembles the structure of tBLMs, on metallurgical titanium naturally coated by the TiO_2 oxide film. We investigated the dilution effect of a spacer in a mixed self-assembled monolayers used for the formation of a mixed hybrid bilayer lipid membrane, which presumably may have some polar reservoir between the bilayer and the substrate, needed for integral protein incorporation, relevant biological fluidity and long-term stability. Considering that hybrid bilayer lipid membranes formed on OTS monolayer can be reused multiple times [26], the ability to reuse a mixed hybrid bilayer lipid membrane was investigated as well. The applicability of mhBLM as a biosensor platform for membrane protein studies was tested with two cytolytic toxins – pneumolysin (PLY) and α-hemolysin (αHL).

2. Experimental

2.1. Preparation of titanium surface

Metallurgical titanium plate (99% purity, Alfa Aesar GmbH & Co KG) was polished with a diamond lapidary paste (200,000 grit, 50% concentration of diamond powder, where the size of the diamond powder was ≤0.1 μm) at the speed of 1000 rpm until a 'mirror finish' was observed. Then polished titanium plate was treated by ultrasound (i) in hexane (≥99%, Reachem, Slovakia), (ii) in 2% laboratory dish cleaning solution of MICRO®-90 (Sigma-Aldrich), (iii) in 2-propanol (≥99.5%, Sigma-Aldrich) and (iv) in water cleaned by Milli Q-plus-Millipore system (USA) for 10 min. After sonication, the titanium plate was dried under a nitrogen stream.

2.2. Self-assembled monolayer formation

Silanization solution was prepared by heating 45 mL of heptane (≥99%, Sigma-Aldrich) to 60–65 °C and then adding the equal amounts (2.5 mM) of octadecyltrichlorosilane (OTS) (> 90%, Sigma-Aldrich) and methyltrichlorosilane (MTS) (97%, Alfa-Aesar). Freshly cleaned titanium plate was immersed into prepared silanization solution and left for 45 min in order to functionalize titanium surface with a self-assembled monolayer. After that, the functionalized titanium plate was rinsed in heptane and dried under a nitrogen stream. Finally, silanized titanium plate was heated at 100 °C for 1 h in air environment to remove adsorbed water and most importantly – solvent residues. This procedure increased the reproducibility of the electrochemical properties of SAMs.

2.3. Phospholipid bilayer lipid membrane formation

Bilayer lipid membranes were formed by vesicle fusion method described in the reference [28]. Vesicle solution was prepared from 1,2-diphytanoyl-sn-glycero-3-phosphocholine (DPhyPC) or a mixture of 1,2-dioleoyl-sn-glycero-3-phosphocholine (DOPC) (Avanti Polar Lipids, Inc., USA) and cholesterol (Chol) (Avanti Polar Lipids, Inc., USA). Molar ratio of lipids in vesicle solution was 60% DOPC and 40% cholesterol, unless indicated otherwise. The lipids were dissolved in chloroform (99%, Sigma-Aldrich) to a concentration of 10 mM. In order to prepare 1.5 mM vesicle solution, a desired amount of lipid-chloroform solution was transferred to a separate vial and evaporated under a nitrogen stream until formation of a lipid film on the bottom of the vial. The lipid film was re-suspended in a phosphate buffered saline (PBS, 0.1 M NaCl (Reachem Slovakia p. a.), 0.01 M NaH_2PO_4 (Reachem Slovakia, p. a.), which pH was adjusted to 4.5 with NaOH (Reachem Slovakia p. a.).

2.4. Electrochemical impedance measurements

Measurements of electrochemical impedance spectroscopy (EIS) were carried out in PBS (pH adjusted to 7.1) at 0 V vs Ag/AgCl/$NaCl_{(sat.)}$ unless indicated differently. EIS were recorded by using either μAutolab (Utrecht, the Netherlands) with conventional three-electrode system configuration in a frequency range from 0.1 Hz to 50 kHz or fast Fourier transform (FFT) electrochemical impedance spectrometer EIS-128/16 [29] (University of Kiel, Germany) in a frequency range from 0.7 Hz to 50 kHz by using four electrode system configuration where titanium plate served as a working electrode, saturated silver-silver chloride (Ag/AgCl/$NaCl_{(sat.)}$) microelectrode (M-401F, Bedford, USA) as a reference electrode, platinum (99.99% purity, Aldrich) wire as an auxiliary electrode, which was coiled around the barrel of the reference electrode and another platinum wire as a quasi-reference electrode, which was connected to 1 μF capacitor to reduce the impedance of the reference electrode at the higher frequencies. All presented data are normalized to the geometric surface area of 0.32 cm^2 of the working electrode.

2.5. Contact angle measurements

Contact angle was measured with Theta Lite Optical Tensiometer from Biolin Scientific (Finland) company by placing 6 droplets of 10 μL Milli-Q water. All contact angle measurements were performed immediately after titanium plate was cleaned or functionalized with different molar ratios of OTS:MTS.

Standard errors were obtained from 6 different titanium plates.

3. Results and discussion

3.1. Formation of mixed silane self-assembled monolayer

To investigate the hydrophobic properties of a monolayer formation, surface wetting characteristics – contact angles (CA) of the water droplets were measured. CA values of titanium surface and functionalized titanium surfaces prepared using silanization solutions of various molar ratios of OTS:MTS are displayed in Fig. 1. Freshly polished and cleaned titanium surface demonstrated hydrophilic properties reaching CA value of 54° ± 3°, while CA increases to 102° ± 2° after the silanization of Ti surface in 2.5 mM OTS solution, as it was reported previously [25]. In this study spacer of short alkyl chain MTS molecules and anchoring unit of long alkyl chain OTS molecules were introduced into silanization solution in order to functionalize the Ti surface with mixed self-assembled monolayer. It was determined that the contact angles of titanium surfaces functionalized with mixed OTS:MTS self-assembled monolayers exceeded a threshold of 90°, which is needed for lipid overlayer formation [30]. However, increasing MTS molar ratio causes lower hydrophobicity of the functionalized Ti surface. Similar

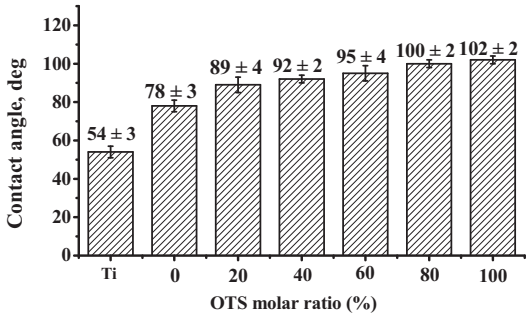

Fig. 1. Contact angles of Ti surface before silanization and after silanization using various molar ratios of OTS:MTS. Standard errors were obtained from 6 different samples.

trend of CA evolution was observed on gold electrodes, using mixture of a short alkyl chain and long alkyl chain thiols [6]. Notably, titanium surface silanized in 100% MTS solution exhibited the lowest CA value of 78° ± 3° and did not produce the sufficient hydrophobicity of the SAM suitable for the formation of compact phospholipid overlayer.

3.2. Mixed hybrid bilayer lipid membrane formation

While the CA measurements indicate the surface wetting characteristics, the electrochemical impedance spectroscopy can be applied for investigations of dielectric properties of the functionalized surfaces [6,31]. Fig. 2 (filled circles) displays EI spectra in Cole – Cole plot of the Ti surfaces after functionalization with SAMs prepared from silanization solutions containing various OTS:MTS molar ratios as well as after formation (open circles) of DOPC/Chol (molar ratio 6:4) bilayer lipid membrane by vesicle fusion method. The obtained complex capacitance plots exhibited semi-circular shapes which are typical for ideally polarizable interphases showing near ideal capacitive behaviour. The diameter of the semicircle is equal to the capacitance of the electrical double layer at the interphase [32]. Therefore, in this study the values of complex capacitances after SAM and bilayer membrane formation were calculated by taking the radius of the semicircle in Cole-Cole plot and multiplying it by two.

In the previous study [25], we have reported the complex capacitance value of 29 ± 4 μF cm^{-2} for Ti electrode covered by the TiO_2 film naturally occurring on the surface. As expected, functionalization of titanium surface using silanization solutions of various molar ratios of OTS:MTS (Fig. 2, filled circles) causes significant decrease of complex capacitances suggesting formation of dielectric layer on the Ti surface. In particular, the values of complex capacitances decrease considerably from 29 ± 4 μF cm^{-2} (before silanization) to 6.17 ± 1.44 μF cm^{-2} (Fig. 2, A, filled circles) after silanization in the solution consisting only of short alkyl chain MTS molecules. Addition of anchoring units of long alkyl chain OTS molecules into silanization solution positively affects functionalization of Ti surface, as suggested by the observed gradual decrease of complex capacitances dependently on OTS:MTS molar ratio in silanization solution. Increasing OTS molar ratio in the OTS:MTS silanization solution enables to obtain lower complex capacitance values (Fig. 2, B–E, filled circles), and the lowest value of 1.02 ± 0.17 μF cm^{-2} was observed when Ti surface was silanized in the solution consisting only of long alkyl chain OTS molecules (Fig. 2, F, filled circles). Gradual variation of the complex capacitance values suggests that modification of Ti surface in OTS:MTS silanization solutions leads to the formation of dielectric layers of mixed silane SAMs and the average thickness of the obtained SAMs is dependent on OTS:MTS molar ratio in silanization solution, since capacitance is inversely proportional to the thickness of the dielectric layer on the surface [33]. Similar trends of the complex capacitance dependence on the fraction of molecular anchor were observed on gold surface, modified with thiols mixed self-assembled monolayers [6]. The experimental results in Fig. 2 correlate well with CA data (Fig. 1), which showed that continuously increasing OTS molar ratio in OTS:MTS silanization solution respectively causes higher CA values of silanized Ti surface. In summary, we conclude that silane-based mixed self-assembled monolayers can be formed on the titanium surface by modifying it in silanization solutions of various molar ratios of OTS:MTS. Furthermore, the obtained EIS and CA data suggest that addition of 20% or 40% of MTS into OTS:MTS silanization solution enables to obtain SAMs which can be tested further for mixed hybrid bilayer lipid membrane formation, since both the values of complex capacitances and contact angles reached the threshold needed for lipid overlayer formation.

Therefore, the next series of experiments were carried out in order to form mhBLM of DOPC/Chol (molar ratio 6:4) by vesicle fusion

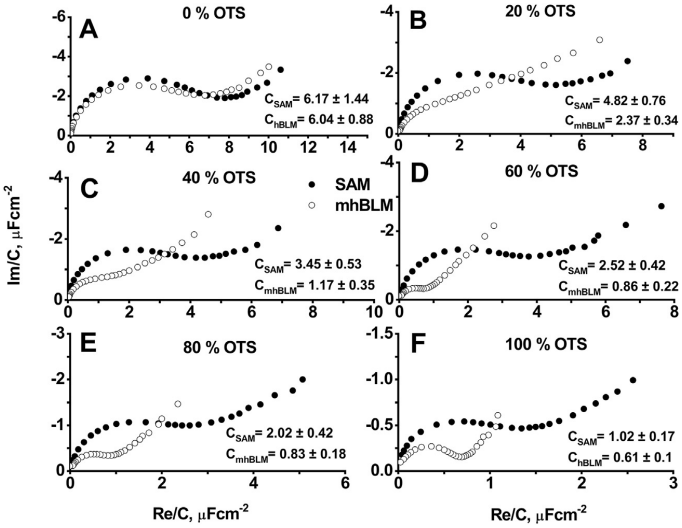

Fig. 2. Cole – Cole plots of FFT electrochemical impedance spectra obtained at 0 V potential vs $Ag/AgCl/NaCl_{(sat.)}$ using Ti electrodes after functionalization with SAMs (filled circles) prepared from silanization solutions of various molar ratios of OTS:MTS: A – 0:10, B – 2:8, C – 4:6, D – 6:4, E – 8:2, F – 10:0 and after mixed hybrid bilayer lipid membrane (mhBLM) formation completed with DOPC/Chol (molar ratio 6:4) after 60 min of vesicle fusion (open circles). Insets – values of the complex capacitances after SAM and mhBLM formation in μF cm^{-2}.

method using Ti surfaces silanized with SAMs obtained from various molar ratios OTS:MTS silanization solutions. The ability of mixed silane SAMs to immobilize bilayer lipid membrane was monitored by EIS method, which enables to indicate a continuous dielectric sheet of a phospholipid [6] covering the surface, if a significant complex capacitance decrease is observed. EIS data in Fig. 2 indicates that formation of bilayer lipid membrane on MTS self-assembled monolayer was not successful because only negligible decrease in complex capacitance was observed after vesicle fusion (Fig. 2, A). This result can be explained by taking into consideration the CA values of titanium surface silanized in 100% MTS solution (Fig. 1) which did not exceed the threshold of 90° needed for successful lipid overlayer formation. Hydrophobic properties of the SAM are dependent on the alkyl chain length of molecule used, because longer alkyl chain molecules are more hydrophobic than shorter alkyl chain molecules [30]. This is due to the density of the non-polar molecules on the surface. The short alkyl chain molecules such as MTS (CH_3SiCl_3) do not produce surface with enough hydrophobicity needed for vesicle fusion to form intact mhBLM.

Meanwhile, the EIS data indicate the formation of additional phospholipid layers after DOPC/Chol (molar ratio 6:4) vesicle fusion on mixed SAMs formed from different silanization solutions (Fig. 2, B–E). This is evident from the decrease of complex capacitance upon exposure of substrates to phospholipid vesicles. However, the EIS response did not displayed complete semi-circular shape after formation of mixed hybrid bilayer lipid membranes on a mixed SAMs prepared from OTS:MTS silanization solution of 2:8 and 4:6 M ratios (Fig. 2, B, C, open circles) indicating high defectiveness of phospholipid membrane [31]. Formation of mhBLMs on SAMs prepared from OTS:MTS silanization solutions of 6:4 and 8:2 M ratios (Fig. 2, D and E, open circles) enabled to obtain EIS spectra exhibiting almost complete semi-circular shapes with complex capacitance values of 0.86 ± 0.22 μF cm^{-2} and 0.83 ± 0.18 μF cm^{-2}, respectively, suggesting that the surface coverage of dielectric phospholipid sheet is approximately similar to hybrid bilayer lipid membrane formed on OTS monolayer (Fig. 2, F, open circles) exhibiting slightly lower complex capacitance value of 0.6 ± 0.1 μF cm^{-2}. Based on the EIS data analysis the surface coverage of mhBLMs was estimated (see details in Supplementary material). Mixed hybrid bilayer lipid membranes formed on SAMs prepared from OTS:MTS silanization solutions of 6:4 and 8:2 M ratios (Fig. 2, D and E, open circles) displayed surface coverage by lipid 0.97 and 0.98 (Table 1S), respectively, indicating that the functionalized titanium surface is almost fully covered with the mixed hybrid bilayer lipid membrane.

All in all, complex capacitance values of mhBLMs (Fig. 2, D, E and F, open circles) on Ti are comparable to the complex capacitances values of tethered bilayer lipid membrane formed on gold surface (C_{tBLM} = 0.8 μF cm^{-2}), which was modified with thiols mixed self-assembled monolayers [6], suggesting that silanes mixed SAMs are suitable for mhBLM formation on Ti surface.

3.3. Mixed hybrid bilayer lipid membrane regeneration

To test reusability of mixed self-assembled monolayer for the formation of the mhBLM, regeneration experiments were carried out by forming and removing mixed hybrid bilayer lipid membrane multiple times. Firstly, mixed self-assembled monolayer on the Ti was prepared from OTS:MTS silanization solution of 6:4 M ratio. The molar ratio of 6:4 in OTS:MTS silanization solution was chosen, expecting that the mixed self-assembled monolayer has more spacer units and should exhibit better mhBLM fluidity than mixed SAMs with higher amount of anchoring units. After formation of mixed SAM, bilayer lipid membrane was immobilized via vesicle fusion method and flushed with isopropanol/Milli-Q water (50/50 vol% ratio) to remove the lipid layer. Then, procedure was repeated multiple times and EIS was registered each time after formation and removal of the mhBLM. The obtained EIS data are depicted in Fig. 3. It is observable that complex capacitance values of the mixed SAM increased slightly after mhBLM was removed for the first time. Possible explanation of this phenomenon may be related to an adsorption and retaining of water molecules by reused SAM. After the next five removals of mhBLMs, there were no significant changes in complex capacitance of the mixed SAM (Fig. 3, A). This result suggests that the Ti surface functionalized with the mixed self-assembled monolayer prepared from OTS:MTS silanization solution of 6:4 M ratio can be used for multiple formations of mhBLMs. As expected, the complex capacitance values remained stable at 0.95 ± 0.03 μF cm^{-2} after multiple formations of the mixed hybrid bilayer lipid membrane (Fig. 4, B), suggesting that exposure to water does not inhibit the repetitive formation of bilayer lipid membrane. Also, these values are in the same range of 0.86 ± 0.22 μF cm^{-2} obtained for mhBLMs formed on 60% OTS SAM as depicted in Fig. 2, D.

3.4. Mixed hybrid bilayer lipid membrane interaction with pore forming toxins pneumolysin and α-hemolysin

To evaluate possible applicability of a mixed hybrid bilayer lipid membrane as a phospholipid biosensor platform, the bilayer lipid membrane containing DOPC/Chol (molar ratio 6:4) was formed on SAM prepared from OTS:MTS (molar ratio 6:4) silanization solution. The cholesterol containing mhBLMs were challenged with a cholesterol dependent cytolysin pneumolysin (PLY), which action on membrane occurs only in the presence of cholesterol [34,35].

The effect of PLY on mhBLMs is seen from the changes of the EIS curves in Fig. 4, A. The addition of 100 nM of PLY to a membrane bathing solution results in a minor increase of the complex capacitance from approximately 0.72 μF cm^{-2} to 0.86 μF cm^{-2}. The process is rather slow, as seen from relatively long time (60 min) necessary to observe the effect. Even though the change of complex capacitance of mhBLM upon exposure to PLY (Fig. 4, A) was quite modest (< 0.14 μF cm^{-2}), the admittance phase minimum of argZ = −60.1 deg. at lg f_{min} = 0.22 slightly shifted up to argZ = −62.7 towards lower frequencies at lg f_{min} = 1.24 (See Supplementary material Fig. 1S, A) and resistivity of the mhBLM decreased consistently in the low frequency range (below 10 Hz) (see Supplementary material, Fig. 1S, B). The calculated percentage values of resistivity change of the mhBLM reached 22.83% and 13% at 8 Hz and 0.1 Hz, respectively (see Supplementary material Table 2S) upon exposure of mhBLM to PLY. These changes were not observed for cholesterol-free mhBLMs (Fig. 4 A, inset): no complex capacitance change was observed for DOPC mhBLMs within 1 h of exposure to 100 nM PLY solution. This allows us to conclude that observed EIS changes are due to a specific interaction between the cholesterol receptor in D4 domain of PLY [35] and cholesterol in phospholipid bilayer.

Taking into account the size of the pore of PLY, which is around 30 nm [36], the EIS response should be in the case of the functional protein pore reconstitution into mixed hybrid bilayer lipid membrane [37]. In the case of such events occurring in tBLMs on gold surface, the EIS phase minimum in the Bode plot (argZ vs. lgf) significantly shifts position of the frequency towards higher frequencies, while also significantly increasing the admittance and decreasing the capacitance of tBLM [16,28,31,37]. Such changes were not observed in the current study. Therefore, we believe that PLY is not undergoing full oligomerization and pore formation. Instead, the observed capacitance increase and slight decrease of the mhBLM resistance are due to the attachment of the PLY monomer to cholesterol in mhBLMs. The absence of functional reconstitution may be related to the excess density of OTS molecules on the surface. Dense OTS layers prevent pore formation due to the rigidity of the bilayer. To overcome the problem and make bilayers suitable for PLY reconstitution as one a solution may be the reduction of molecular anchor concentration in the silanization solution. Such reduction of the density is presumably possible by using longer-chain unsaturated anchor molecules [38], which however, currently are not available in the silane group terminated form.

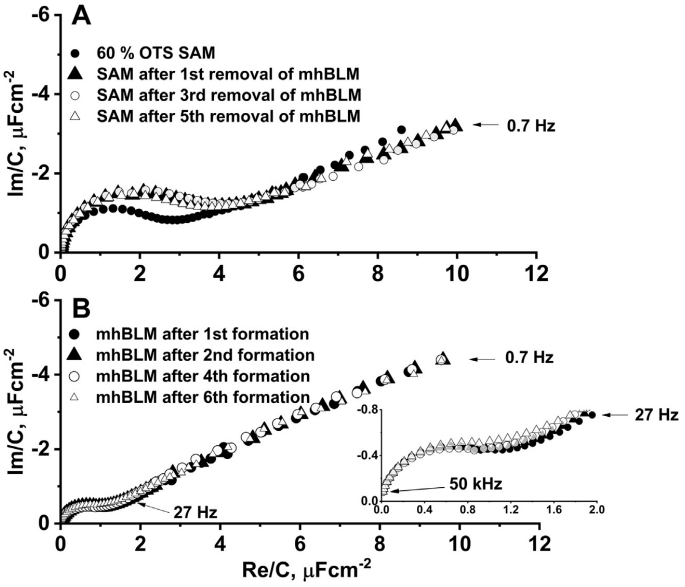

Fig. 3. Cole – Cole plots of electrochemical impedance spectra recorded over several times of vesicle fusion and removal of the phospholipid layer; A – a mixed SAM (OTS:MTS molar ratio 6:4) after removals of bilayer lipid membrane; B – mixed hybrid bilayer lipid membrane formation (DOPC/Chol, molar ratio 6:4) after removing the previously formed mhBLM. Electrode potential: 0 V vs Ag/AgCl/$NaCl_{(sat.)}$.

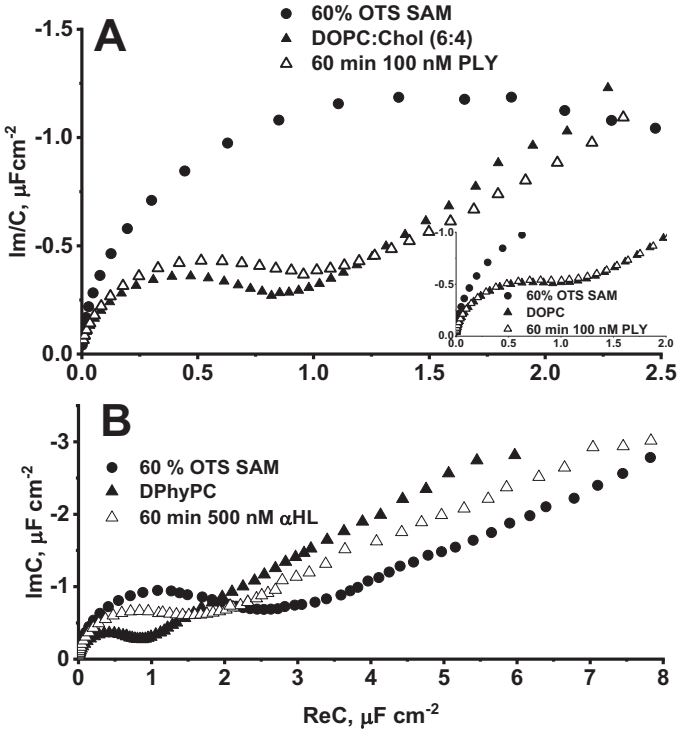

Fig. 4. Cole – Cole plots of electrochemical impedance spectra obtained at 0 V potential vs Ag/AgCl/$NaCl_{(sat.)}$ using Ti electrode functionalized with SAM prepared from silanization solution containing OTS:MTS molar ratio of 6:4; A – mixed hybrid bilayer lipid membrane (DOPC:Chol) interaction with 100 nM pneumolysin (PLY), B - mixed hybrid bilayer lipid membrane (DPhyPC) interaction with 500 nM α-hemolysin (αHL). Inset – control experiment - mhBLM (DOPC) interaction with 100 nM of PLY.

We also challenged the diphytanoyl phosphatidylcholine (DPhyPC) bilayer lipid membranes with α-hemolysin expecting spontaneous incorporation of αHL into DPhyPC membrane by the formation of heptameric pores [39]. As it can be seen from Fig. 4 B, the deviation in complex capacitance from 0.71 μF cm^{-2} to 1.32 μF cm^{-2} was observed after 1 h of injection of 500 nM αHL. The observed change in coefficient value of $C_{bilayer}/C_{bilayer+\alpha HL} = 0.54$ is more considerable than in case of PLY ($C_{bilayer}/C_{bilayer+PLY} = 0.84$). Also, the change of phase angle and

resistivity (see Supplementary material Fig. 1S, C and D) of the mhBLM in the low frequency range (below 10 Hz) was quite noticeable after introduction of αHL. Particularly, the percentage resistivity change of mhBLM was calculated to be equal to 44.68% and 25.93% for 8 Hz and 0.1 Hz, respectively (see Supplementary material Table 2S). Also, the coefficient value of $C_{bilayer}/C_{bilayer+\alpha HL} = 0.54$ is comparable to $C_{tBLM}/C_{tBLM+\alpha HL} = 0.50$, which was obtained on DPhyPC tethered bilayer lipid membrane formed on gold surfaces, where functional reconstitution of αHL was reported [39]. Therefore, we assume that such considerable change of the complex capacitance as well as a decrease of the resistance of mhBLM attest for functional reconstitution of αHL into mhBLM [40].

To conclude, both membrane damaging proteins – PLY and αHL – displayed effects on the EIS of mhBLM anchored to a mechanically polished Ti surface functionalized with mixed silane self-assembled monolayer. These effects are large enough and can be employed as a signal for the development of electrochemical/electroanalytical biosensor platforms based on modified titanium surface. Such substrates are relatively inexpensive compared to gold substrates and exhibit high biocompatibility, mechanical resistance and non-toxicity.

4. Conclusions

In this study, we explored a dilution effect of a spacer for fabrication of mixed hybrid bilayer lipid membranes on a metallurgical titanium plate electrode. We showed that a mechanically polished titanium surface can be tailored via simple silanization procedure with the mixed OTS:MTS self-assembled monolayer acting as molecular anchors for phospholipid bilayer. Experimental data suggest that having > 20% OTS in silanization solutions leads to a formation of the hydrophobic surfaces with properties suitable for triggering vesicle fusion and mhBLM formation. Furthermore, we established that the increase of MTS molar ratio decreases mhBLM's conductivity, which is primarily related to the increased number of defects in membranes. We determined that the optimal molar ratio of the MTS in the silanization solution is 40%. Such dilution of OTS provides surface coverage 0.97 which is sufficient to obtain compact phospholipid bilayers as well as flexibility of mhBLM necessary for functional reconstitution of membrane proteins [20]. We found that regeneration of a mixed self-assembled monolayer for mhBLM formation can be performed at least 6 times, with no loss of dielectric properties of the lipid membranes.

The EIS of mhBLMs indicate clear response to the membrane damaging proteins, such as PLY and αHL. The observed effects were noticeably different. Large pore-forming PLY showed effects consistent with the binding of the protein to cholesterol in mhBLM. Interaction of PLY monomers with mhBLM results in an increase of their capacitance and conductance. However, no clear indications of a pore-formation were observed. Most likely this is due to the lack of plasticity of the mbBLMs which prevents functional reconstitution PLY, as reported earlier for hybrid bilayers on gold [41]. Conversely, αHL exhibited more pronounced effects on DPhyPC mhBLM consistent with the dielectric damage and functional reconstitution of the protein.

This study proves that phospholipid layers can be immobilized using a metallurgical titanium surface. mhBLMs formed on titanium surface can provide a convenient platform for reusable phospholipid biosensors for the detection of membrane protein interactions. Titanium exhibits good protein resistance and compatibility with tissues, and it is widely used in surgery and medical implants [42]. The biocompatibility and reusability, in our opinion, is a major advantage of the metallurgical titanium over the gold substrates, which so far were not proven to allow regeneration of tBLMs without deterioration of their dielectric properties [43].

Declaration of competing interest

The authors declare that they have no known competing financial interests or personal relationships that could have appeared to influence the work reported in this paper.

Acknowledgement

This study was supported by Research Council of Lithuania. Project number P-MIP-19-394 (2019).

Appendix A. Supplementary data

Supplementary data to this article can be found online at https://doi.org/10.1016/j.bbamem.2020.183232.

References

[1] R. Naumann, E.K. Schmidt, A. Jonczyk, K. Fendler, B. Kadenbach, T. Liebermann, A. Offenhäusser, W. Knoll, The peptide-tethered lipid membrane as a biomimetic system to incorporate cytochrome c oxidase in a functionally active form, Biosens. Bioelectron. 14 (1999) 651–662, https://doi.org/10.1016/S0956-5663(99)00036-6.

[2] L.J.C. Jeuken, S.D. Connell, P.J.F. Henderson, R.B. Gennis, S.D. Evans, R.J. Bushby, Redox enzymes in tethered membranes, J. Am. Chem. Soc. 128 (2006) 1711–1716, https://doi.org/10.1021/ja056972u.

[3] G. Krishna, J. Schulte, B.A. Cornell, R.J. Pace, P.D. Osman, Tethered bilayer membranes containing ionic reservoirs: selectivity and conductance, Langmuir 19 (2003) 2294–2305, https://doi.org/10.1021/la026238d.

[4] H.M. Keizer, B.R. Dorvel, M. Andersson, D. Fine, R.B. Price, J.R. Long, A. Dodabalapur, I. Köper, W. Knoll, P.A.V. Anderson, R.S. Duran, Functional ion channels in tethered bilayer membranes—implications for biosensors, ChemBioChem 8 (2007) 1246–1250, https://doi.org/10.1002/cbic.200700094.

[5] J.D. Taylor, M.J. Linman, T. Wilkop, Q. Cheng, Regenerable tethered bilayer lipid membrane arrays for multiplexed label-free analysis of lipid−protein interactions on poly(dimethylsiloxane) microchips using SPR imaging, Anal. Chem. 81 (2009) 1146–1153, https://doi.org/10.1021/ac8023137.

[6] D.J. McGillivray, G. Valincius, D.J. Vanderah, W. Febo-Ayala, J.T. Woodward, J.J. Kasianowicz, M. Löscheb, Molecular-scale structural and functional characterization of sparsely tethered bilayer lipid membranes, Biointerphases 2 (2007) 21–33, https://doi.org/10.1116/1.2709308.

[7] B.A. Cornell, V.L.B. Braach-Maksvytis, L.G. King, P.D.J. Osman, B. Raguse, L. Wieczorek, R.J. Pace, A biosensor that uses ion-channel switches, Nature 387 (1997) 580–582 https://doi https://doi.org/10.1038/42432.

[8] L.J.C. Jeuken, N.N. Daskalakisa, X. Hana, K. Sheikha, A. Erbea, R.J. Bushbyb, S.D. Evansa, Phase separation in mixed self-assembled monolayers and its effect on biomimetic membranes, Sensors Actuators B Chem. 124 (2007) 501–509, https://doi.org/10.1016/j.snb.2007.01.014.

[9] B. Raguse, V. Braach-Maksvytis, B.A. Cornell, L.G. King, P.D.J. Osman, R.J. Pace, L. Wieczorek, Tethered lipid bilayer membranes: formation and ionic reservoir characterization, Langmuir 14 (1998) 648–659, https://doi.org/10.1021/la9711239.

[10] A. Valiūnienė, Ž. Margarian, I. Gabriūnaitė, V. Matulevičiūtė, T. Murauskas, G. Valinčius, Cadmium stannate films for immobilization of phospholipid bilayers, J. Electrochem. Soc. 163 (2016) H762–H767, https://doi.org/10.1149/2.0331609jes.

[11] O. Eicher-Lorka, T. Charkova, A. Matijoška, Z. Kuodis, G. Urbelis, T. Penkauskas, M. Mickevičius, A. Bulovas, G. Valinčius, Cholesterol-based tethers and markers for model membranes investigation, Chem. Phys. Lipids 195 (2016) 71–86, https://doi.org/10.1016/j.chemphyslip.2015.12.006.

[12] R. Naumann, S.M. Schiller, F. Giess, B. Grohe, K.B. Hartman, I. Kärcher, I. Köper, J. Lübben, K. Vasilev, W. Knoll, Tethered lipid bilayers on ultraflat gold surfaces, Langmuir 19 (2003) 5435–5443, https://doi.org/10.1021/la0342060.

[13] S.M. Schiller, R. Naumann, K. Lovejoy, H. Kunz, W. Knoll, Archaea analogue thiolipids for tethered bilayer lipid membranes on ultrasmooth gold surfaces, Angew. Chem. Int. Ed. Engl. 42 (2003) 208–211, https://doi.org/10.1002/anie.200390080.

[14] B.R. Dorvel, H.M. Keizer, D. Fine, J. Vuorinen, A. Dodabalapur, R.S. Duran, Formation of tethered bilayer lipid membranes on gold surfaces: QCM-Z and AFM study, Langmuir 23 (2007) 7344–7355, https://doi.org/10.1021/la0610396.

[15] S. Terrettaz, M. Mayer, H. Vogel, Highly electrically insulating tethered lipid bilayers for probing the function of ion channel proteins, Langmuir 19 (2003) 5567–5569, https://doi.org/10.1021/la034197v.

[16] G. Valincius, R. Budvytyte, T. Penkauskas, M. Pleckaityte, A. Zvirbliene, Phospholipid sensors for detection of bacterial pore-forming toxins, ECS Trans. 64 (2014) 117–124, https://doi.org/10.1149/06401.0117ecst.

[17] S. Saraf, C.J. Neal, S. Park, S. Das, S. Barkam, H.J. Cho, S. Seal, Electrochemical study of nanoporous gold revealing anti-biofouling properties, RSC Adv. 5 (2015) 46501–46508 https://10.1039/C5RA05043J.

[18] E.F. Bowden, F.M. Hawkridge, H.N. Blount, Interfacial electrochemistry of cytochrome c at tin oxide, indium oxide, gold, and platinum electrodes, J. Electroanal. Chem. Interfacial Electrochem. 161 (1984) 355–376, https://doi.org/10.1016/S0022-0728(84)80193-X.

[19] M. Long, H.J. Rack, Titanium alloys in total joint replacement — a materials science

perspective, Biomaterials 19 (1998) 1621–1639, https://doi.org/10.1016/S0142-9612(97)00146-4.
[20] I. Gabriūnaitė, A. Valiūnienė, G. Valincius, Formation and properties of phospholipid bilayers on fluorine doped tin oxide electrodes, Electrochimica Acta 283 (2018), https://doi.org/10.1016/j.electacta.2018.04.160.
[21] H. Hillebrandt, M. Tanaka, Electrochemical characterization of self-assembled alkylsiloxane monolayers on indium − tin oxide (ITO) semiconductor electrodes, J. Phys. Chem. B 105 (2001) 4270–4276, https://doi.org/10.1021/jp004062n.
[22] K. Kumar, C.S. Tang, F.F. Rossetti, M. Textor, B. Keller, J. Vörös, E. Reimhult, Formation of supported lipid bilayers on indium tin oxide for dynamically-patterned membrane-functionalized microelectrode arrays, Lab Chip 9 (2009) 718–725, https://doi.org/10.1039/B814281E.
[23] J.A. Jackman, S.R. Tabaei, Z. Zhao, S. Yorulmaz, N.-J. Cho, Self-assembly formation of lipid bilayer coatings on bare aluminum oxide: overcoming the force of interfacial water, ACS Appl. Mater. Interfaces 7 (2015) 959–968, https://doi.org/10.1021/am507651h.
[24] A. Valiūnienė, T. Petrulionienė, I. Baleviciūtė, L. Mikoliūnaitė, G. Valinčius, Formation of hybrid bilayers on silanized thin-film Ti electrode, Chem. Phys. Lipids 202 (2017) 62–68, https://doi.org/10.1016/j.chemphyslip.2016.12.001.
[25] T. Sabirovas, A. Valiūnienė, G. Valincius, Mechanically polished titanium surface for immobilization of hybrid bilayer membrane, J. Electrochem. Soc. 165 (2018) G109–G115, https://doi.org/10.1149/2.0101810jes.
[26] X. Liu, P.K. Chu, C. Ding, Surface modification of titanium, titanium alloys, and related materials for biomedical applications, Mater. Sci. Eng. R Rep. 47 (2004) 49–121, https://doi.org/10.1016/j.mser.2004.11.001.
[27] J.A. Jackman, W. Knoll, N.-J. Cho, Biotechnology applications of tethered lipid bilayer membranes, Materials (Basel) 5 (2012) 2637–2657, https://doi.org/10.3390/ma5122637.
[28] T. Ragaliauskas, M. Mickevicius, B. Rakovska, T. Penkauskas, D.J. Vanderah, F. Heinrich, G. Valincius, Fast formation of low-defect-density tethered bilayers by fusion of multilamellar vesicles, Biochim. Biophys. Acta Biomembr. 1859 (2017) 669–678, https://doi.org/10.1016/j.bbamem.2017.01.015.
[29] G.S. Popkirov, R.N. Schindler, A new impedance spectrometer for the investigation of electrochemical systems, Rev. Sci. Instrum. 63 (1992) 5366–5372, https://doi.org/10.1063/1.1143404.
[30] V.I. Silin, H. Wieder, J.T. Woodward, G. Valincius, A. Offenhausser, A.L. Plant, The role of surface free energy on the formation of hybrid bilayer membranes, J. Am. Chem. Soc. 124 (2002) 14676–14683, https://doi.org/10.1021/ja026585+.
[31] G. Valincius, M. Mickevicius, Chapter two - tethered phospholipid bilayer membranes: an interpretation of the electrochemical impedance response, in: A. Iglič, C.V. Kulkarni, M. Rappolt (Eds.), Advances in Planar Lipid Bilayers and Liposomes, Academic Press, 2015, pp. 27–61, , https://doi.org/10.1016/bs.adplan.2015.01.003.
[32] M. Itagaki, S. Suzuki, I. Shitanda, K. Watanabe, Electrochemical impedance and complex capacitance to interpret electrochemical capacitor, Electrochemistry 75 (2007) 649–655, https://doi.org/10.5796/electrochemistry.75.649.
[33] Allen J. Bard, Larry R. Faulkner, Electrochemical Methods: Fundamentals and Applications, 2nd ed., Wiley, New York, 2001.
[34] D.R. Neill, T.J. Mitchell, A. Kadioglu, Chapter 14 - pneumolysin, in: J. Brown, S. Hammerschmidt, C. Orihuela (Eds.), Streptococcus pneumoniae, Academic Press, Amsterdam, 2015, pp. 257–275, , https://doi.org/10.1016/B978-0-12-410530-0.00014-4.
[35] J. Rossjohn, R.J.C. Gilbert, D. Crane, P.J. Morgan, T.J. Mitchell, A.J. Rowe, P.W. Andrew, J.C. Paton, R.K. Tweten, M.W. Parker, The molecular mechanism of pneumolysin, a virulence factor from Streptococcus pneumoniae11Edited by J. Thornton, J. Mol. Biol. 284 (1998) 449–461, https://doi.org/10.1006/jmbi.1998.2167.
[36] S.L. Lawrence, S.C. Feil, C.J. Morton, A.J. Farrand, T.D. Mulhern, M.A. Gorman, K.R. Wade, R.K. Tweten, M.W. Parker, Crystal structure of Streptococcus pneumoniae pneumolysin provides key insights into early steps of pore formation, Sci. Rep. 5 (2015) 14352, https://doi.org/10.1038/srep14352.
[37] T. Raila, T. Penkauskas, M. Jankunec, G. Dreižas, T. Meškauskas, G. Valincius, Electrochemical impedance of randomly distributed defects in tethered phospholipid bilayers: finite element analysis, Electrochim. Acta 299 (2019) 863–874, https://doi.org/10.1016/j.electacta.2018.12.148.
[38] R. Budvytyte, G. Valincius, G. Niaura, V. Voiciuk, M. Mickevicius, H. Chapman, Haw-Zan Goh, Prabhanshu Shekhar, F. Heinrich, Siddharth Shenoy, M. Lösche, D.J. Vanderah, Structure and properties of tethered bilayer lipid membranes with unsaturated anchor molecules, Langmuir 29 (2013) 8645–8656, https://doi.org/10.1021/la401132c.
[39] I.K. Vockenroth, P.P. Atanasova, A.T.A. Jenkins, I. Köper, Incorporation of α-hemolysin in different tethered bilayer lipid membrane architectures, Langmuir 24 (2008) 496–502, https://doi.org/10.1021/la7030279.
[40] D.J. McGillivray, G. Valincius, F. Heinrich, J.W.F. Robertson, D.J. Vanderah, W. Febo-Ayala, I. Ignatjev, M. Lösche, J.J. Kasianowicz, Structure of functional Staphylococcus aureus alpha-hemolysin channels in tethered bilayer lipid membranes, Biophys. J. 96 (2009) 1547–1553, https://doi.org/10.1016/j.bpj.2008.11.020.
[41] S.A. Glazier, D.J. Vanderah, A.L. Plant, H. Bayley, G. Valincius, J.J. Kasianowicz, Reconstitution of the pore forming toxin α-hemolysin in phospholipid/18-n-C18H37-1-thiahexa(ethylene oxide) and phospholipid/n-octadecanethiol supported bilayer membranes, Langmuir 16 (2000) 10428–10435, https://doi.org/10.1021/la000690k.
[42] M. Saini, Y. Singh, P. Arora, V. Arora, K. Jain, Implant biomaterials: a comprehensive review, World J Clin Cases 3 (2015) 52–57, https://doi.org/10.12998/wjcc.v3.i1.52.
[43] B. Rakovska, T. Ragaliauskas, M. Mickevicius, M. Jankunec, G. Niaura, D.J. Vanderah, G. Valincius, Structure and function of the membrane anchoring self-assembled monolayers, Langmuir 31 (2015) 846–857, https://doi.org/10.1021/la503715b.

NOTES

NOTES

NOTES

Vilniaus universiteto leidykla
Saulėtekio al. 9, LT-10222 Vilnius
El. p. info@leidykla.vu.lt,
www.leidykla.vu.lt
Tiražas 20 egz.